

**PREMATURE FAILURE ANALYSIS OF SINGLE ROW, DEEP
GROOVE BEARINGS FROM IDLER ROLLERS USED ON MINE
SITES**

Patrick O'Farrell

Bachelor of Engineering (Honours)
with a Major in Mechanical Engineering



Department of Mechanical Engineering
Macquarie University

November, 7 2016

Supervisor: Professor Candace Lang

ACKNOWLEDGEMENTS


I would like to acknowledge the help of my academic supervisors' Dr Abdul Mazid and Professor Candace Lang as well as industry engineer Jamie Overend from Gladstone Port Corporation for supplying idler rollers, without which this project would not be possible. The objective of this project is to analyse failed bearings from idler rollers to investigate their premature failure. The results will be beneficial for mine sites in order to reduce the number and types of premature failures of idler rollers on belt conveyors. I would also like to thank Macquarie Engineering and Technical Services (METS) for helping and supplying tools for work on the idler rollers.

STATEMENT OF CANDIDATE

I, Patrick O'Farrell, declare that this report is entirely my own work unless stated or referenced otherwise. This document is part of the requirement for a Bachelor of Engineering, Majoring in Mechanical, by Macquarie University. This document has not been submitted for assessment at any other academic institution.

Student name: Patrick O'Farrell

Student ID: 43273246

Students Signature: 

Date: 7 November, 2016

ABSTRACT

Bearings are vital to the operation and efficiency of millions of systems as they allow components to rotate freely with minimal resistance or stress. They are particularly important on belt conveyors which are widely used on mine sites (the specifics of a belt conveyor system will be discussed in more detail later on). It is a common occurrence for idler rollers (the cylindrical pipes upon which the belt slides across) to fail prematurely, causing damage to the belt conveyor resulting in down-time of the mining operations, consequently costing mining companies hundreds of thousands of dollars. For this reason, it is beneficial to perform a detailed failure analysis of these idler rollers, focussing on the bearings as they are the common point of premature failure. This thesis paper will contain mathematical models simulating the mechanical loads on a bearing using computer simulations in ANSYS Workbench as well as practical work on damaged idler rollers where a failure analysis will be carried out. This experimental work will consist of a series of pictures taken using a camera as well as an optical microscope for detailed views of the internal surfaces of the bearings. A detailed analysis of the findings will be presented in the discussion.

TABLE OF CONTENTS

ACKNOWLEDGEMENTS	3
STATEMENT OF CANDIDATE	5
ABSTRACT.....	7
LIST OF FIGURES	11
1 INTRODUCTION	15
1.1 Project Overview	15
1.2 Belt Conveyor System	15
1.3 The Question	17
2 LITERATURE REVIEW	18
2.1 The Idler Roller.....	18
2.1.1 Manufacturing and Assembly of Components of an Idler Roller	19
2.2 Bearings	21
2.2.1 General Information about Bearings	21
2.2.2 Project Bearings	22
2.2.3 Bearing Sealing	23
2.2.4 Lubrication	24
2.3 Bearing Damage Analysis.....	25
2.3.1 Wear.....	25
2.3.2 Overheating.....	28
2.3.3 Loading and Movement	31
2.3.4 Installation.....	34
2.3.5 Bearing Misalignment.....	35
2.4 Wear Mechanisms	36
2.4.1 Two body Abrasive Wear	37
2.4.2 Three Body Abrasive Wear.....	38
2.4.3 Lubricant Related Abrasive Wear.....	38
3 EXPERIMENTAL PROCEDURES	40
3.1 Theoretical Work	40
3.1.1 Model Development.....	40
3.1.2 FEA.....	41
3.2 Experimental Work.....	58
3.2.1 Removal of Bearings from Idler Rollers	58
3.2.2 Bearing Preparation.....	65
3.2.3 Cutting Bearings	67
3.2.4 Microscopic Images	68
3.2.5 Hardness Test.....	69
4 RESULTS	72

4.1	FEA.....	72
4.2	Experimental Results	75
4.2.1	Idler Roller 1	76
4.2.2	Idler Roller 2	81
4.2.3	Idler Roller 3	86
4.2.4	Idler Roller 4	91
4.2.5	Idler Roller 5	94
4.2.6	Idler Roller 6	99
4.3	Micrographs	104
4.3.1	Surface damage.....	104
4.3.2	Pitting/Bruising	118
4.3.3	Fatigue Spalling	122
4.3.4	Chips	125
4.3.5	Surface Contamination.....	126
4.3.6	Corrosion/Etching	129
4.3.7	Heat Damage.....	130
4.3.8	Ball damage	131
4.3.9	Cage Damage.....	136
4.4	Hardness Test.....	140
5	DISCUSSION.....	141
5.1	FEA Component	141
5.1.1	Total Deformation.....	142
5.1.2	Stress	142
5.1.3	Pressure.....	142
5.2	Lubrication samples	144
5.3	Micrographs	145
5.3.1	Surface Damage	146
5.3.2	Pitting/Bruising	148
5.3.3	Fatigue Spalling	149
5.3.4	Chips	149
5.3.5	Surface Contamination.....	150
5.3.6	Corrosion/Etching	151
5.3.7	Heat Damage.....	152
5.3.8	Frequency of Various Damage Types.....	153
6	CONCLUSIONS.....	154
7	FUTURE WORK.....	156
	REFERENCES	157
	APPENDICES	159

LIST OF FIGURES

Figure 1: A simple belt conveyor system.....	16
Figure 2: Front cross-section of a trough layout belt conveyor	16
Figure 3: Components of an idler roller [3]	18
Figure 4: A labyrinth seal [7].....	20
Figure 5: Single row deep groove ball bearing [8]	21
Figure 6: ZZ Shielded bearing [9].....	23
Figure 7: Example of GSC spalling [13]	26
Figure 8: Example of PSO spalling [13]	26
Figure 9: Etching and corrosion on the races of the bearing [13]	27
Figure 10: False Brinelling shown on the race.....	28
Figure 11: Total Bearing Seizure due to extreme material deformation [13]	30
Figure 12: Total bearing seizure due to external bodies	31
Figure 13: Example of excessive loading on the races and rolling elements [13]	32
Figure 14: An example of brinelling [13]	34
Figure 15: Wear mechanisms [15].....	36
Figure 16: Two modes of abrasive wear [16]	37
Figure 17: Three body abrasion of ball and raceway of a bearing [17]	38
Figure 18: SKF 6306-2Z single row deep groove ball bearing model.....	41
Figure 19: The main screen of ANSYS Workbench with the desired simulation highlighted	42
Figure 20: An overall look at the settings for preparing a simulation in FEA	43
Figure 21: Cage (highlighted green) set to have flexible 'Stiffness Behaviour' and material Stainless Steel.	44
Figure 22: Cartesian coordinate system	45
Figure 23: Cylindrical coordinate system	46
Figure 24: Frictional contact between the ball (blue) and the inside race (red).....	47
Figure 25: Frictional coefficient between the ball (blue) and the outside race (red)	48
Figure 26: Frictionless contact between the ball (blue) and the inside ring of the cage (red)	49
Figure 27: Fixed joint of the inner ring	50
Figure 28: Revolute joint of outer ring	51
Figure 29: Revolute ground to cage.....	51
Figure 30: Face sizing of mesh (inner race, outer race balls)	52
Figure 31: Face Sizing 3, cage and balls.....	53
Figure 32: Patch Conforming Method of the mesh.....	54
Figure 33: Mesh Details.....	55
Figure 34: Bearing Load:	56
Figure 35: Joint Rotation of outside ring	57
Figure 36: Idler roller with aluminium shell before disassembly	58
Figure 37: Cutting of idler roller in progress (150mm from end) in the abrasive cutter.....	59
Figure 38: The result of the first cutting process	59
Figure 39: Hydraulic press in action, pressing the shaft through the bearing housing	60
Figure 40: Removed bearing housing from the shaft and bearing using a hydraulic press	61
Figure 41: Small shaft section which the bearing and end cap are press fitted too.....	61
Figure 42: Two layers of press fitted sheet metal to prevent debris contamination to the bearing.....	62
Figure 43: The bearing, isolated from all other components	62
Figure 44: The shaft, with bearings and seals	63
Figure 45: End of shaft with bearing, two sheets of metal, rubber seal (left to right)	63
Figure 46: Internal side of the bearing on the shaft	64
Figure 47: The aluminium shell from the shaft in figure 42.....	64

Figure 48: Uncleaned bearing observations	65
Figure 49: Scrubbing grease off bearings with a toothbrush	66
Figure 50: After the cleaning process	66
Figure 51: Diagram showing the line which bearings were cut.....	67
Figure 52: Jig used to cut bearings in half	67
Figure 53: Optical Microscope used for detailed images.....	68
Figure 54: Struers Secotom-50 cutting tool	69
Figure 55: Abrasive cutting tool settings	69
Figure 56: After first stage of cutting, this piece is cut in half horizontally	70
Figure 57: Bearing pieces in the mould ready after being polished.....	70
Figure 58: Hardness test result.....	71
Figure 59: FEA Total Deformation of outer ring.....	72
Figure 60: Equivalent stresses in a bearing.....	73
Figure 61: FEA Equivalent stress cage edge	74
Figure 62: FEA pressure points on rolling elements.....	74
Figure 63: Bearing 1.1	76
Figure 64: Bearing 1.1	76
Figure 65: Bearing 1.1 lubrication	77
Figure 66: Bearing 1.1 clean	78
Figure 67: Bearing 1.1 outside of outer ring	78
Figure 68: Bearing 1.2	79
Figure 69: Bearing 1.2 lubrication	79
Figure 70: Bear 1.2 clean	80
Figure 71: Bearing 2.1	81
Figure 72: Bearing 2.1	81
Figure 73: Bearing 2.1 lubrication	82
Figure 74: Bearing 2.1 clean	82
Figure 75: Bearing 2.1 outer ring face	83
Figure 76: Bearing 2.2	84
Figure 77: Bearing 2.2 lubrication	84
Figure 78: Bearing 2.2 clean	85
Figure 79: Bearing 2.2 outer ring face	85
Figure 80: Bearing 3.1	86
Figure 81: Bearing 3.1	86
Figure 82: Bearing 3.1 lubrication	87
Figure 83: Bearing 3.1 clean	87
Figure 84: Bearing 3.2	88
Figure 85: Bearing 3.2 lubrication	88
Figure 86: Bearing 3.2 clean	89
Figure 87: Bearing 3.2, inner edge of outer ring.....	89
Figure 88: Bearing 3.2 outer ring face	90
Figure 89: Bearing 4.1	91
Figure 90: Bearing 4.1	91
Figure 91: Bearing 4.1 clean, outer ring face.....	92
Figure 92: Bearing 4.2	93
Figure 93: Bearing 4.2 clean, outer ring face.....	93
Figure 94: Bearing 5.1	94
Figure 95: Bearing 5.1 Lubrication.....	94
Figure 96: Bearing 5.1 lubrication	95
Figure 97: Bearing 5.1 clean	95
Figure 98: Bearing 5.1 outer ring face	96

Figure 99: Bearing 5.2	96
Figure 100: Bearing 5.2 lubrication	97
Figure 101: Bearing 5.2 clean	97
Figure 102: Bearing 5.2 outer ring face	98
Figure 103: Bearing 5.2 inner ring edge	98
Figure 104: Bearing 6.1	99
Figure 105: Bearing 6.1	99
Figure 106: Bearing 6.1 lubrication	100
Figure 107: Bearing 6.1 clean	100
Figure 108: Bearing 6.1 outer ring face	101
Figure 109: Bearing 6.2	102
Figure 110: Bearing 6.2 lubrication	102
Figure 111: Bearing 6.2 clean	103
Figure 112: Bearing 6.2 outer ring face	103
Figure 113: Bearing 1.1 outer ring scratches	104
Figure 114: Bearing 2.1 outer race scratches	105
Figure 115: Bearing 2.2 outer race scratches	106
Figure 116: Bearing 2.1 outer race	106
Figure 117: Bearing 3.1 inner race scratches	106
Figure 118: Bearing 3.2 outer race scratches	107
Figure 119: Bearing 3.2 outer race scratches	107
Figure 120: Bearing 4.2 outer race scratches	108
Figure 121: Bearing 5.1 inner race scratches	108
Figure 122: Bearing 5.2 inner race scratches	109
Figure 123: Bearing 6.1 outer race scratches	109
Figure 124: Bearing 6.1 outer race scratches	110
Figure 125: Bearing 6.2 outer race scratches	111
Figure 126: Bearing 1.1 inner race edge	112
Figure 127: Bearing 2.1 outer race gouges near edge of race	113
Figure 128: Bearing 4.1 inner race gouge	114
Figure 129: Bearing 4.2 outer race gouge and surface contamination	114
Figure 130: Bearing 5.1 outer race gouges and pitting	115
Figure 131: Bearing 5.2 inner race gouge	115
Figure 132: Bearing 6.1 outer race gouge	116
Figure 133: Bearing 3.1 outer race groove	117
Figure 134: Bearing 4.1 inner race groove and bruising	117
Figure 135: Bearing 5.1 outer race groove	117
Figure 136: Bearing 1.1 inner ring pitting	118
Figure 137: Bearing 3.1 inner race bruising	119
Figure 138: Bearing 4.1 outer race pitting	119
Figure 139: Bearing 4.2 outer race pitting	120
Figure 140: Bearing 4.2 inner race series of chips	120
Figure 141: Bearing 5.1 outer race bruising	121
Figure 142: Bearing 6.2 inner race pitting and bruising	121
Figure 143: Bearing 1.1 outer ring spalling	122
Figure 144: Bearing 2.1 inner race spalling	122
Figure 145: Bearing 3.2 inner race spalling	123
Figure 146: Bearing 4.1 inner race spalling	123
Figure 147: Bearing 4.2 inner race PSO spalling	124
Figure 148: Bearing 6.1 outer race chip on edge	125
Figure 149: Bearing 1.2 outer race surface contamination	126

Figure 150: Bearing 2.2 inner race surface contamination by polymer of bearing housing	126
Figure 151: Bearing 5.1 outer race surface contamination	127
Figure 152: Bearing 5.2 inner race surface contamination	127
Figure 153: Bearing 6.1 outer race surface contamination	128
Figure 154: Bearing 2.2 inner race corrosion/etching.....	129
Figure 155: Bearing 4.1 outer race surface breakdown due to heat.....	130
Figure 156: Bearing 1.1 ball surface scratches	131
Figure 157: Bearing 2.2 ball surface scratches and pitting	131
Figure 158: Bearing 3.1 ball surface scratches	132
Figure 159: Bearing 3.2 ball scratches.....	132
Figure 160: Bearing 4.1 ball surface scratches and wear.....	133
Figure 161: Bearing 5.1 ball scratches.....	133
Figure 162: Bearing 5.2 ball scratches and pitting.....	133
Figure 163: Bearing 6.1 ball scratches.....	134
Figure 164: Bearing 6.2 ball scratches (arrow) and surface contamination (red circle)	134
Figure 165: Bearing 2.1 ball scratches and pitting.....	135
Figure 166: Bearing 3.2 ball pitting with surface wear.....	135
Figure 167: Bearing 4.2 ball pitting	135
Figure 168: Bearing 1.1 cage edge wear.....	136
Figure 169: Bearing 3.1 cage edge wear.....	136
Figure 170: Bearing 4.1 melted cage edge.....	136
Figure 171: Bearing 4.2 melted cage edge and wear	137
Figure 172: Bearing 5.1 melted cage edge and wear	137
Figure 173: Bearing 5.2 cage edge wear.....	138
Figure 174: Bearing 6.1 cage edge wear.....	138
Figure 175: Bearing 6.2 cage wear	139
Figure 176: Frequency of various damage types	153
Figure 177: Fine particle contamination examples [9]	159
Figure 178: Heat Damage at roller ends [13].....	159
Figure 179: Example of excessive end play damage [13].....	160
Figure 180: Example of impact damage to the races of the bearing [13]	160
Figure 181: Shaft misalignment and bearing housing misalignment [13]	161
Figure 182: Uneven load distribution and ball path due to bearing misalignment [13].....	161
Figure 183: SKF 6306-2Z single row deep groove ball bearing specifications [20]	162
Figure 184: Coefficient of Friction for various SKF bearings [21]	163
Figure 185: Consultation sheet	164

1 INTRODUCTION

1.1 PROJECT OVERVIEW

This section outlines a brief overview of the paper, allowing the reader to clearly visualise the structure and methodical progress throughout the report.

The introduction will explain exactly what is to be investigated during this project and the reasoning behind it. A description of a belt conveyor system will also be provided with details on the key components within the system.

Having discussed the components of the belt conveyor and chosen a focus area, the bearing inside the idler roller, the workings of a bearing are analysed in further detail. This includes bearing selection for mining related applications as well as lubrication which is vital to the function and efficiency of a bearing in motion.

Following the discussion of the bearing mechanisms, a damage analysis guide is provided which supplies the reader an abundance of information on the numerous types of damage and reasons for bearings failure, along with the consequential effects of these incidents.

A methodology guides the reader through the various stages of computer simulations and experimental work. Experimental work consists of both macro (large) and micro (small) photographs covering the overall picture and detailed components of bearings and their internal structure.

The results will then be discussed to determine the root cause of premature bearing failure.

1.2 BELT CONVEYOR SYSTEM

A belt conveyor system is primarily used for automated, bulk transportation of a diverse range of products in high flow rates over large distances. They are widely used in mining processes, production lines in factories and other tasks which require consistently high movement of products over sizable distances.

A belt conveyor system is made up of very few components. The belt itself is an endless strap of flexible, flat material stretched between two large drums or pulleys at either end [1]. One pulley is powered, making it the driver pulley and allows the belt to move. The other is called an idler pulley as it has no means of power. As the belts run over large distances it is necessary to have a way of assisting the belts' movement and providing support so it so it doesn't sag.

The job is done by idler rollers which are similar to the idler pulley. They are not driven but provide load support with minimal resistance to movement [2].

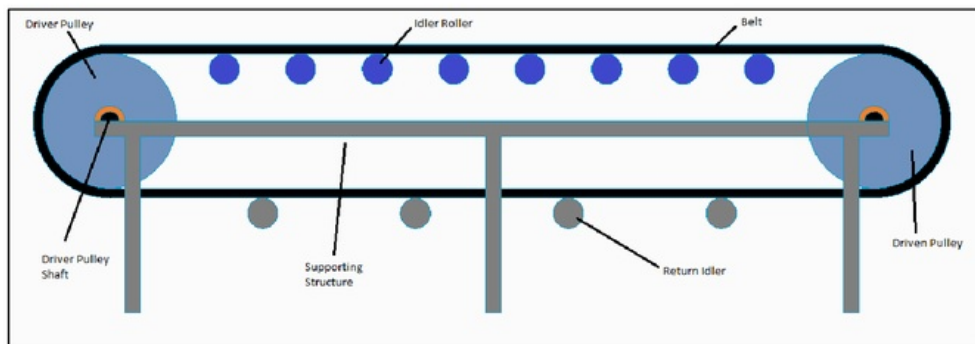


Figure 1: A simple belt conveyor system

The figure above is a drawing of a very simple belt conveyor system (very different from those used to transport minerals and ores). We can see the belt is moved by a driver pulley and travels across a series of idlers designed to support the belt and spread the load. On the belts return it passes over a series of return idlers which are designed to support small loads but keep the belt moving efficiently.

Every few metres a series of idler rollers support the belt and keep it moving at the highest possible efficiency. In mining applications, they are usually assembled in a 'V' trough formation so the belt is curved, allowing more material to be contained and efficiently transported without spillage. [2]

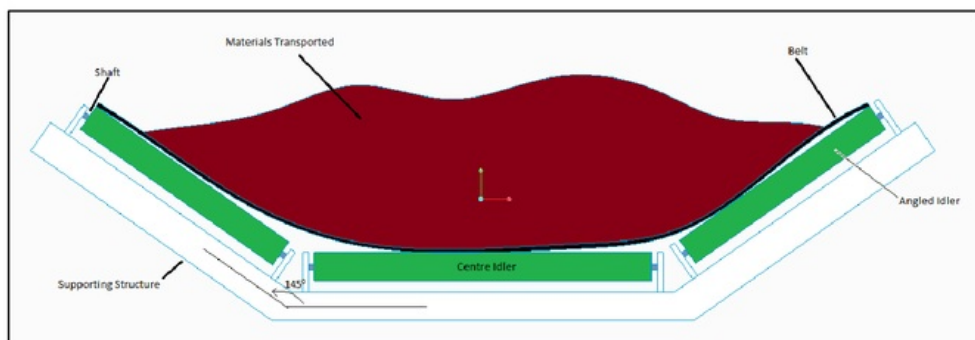


Figure 2: Front cross-section of a trough layout belt conveyor

The above diagram shows us a cross-sectional cut of the belt conveyor typically used on mine sites. The angle of the left and right idlers with respect to the centre idler. As the angle (currently 145°) changes so does the load and load angle applied by the material on each idler.

Belt conveyors are essentially the backbone of mine sites, used for transportation of large quantities of materials such as ores, over long distances. A typical belt conveyor may run over tens of kilometres for much of the day. However, ideally a belt conveyor system would run 24/7 with minimal downtime for maintenance and equipment check-ups.

1.3 THE QUESTION

The aim of this thesis paper is to understand in more detail, the cause and effects of premature failure of idler rollers used in belt conveyor systems on mine sites. To provide enough detail a narrower scope is required. The most common point of failure on these idler rollers is the bearing as it is what allows the idler to rotate freely and efficiently, so this paper will focus on failure analysis of the bearing. It is predicted the root cause of failure is wear due to foreign particles which cause several secondary problems (such as vibration, deformation and thermal effects) resulting in bearing failure.

Computer simulations of a model bearing of the same type as the one used in the idlers on the mine site will be ran to test whether the design of the bearing cannot support the stresses and strains it is subjected too. While it is expected that fatigue is not the primary cause of failure, validating this theory will eliminate the need to continue that avenue of research. Following this, several idler rollers will be disassembled and the bearings singled out. A close look at the bearings and the surrounding areas will be investigated to determine failure cause. Theoretical and experimental data will be compared to determine whether the expected fatigue failures are occurring in real situations.

Experimental work consists of using microscopes to study the surfaces of internal components of the bearings to understand exactly what is going on. This does not look at fatigue but rather wear of the bearing which is a suspected cause of premature failure.

We cannot simply look at the bearing in isolation and expect to come out with a meaningful conclusion. Therefore, it is important to understand the basics of a belt conveyor system and how each component works with each other. Then we can fully understand the damage itself and possible causes of damage to the bearings inside the idler roller.

2 LITERATURE REVIEW

2.1 THE IDLER ROLLER

Breaking down the system, we get to this paper's area of focus, the idler roller. It is a very simple piece of equipment, consisting of a stationary shaft with two bearings mounted at either end, encased in a rotating shell upon which the belt runs. The parameters of each component can vary depending on belt width, belt speed, weight and type of material being transported but the construction remains almost identical [2].

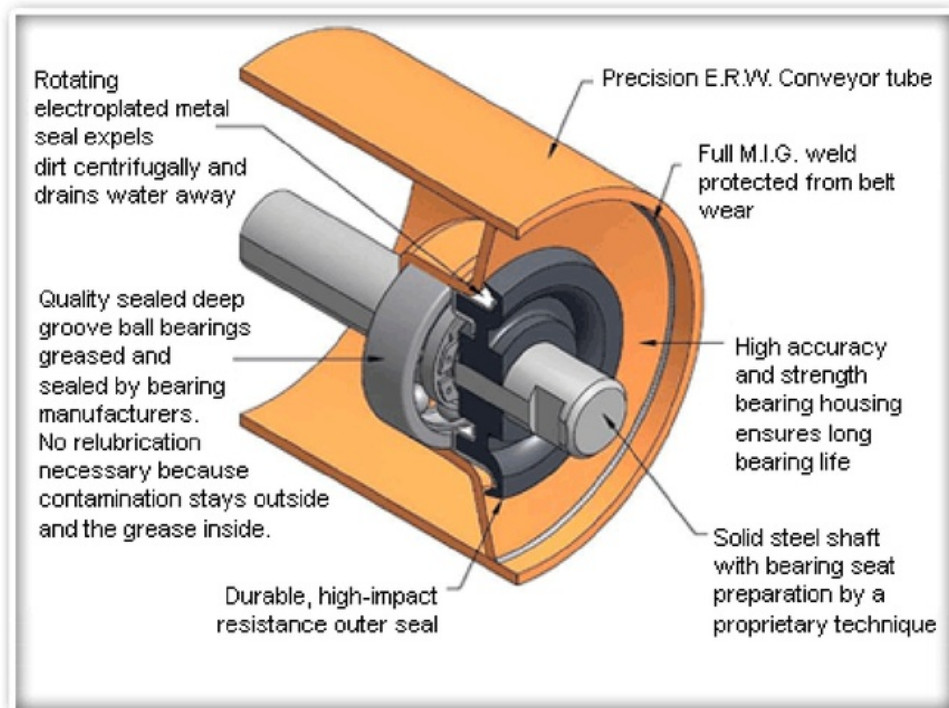


Figure 3: Components of an idler roller [3]

The diagram above is an example of an idler rollers construction as per *Lorbrand*, who develop mine site equipment. We can see the idler consists of a shaft fixed to the structure of the belt conveyor. A single row deep groove ball bearing is fitted to the shaft and sealed using a labyrinth seal. Attached to the outer ring of the bearing is a shell (usually steel or an aluminium alloy) with an end plate filling the gaps and protecting the insides of the idler.

2.1.1 Manufacturing and Assembly of Components of an Idler Roller

While each roller manufacturer may have slight variations in manufacturing, it is presumed the design would be very similar as well as the materials chosen (this being due to the environment and task they are designed for).

Roller shafts are manufactured from solid steel due to its strong mechanical properties. In some cases, the shafts are hollow to reduce roller mass but for idler roller applications the shafts are solid steel [4]. Structural Steel has a Young's Modulus of 200 GPa and an Ultimate Tensile Strength of 400 MPa. These high values are valuable in preventing deflection from impacts and sustained high loads [5].

The shell of the roller is usually made from steel as well for the same reasoning, although aluminium alloy is also commonly used these days. The end caps are welded to the shell (meaning the material needs to be compatible) so they are also a steel or aluminium alloy [4].

Bearings are secured with an interference fit according to international standards and afterwards locked in so lateral movement cannot occur. Due to the nature of the loads single row deep groove ball bearings with C3 or C4 clearance. These bearings give up to $0^{\circ} 10'$ angular deflection in operation, with even load distribution in the race [4].

The seal for the bearing provides effective protection from common contaminants such as dust and water with minimal rotational resistance. This also helps prevent shell wear due to differential speeds between the roller and the belt. The seal is known as a labyrinth seal and is located on the outer face of the bearing [4]. The clue is in the name, the seal is made up of a labyrinth, of sorts, which particles must traverse to penetrate the seal. This type of seal is non-contact seal, meaning it will not wear out, and is made up of many grooves which particles get trapped in due to the centrifugal forces from the spinning components [6]. The figure below shows in detail the labyrinth seal.

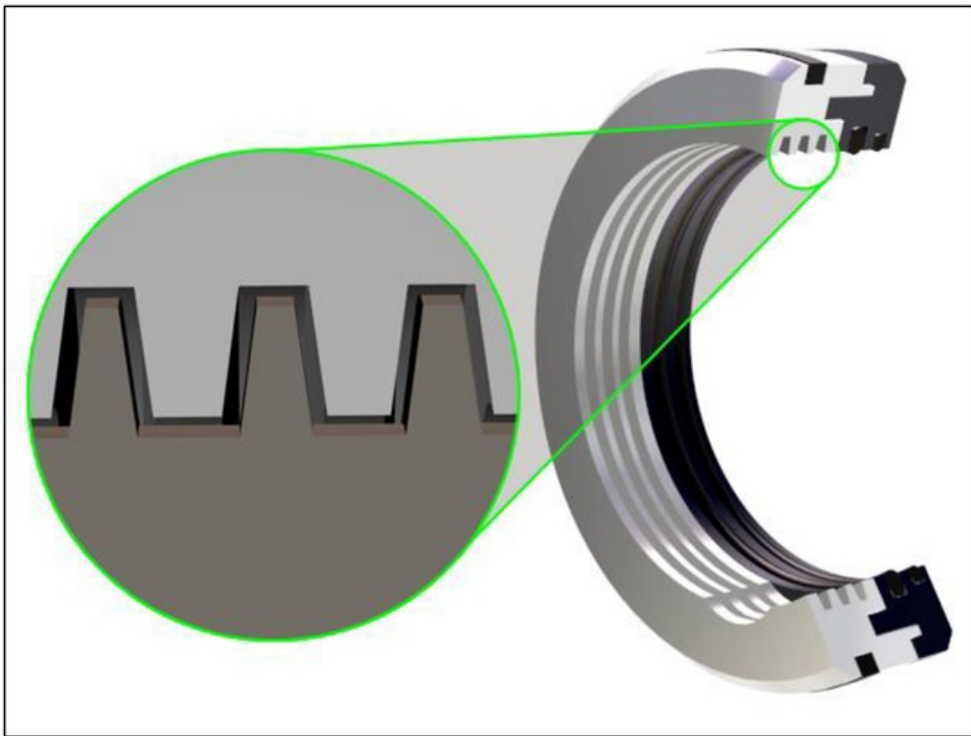


Figure 4: A labyrinth seal [7]

The expected life expectancy of these idler rollers is approximately ten years but due to the high load working of these rollers, some of the bearings fail after 2 or 3 years. There are many factors involved when investigating premature failure and collaborating as much informative data as possible on the subject will be hugely beneficial. Past research on the known types and causes of fatigue damage will be useful when analysing the various forces acting upon the rollers as well as the environmental effects. The data can be compiled to create a theoretical model of a roller bearing to demonstrate premature failure and how it can be avoided.

2.2 BEARINGS

2.2.1 General Information about Bearings

This section describes the components of a roller bearing, how they are assembled and how each part works with each other to form a functioning bearing. The inner and outer rings contain the rolling elements and the cage. The surface upon which the rolling elements roll on is known as a race. This is curved to keep the balls in place and on the same path. In this case the rolling elements are balls which are held in place by a cage. The cage keeps the balls in the same position relative to each other so that they do not roll around and bunch up together. This keeps the loading area uniform and allows the balls to rotate freely and smoothly. A lubricant is used inside the rings and cage to create frictionless surfaces to prevent heat and wear.

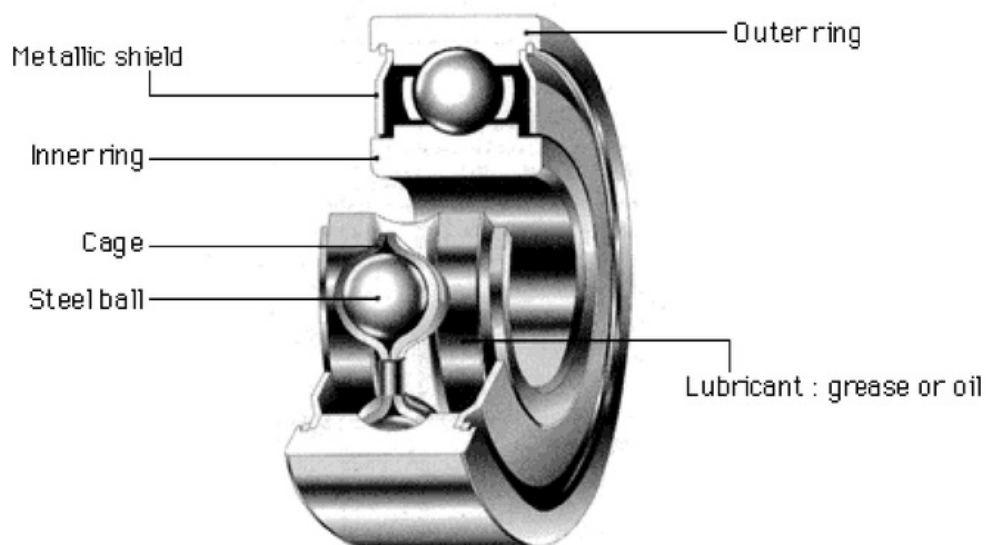


Figure 5: Single row deep groove ball bearing [8]

Bearings used in rollers are selected for their load rating, speed and are the key to a long lasting idler roller [2]. Bearings nowadays are precision machined, hardened, ground and polished elements designed to roll in similarly treated and lubricated races. The objective is to create as close as possible to zero friction or letting the balls slide. This allows for a longer life as the balls are not designed for radial or axial movement

The bearings used in the idler rollers in mine site belt conveyors are single row, deep groove ball bearings. Single row refers to the number of rows of rolling elements, in this case the one row. A deep groove means the race runs deeper into the bearing ring, preventing the rolling

element moving in the axial direction. Deep groove ball bearings are designed to support high radial loads and small amounts of axial loads in either direction simultaneously. They can run at high speeds and come in a variety of sizes with a variety of shields and seals [9]. These bearings give up to $0^{\circ} 10'$ angular deflection in operation, with even load distribution in the race [4].

2.2.2 Project Bearings

This report will study the bearings removed from the idler rollers attained from a mine site. After disassembly, the bearings were found to be a single row deep groove ball bearing, as expected. The exact model is an SKF Explorer Deep Groove, Single Row ball bearing, a 6306/C3-2Z SKF Explorer (dimensions specified in the appendix, figure 184). As explained earlier, '6306' refers to the dimensions, 'C3' the internal radial clearance (in this case greater than normal) '2Z' referring to the shield of pressed sheet steel on either side of the bearing, and 'Explorer' the series of deep groove single row ball bearings [10].

Principle dimensions are as follows:

Table 1: General specifications of SKF Explorer 6306/C3 - 2Z [11]

SKF Explorer 6306/C3-2Z	
Inside Diameter	30 mm
Outside Diameter	72 mm
Width	19 mm
Dynamic Load Rating	29.6 KN
Static Load Rating	16 KN
Reference Speed Rating	20,000 rpm
Limiting Speed Rating	13,000 rpm

They are made of a through hardening carbon chromium steel (100Cr6), with approximately 1% carbon and 1.5% chromium. The steel undergoes heat treatment to obtain a hardness between 58 and 65 HRC (a value on the Rockwell scale of hardness) [12].

The following table provides material properties of bearing steel 100Cr6.

Table 2: Material properties of bearing steel 100Cr6 [10]

Material Properties	Bearing Steel 100Cr6
Density [g/cm ³]	7.9
Hardness	700 HV10
Modulus of Elasticity [kN/mm ²]	210
Thermal Expansion	12
Coefficient of friction (ball/inside race) [N]	0.3
Coefficient of friction (ball/outside race) [N]	0.01

2.2.3 Bearing Sealing

Due to the nature of the loads and environment, ZZ shields using labyrinth seals are used. What this means is that a labyrinth seal exists on both the inside and outside of the bearing. However, in our case there is no seal on the inside of the bearing as all the sealing components are located on the outside in the bearing housing.


Type	Shields ZZ
Construction	
Material	Low carbon pressed steel
Speed Capability	High speed
Operating Temperature	-50 to +120° C
Grease Retention	Good
Dust Resistance	Good
Torque	Low

Figure 6: ZZ Shielded bearing [9]

2.2.4 Lubrication

Lubrication is vital to the efficient and prolonged operation of bearings. Essentially it provides a film over the surfaces where there is contact to reduce friction (main cause of heat and wear). There are many types, grades and forms of lubricant around but roller bearings typically use lithium based grease with high heat resistance. This will prevent the lubricant from breaking down when subjected to high heat [4].

Lubrication is also an important factor when studying the seal of a bearing as the bearings operate at high speeds, generating large amounts of friction and heat. Selecting the right lubricant and using the right amount will greatly prolong the life of the bearing.

2.3 BEARING DAMAGE ANALYSIS

Premature bearing failure can occur for multiple reasons and at any time depending on the factors involved. Failure results in loss of function of the bearing. This is often preceded by loss of efficiency from overheating or excessive internal movement of components other than rotating as per usual. Most of the time the result is the same, a seized bearing, whether this be due to overheating, or deformation. These are known as secondary failures which simply tell us the secondary damage cause. For example, an overheating bearing can be the result of numerous damages from lubrication breakdown to abrasive wear, one damage leading to the next.

Quite often a root problem will lead to other modes of damage making it difficult to pinpoint the root cause. This means that to find the root cause of bearing failure we need to understand all the damage types, what they look like and how each of them are caused. We can group various types of damage together as they are closely linked. The primary groupings would be wear, lubrication failure, excessive movement and loads, installation issues. Nearly of these issues lead to overheating and/or deformation.

2.3.1 Wear

2.3.1.1 Abrasive wear

One of the most common damage modes in ball bearings is due to foreign particles making their way into the bearing causing abrasive wear, bruising and grooving, circumferential lining or debris contamination [13]. Fine particles like coal dust (common in the mining environment) can contaminate the bearing through worn or defective seals. The can cause excessive damage over time to the races and balls. This type of damage will worsen as time goes on and can cause an increase in internal clearance allowing the movement of the ball bearing, therefore reducing fatigue life and misalignment of the bearing [13].

Hard particles rolling around inside the bearing may cause pitting and bruising of the rolling elements and races. The lubrication allows particles to travel within it and damage the surfaces through bruising, scratching, cutting or denting. This can include metal chips or hardened dirt which can become lodged inside the bearing and create grooves in the spinning elements. These types of damage affect the contact geometry of the bearing and reduce the life of the components. Raised points on the surface due to dents and bruises act as surface-stress risers and cause premature spalling and bearing life [13]. Abrasive wear leads to other forms of damage including spalling which is a form of wear.

2.3.1.2 Fatigue Spalling

Spalling is generally seen as usual fatigue wear as the ball continuously runs over the inner and outer race. As time goes on, small particles of metal flake away, amounting to a larger visible area of metal damage [14].

This is where the material simply flakes away and mainly occurs on the races and rolling elements. Spalling is an outcome of a primary damage cause. There are 3 main types of spalling according to Timken's Bearing Damage Analysis Guide which are Geometric Stress Concentration (GSC), Point Surface Origin (PSO) and Inclusion Origin Spalling (IOS) [13].

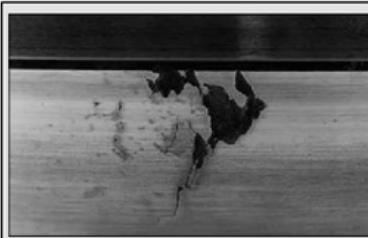
GSC is a result of bearing misalignment, deflection or edge loading that initiates points of high stress in regions of the bearing. This type of spalling occurs at the outer edge of the race. Another cause could be a machining error [13].



Fig. 22. Misalignment, deflections or heavy loading on this tapered roller bearing caused GSC spalling.

Figure 7: Example of GSC spalling [13]

PSO is caused by extremely high localized stress usually due to etching, foreign debris contamination which results in dents and bruises. This type of spalling is the most common where the shapes are often triangular, pointing in the direction of rotation [13].



Point Surface Origin (PSO) Spalling

This mode is the result of very high and localized stress (Fig. 23). The spalling damage is typically from nicks, dents, debris, etching and hard-particle contamination in the bearing. PSO spalling is the most common spalling damage, and it often appears as arrowhead shaped spalls, propagating in the direction of rotation.

Fig. 23. PSO spalling resulted from debris or raised metal exceeding the lubricant film thickness on this tapered roller bearing inner ring.

Figure 8: Example of PSO spalling [13]

ISO is a result of bearing material fatigue in localised areas after millions and millions of load cycles. The material properties of bearings have advanced over the years so this type of failure is much less common [13].

2.3.1.3 Corrosion/Etching

Another form of wear, corrosion or etching, takes place when the contaminants are oxidising particles which build up over time and use.

Corrosion, otherwise known as etching, is caused by water contaminating the internal surfaces of the bearings. It is most often caused by condensate collecting in the housing due to vast temperature ranges. Again, faulty or worn seals are the primary cause of moisture finding its way inside the bearing [13]. During servicing if the components are not washed and cleaned correctly then traces of water will be left inside the bearings, although in the case of a mine site it's not likely the bearings will be taken apart to that degree as they should be sealed for life. As the race or balls are worn away, the internal clearances increase, leading to increased vibrations followed by further wear and loss of preload.

Etching leaves uneven surfaces, resulting in unwanted movement of the internal components as well as increasing friction of the bearing. This leads to heat becoming a huge contributor to premature failure of bearings.

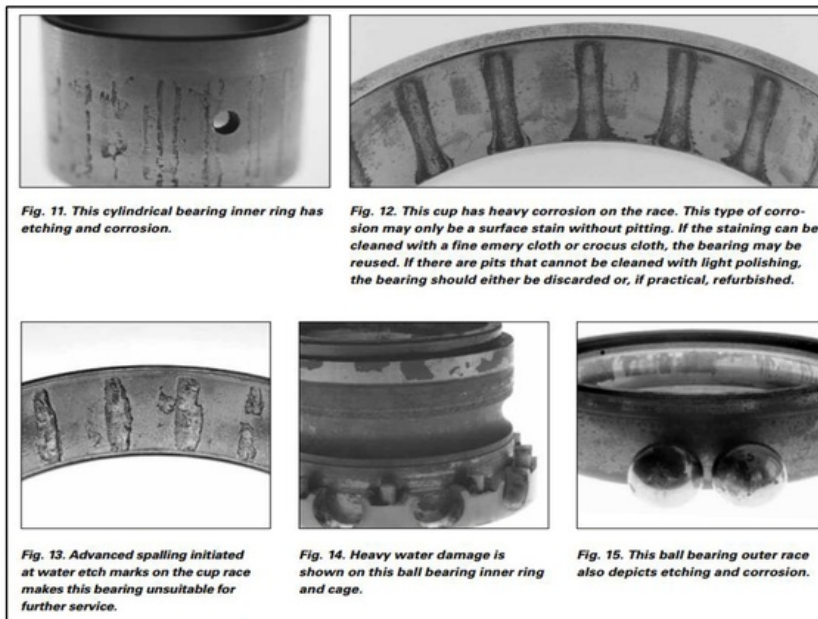


Figure 9: Etching and corrosion on the races of the bearing [13]

2.3.1.4 False Brinelling

Another form of wear is False Brinelling, which is quite different to brinelling (which is explained later in this paper). Damage analysis may point to brinelling but on closer inspection, false brinelling is fretting wear. Its cause is small axial movement of the rolling elements while the bearing is stationary and a groove is worn into the race by the sliding roller due to vibrations. False brinelling wears away the surface of the material while true brinelling simply deforms it [13].

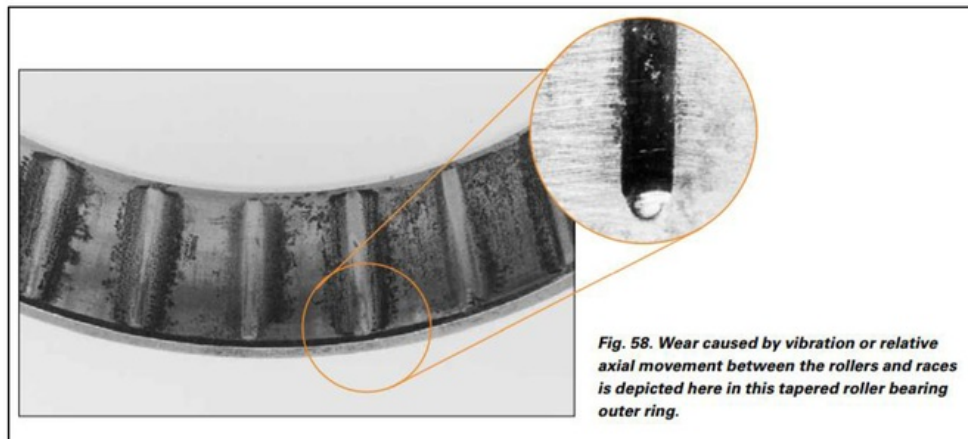


Figure 10: False Brinelling shown on the race

It can be detected by small bright marks on the race from where the rolling element has been rubbing off the surface finish. Without bearing movement the oil cannot access the contact point between the race and ball, permitting race wear to continue. This type of damage is disastrous when the wear debris oxidizes [14].

2.3.2 Overheating

Overheating can be a result of many issues. Symptoms include discolouration of the rolling elements, cage or race and result in changes in material properties. The high heat, often more than 120°C, can anneal the metal resulting in loss of hardness in the bearing. This leads to deformation of the elements and in turn, bearing seizure [14].

We can study the effects of overheating failure in stages, ranging from small forms of damage to catastrophic failure

2.3.2.1 Inadequate Lubrication

Another consequence of extremely high heat is the degradation or lack of lubricant, although the degradation could have been one reason for mass overheating [14].

Ball bearings depend heavily on a continuous presence of a very thin film of lubricant between the balls and the races. As discussed earlier, bearings create a 'frictionless' surface for an axial to rotate without generating heat. For the bearing to provide a frictionless environment lubrication is needed. Lubrication makes the surfaces extremely slippery so when the substance breaks down, is contaminated by foreign particles or increases its viscosity, damage begins to occur.

Lubrication is vital to maintaining the performance of the bearing. Inadequate lubrication can cause a wide variety of damage such as discolouration, scoring and peeling, excessive roller end heat and total bearing seizure. For these reasons its paramount the correct lubricant type, amount, grade and viscosity is used [13].

There are multiple reasons why a lubricant should break down which explained earlier. A brief reminder on the requirements of a lubricant.

1. Weight
2. Speed
3. Viscosity
4. Heat resistivity

2.3.2.2 Discolouration

Metal to metal contact creates high amounts of friction and therefore heat. This high heat affects the material properties in such a way the metal is stained or worse, discoloured. Although there is no damage at this point it is a clear sign there is lack of lubricant or that the current lubricant is incorrect [13].

This discolouration is a clear sign that either the lubricant is lacking or that it is the wrong grade for the application and can lead to scoring and peeling if not adhered to.

2.3.2.3 Scoring and Peeling

The next stage after discolouration is the scoring and peeling of the races and rolling elements. The metal is scored by heat and the metal begins to peel away. This can be due to:

- Lack of lubricant
- Incorrect lubricant
- Sudden changes in operating conditions such as temperature changes [13]

2.3.2.4 Excessive End Heat and Bearing Seizure

Excessive heat at the ends of the rollers is transferred from the bearings inside to the outer shell defined by the Principles of Heat Transfer. For the roller shell to be affected to this degree the heat generated inside the bearing would be massive. At this point scoring and peeling would have occurred and the structural properties of the bearing would be changing.

Essentially the bearing is heat treating itself, something it was not designed to do. During heat treatment, the material properties are altered. The metal becomes malleable and the tensile strength reduces. Now, loads that the bearing could normally withstand easily, being well within the elastic region, are now bordering on plastic deformation or have already entered the plastic region. Thus, the structure of the bearing changes and can no longer operate efficiently or at all. This is known as total bearing seizure and is irreversible and is pictured below

Inadequate lubrication results in localised high temperatures and scoring at the ends of the rollers where the bearings are located [13].



Fig. 20. Level 4 – Excessive heat generation caused advanced metal flow of the rollers, as well as cone rib deformation and cage expansion.



Fig. 21. Level 4 – Total bearing lockup is depicted here.

Figure 11: Total Bearing Seizure due to extreme material deformation [13]



Figure 12: Total bearing seizure due to external bodies

2.3.3 Loading and Movement

This refers to excessive movement of the bearing (meaning movement with respect to the shaft or shell) as well as internal movement such as the rolling elements in relation to the inner and outer rings and/or the cage. Both results in uneven load distribution and dramatically increase the likelihood of premature bearing failure.

2.3.3.1 Preload

Excessive preload can generate large amounts of heat and cause damage similar to that caused by inadequate lubrication. This is partly due to an incorrect choice of lubricant and it would seem the causes are the same. However, a lubricant may be correctly selected under normal operating conditions, but if subjected to a heavy preload then the film strength of the lubricant may not be able to withstand the high loads. The type of damage caused is the same [13].

Excessive preloading or overloading can still cause large amounts of damage even with the correct lubricant. This includes fatigue spalling on the roller bearing and the race as well as fractures and similar fatigue failures [13].

2.3.3.2 Excessive Loads

Excessive loading damage could be a result of tight fits between the internal components, extreme loads applied by the roller shell and material on top of the belt as well as excessive preloading. This is indicated by wearing on the race along the ball path as the ball appears to be heavy, continuously pressing into the race. The ball will become overloaded resulting in increasing temperature and torque, obviously resisting rotation. This can be avoided by lessening the load, redesigned bearings or a bearing with a higher load capacity [14].

High spots are formed at the outer edges of dents or gouges. They significantly increase vibration and can cause grooving in the rolling elements. High spots are a point of high stress resulting in increased fatigue of the metal [13].

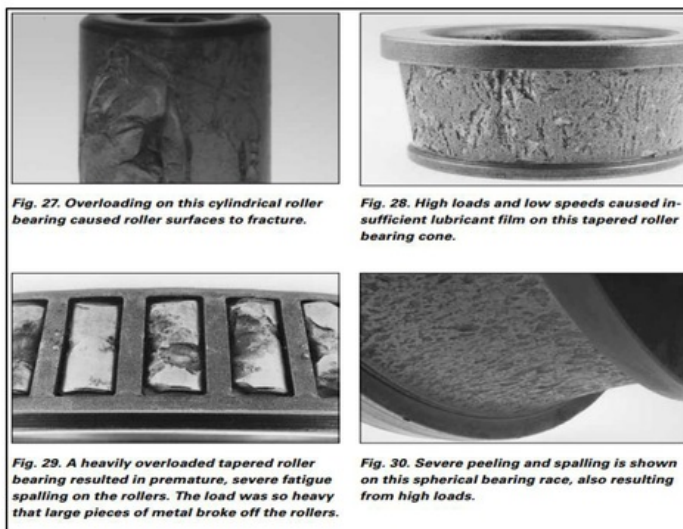


Figure 13: Example of excessive loading on the races and rolling elements [13]

The figure above displays large amounts of damage caused by the overloading of a bearing. The surface of the race is subjected to plastic deformation, becoming an uneven surface which the rolling elements roll across. Damage to this extent generates large amounts of friction and therefore heat. This heat then creates the damage as explained earlier in 'Overheating'.

This then allows for endplay, which is where the rolling elements can move in the radial direction before being applied a load.

2.3.3.3 Endplay

Endplay is the situation where the rolling elements are allowed small amounts of movement before being applied a load. Essentially, the rolling elements go through a very small load zone into a sudden high load zone. Initially, the internal clearances are incredibly small but whether through a manufacturing error, assembling error or over time due to fatigue, abrasive wear, corrosion or overloading. This looseness between the rollers, cage and/or race leads to roller skidding, greater axial movement and skewing. Endplay has the added effect of introducing vibration, which in turn amplifies the magnitude of loading, endplay and wear. Sudden changes in the magnitude, location and direction of the load severely impacts fatigue life of all the elements of the bearing [13].

Endplay can also be the result of brinelling and impact damage.

2.3.3.4 Brinelling and impact damage

Brinelling is caused by high impacts in the axial or radial direction, most likely during improper assembly of the bearing or during installation of the roller at the site. The roller could be dropped onto its end or have a large amount of material dropped on the end during operation. These short but high impact loads deform the metal of the race and possibly cause fractures on the rolling elements or on the race [13].

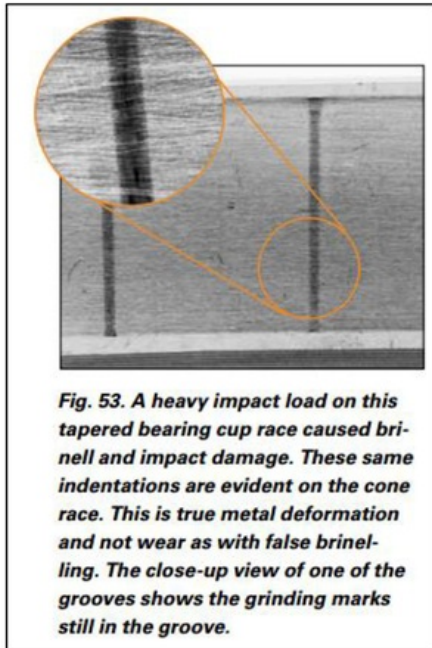


Figure 14: An example of brinelling [13]

As you can see the indentations in the metal are from impacts, not wear, as the wear on the race is consistent across the indentation. The loads exceed the elastic limit of the metal. As the rolling elements continue to pass over the indentations, vibrations increase and reduce fatigue life [14].

2.3.4 Installation

Quite often the root reason for premature failure is damage taken before the bearing is installed. Knocks, dents and deep gouges on the surfaces of the cage, rolling elements or the races during assembly act as a catalyst for fatigue. These weak points get worse and worse and greatly reduce the life of the bearing. These faults can be caused with improper tools, carelessness during handling or assembly. Initial faults like these lead to failure causes such as spalling and abrasive wear [13].

High spots, mentioned earlier, are formed at the outer edges of dents or gouges. They significantly increase vibration and can cause grooving in the rolling elements. High spots are a point of high stress resulting in increased fatigue of the metal.

2.3.5 Bearing Misalignment

The life of the bearing will depend on the degree of misalignment. The greater the misalignment the more uneven the load distribution will be on the rolling elements and the races. This results in only a portion of the rollers taking the full load, a higher load to surface area ratio, greatly reducing the life of the material. Bearings can become misaligned through inaccurate machining or assembly, deflection or distortion from high loads or impacts [13].

This problem is evident from examining the race, where the ball path will have worn into the race. If the path is not parallel with the edges, then the bearing is misaligned, which will result in a temperature increase, potentially spalling on the outer edges and heavy wear on the cage pockets [14].

2.4 WEAR MECHANISMS

Wear is generally a result of multiple wear mechanisms, so understanding each one is important when identifying causes of wear. Essentially, wear is the result of a harder material interacting with a softer material resulting in material removal, plastic deformation and other forms of damage explained earlier in 'Bearing Damage Analysis'. The type of contact between the two materials means different types of wear will occur and whether the contact causes elastic or plastic deformation also plays a role in the wear of the material.

The figure below can be used to follow the wear 'path'. The cause and effect of material interaction and wear modes can be followed.

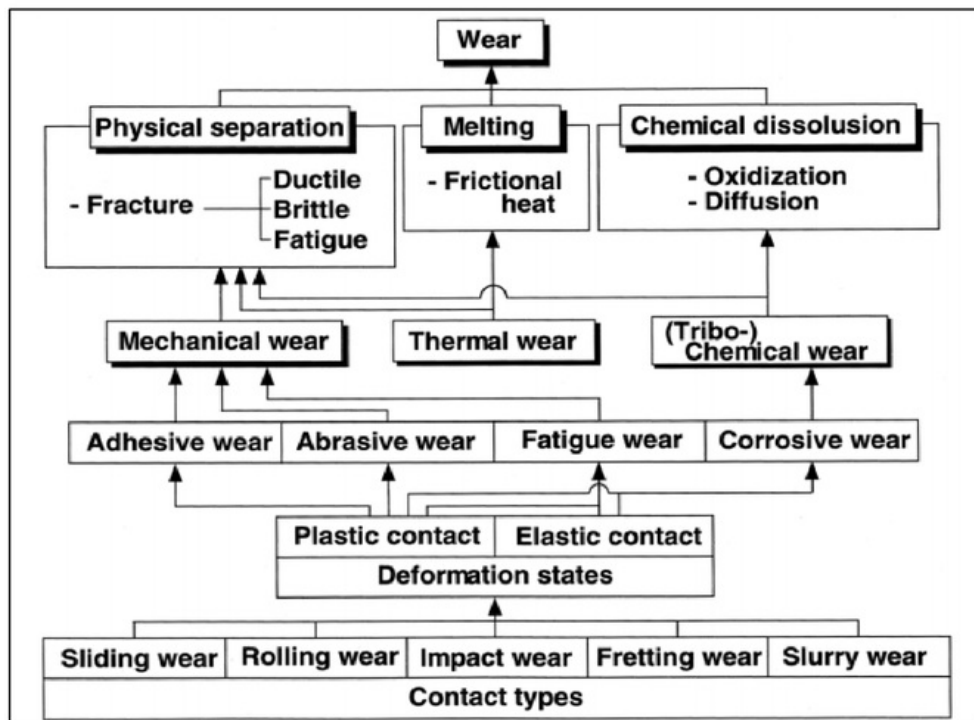


Figure 15: Wear mechanisms [15]

The main types of wear can be boiled down to adhesive wear, abrasive wear, fatigue wear and corrosive wear.

Abrasive wear is estimated to be the primary cause of premature bearing failure with many side effects leading to failure such as vibration increase, increase in operating temperatures which subsequently affect the lubrication used. There are two common types of abrasive wear, two-body and three-body abrasion.

2.4.1 Two body Abrasive Wear

Two body wear is the simplest form of abrasive wear in which hard particles are forced to move across a softer metal surface to form grooves. It is called two body as only two bodies are involved, the particle causing wear and the surface the particle moves across. This process leads to metal removal in the form of a chip or a ploughing, a plastic deformation. [16]

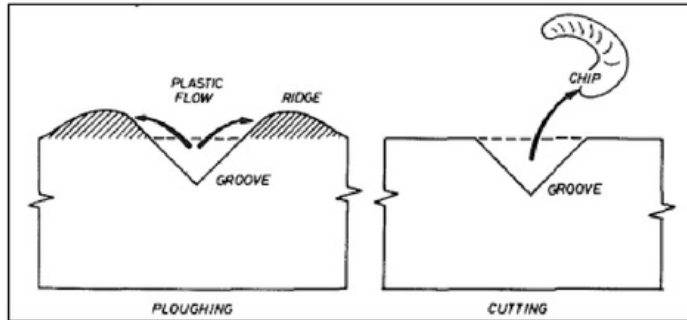


Figure 16: Two modes of abrasive wear [16]

Ploughing, rubbing or plastic grooving results in plastic deformation of the metal, with the metal continually displaced to the grooves' edges where ridges are formed. No metal is removed in this case. A second form of groove formation is cutting where chips of metal are cuts out of surface. Ploughing can also occur during this process although it is possible in extreme cases for the volume of the groove to match the volume of the chip. [16]

In the case of the ball bearing, three body abrasion is the primary focus due to the three bodies present, the race, particle and the rolling element. It is highly likely three body abrasion can then lead to two body abrasion.

2.4.2 Three Body Abrasive Wear

During three body abrasion, particles between two surfaces cause wear from one or both surfaces. This is significant in a bearing due to the high loads relative between the ball and the race, which particles can get stuck. The relative movement between the three bodies and scratch the surface and result in grooves, gouges after consistent abrasion.

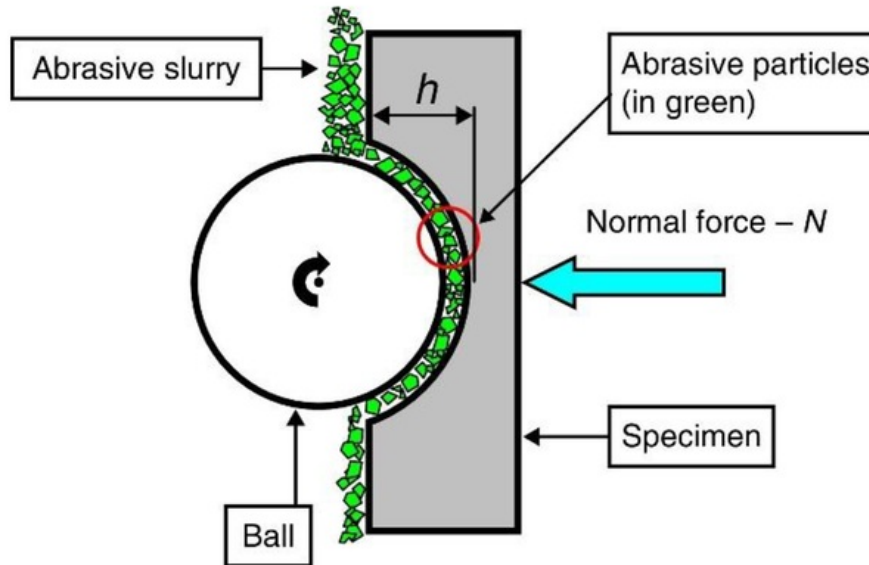


Figure 17: Three body abrasion of ball and raceway of a bearing [17]

The figure above exaggerates what happens during three body abrasion. As the ball rotates and a force is applied by the load, the abrasive particles (green) are ground against the race (specimen). The abrasive particles will chip, scratch or pit both surfaces and create even more abrasive particles, leaving uneven and worn surfaces. This process can lead to the added effect of two body abrasion, with the uneven surfaces wearing against each other.

As with two body abrasion, the softer surface will be pitted and the harder surface scratched. The third body, the particle, will either be plastically deformed or crushed into small fragments depending on the size, shape and brittleness of the particle.

2.4.3 Lubricant Related Abrasive Wear

Debris within the lubricant contributes greatly to abrasive wear. The particles can become lodged at the contacts between bodies and result in three body abrasion. When either or both the bodies are applied a force, the particle can scratch and gouge the surfaces, removing material and adding to the amount of lubricant debris.

As discussed earlier, it is common for lubricant to accumulate particles over time from the environment, such as dust and rocks as well as wear particles from the surfaces. Rolling elements function much more efficiently when surrounded by non-contaminated lubricant. A microscopically thin film between the contact points reduces friction massively. Many of the particles within the lubricant are much larger than this film thickness and so any interference can initiate fatigue initiation. [18]

Smaller particles are also an issue as when they become between the contact areas, different varieties of damage modes can occur. Repeated damage by these small particles is known as three body abrasion in which material is removed from the surfaces. [18]

A study into predicting the wear of ball bearings by lubricant debris [18], generated a model which considers the wear as the sum of the individual actions of each particle. A suitable ratio of lubrication to debris particles as well as particle size was determined with results comparable to the predictions made by the paper. [18]

The paper describes two kinds of particles, ductile particles which are deformed and rolled into platelets and brittle particles, which are crushed into fragments, depending on the hardness and toughness respectively. The main concern is wear caused by the brittle fragments which pass through the contact areas. Diamond abrasives are used in this papers experiment and while diamond particle abrasion is largely distant from practical contamination in the real world. The reasoning, small brittle diamond particles will cause abrasion on both the race and the ball, causing scratches, gouges and material removal. [18]

Due to the toughness of diamond and the high loads, the particles are pressed into the surfaces at a depth which correlates to the hardness of the materials and the magnitude of the force. It was found that increasing magnitude of the force had no effect on the depth of immersion of the particle, contrasting to two body abrasion where wear is increased with increasing load. As the balls have a higher hardness value than the races, more material is removed from the races than the rolling elements in the case of wear. It also means the harder surface, balls, are scratched as opposed to the softer surface being indented, the races [18].

3 EXPERIMENTAL PROCEDURES

The section details the experimental procedures involved with this research project. This will allow potential future researchers to replicate the experiments to either validate results or continue research. To investigate premature bearing failure in full the bearings must be fully removed from the idler roller and then dissected to inspect the internal components.

Firstly, a theoretical simulation will be run to validate whether the bearings can support the loads they were designed to take. It is expected that it will be a null result but by testing, the result will demonstrate whether the loads are too high.

This will lead into a practical examination of the damaged bearings where the modes of failure will be evident after removal, cleaning and dissecting of the bearings.

3.1 THEORETICAL WORK

The first step when performing a failure analysis in this case is to test whether the design of the system is sufficient for this application. This means that the selected bearings must meet all the requirements of the idler roller operation, including loading capabilities, design life, stress resistivity and so on.

These real-life situations that are normally time consuming, tedious and sometimes expensive to run can be easily replaced with computer simulations. Computer programs such as ANSYS Workbench offer FEA (Finite Element Analysis) software for just such tasks. FEA is a computerized method for predicting how a product reacts to real world forces, vibrations, heat, fluid flow and other physical effects [19].

In this case the model will be subjected to bearing load and external forces while in motion.

3.1.1 Model Development.

These parameters can be measured in computer simulations by making a 3D model and computer software. The program used to generate the 3D model of the bearing is Creo Parametric 2.0, a Computer Aided Design (CAD) modelling program used to create complex or simple geometries. The bearing dimensions and/or model was obtained from the SKF website as a CAD model download (shown below) [20]. By using the model direct from the manufacturer, we can be sure the results can be beneficial to our discussion.

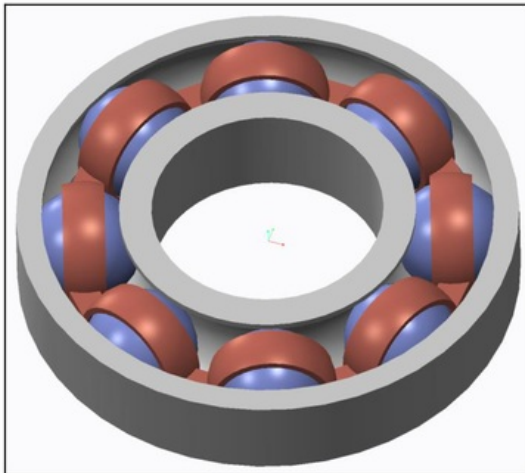


Figure 18: SKF 6306-2Z single row deep groove ball bearing model

The CAD model above is the one which will be ran through Finite Element Analysis (FEA). It was obtained direct from SKF with the dimensions specified in the appendix (figure 185).

3.1.2 FEA

The CAD model is exported from Creo Parametric 2.0 as a STP file, then into ANSYS Workbench 15.0 where the analysis is run. An STP file, known as a 'step' file is often used for CAD models as it can easily be imported into other CAD software or Analysis programs.

ANSYS Workbench is used for various types of simulations from fluid flows, thermodynamics to structural mechanics. The simulation relevant to the bearing is a Static Structural simulation where a structure is subject to various types of loadings and movements. It is vital that the program recognise the model is a bearing with moving parts. At this stage, we insert parameters to allow the program to identify features so it can find a solution. The required steps will be talked through here, allowing the simulation to be redone in the future for future work.

Selecting the Static Structural function brings up the menus for editing the Engineering Data Geometry, Model preparation, solution and results (as shown in figure. 19 below).

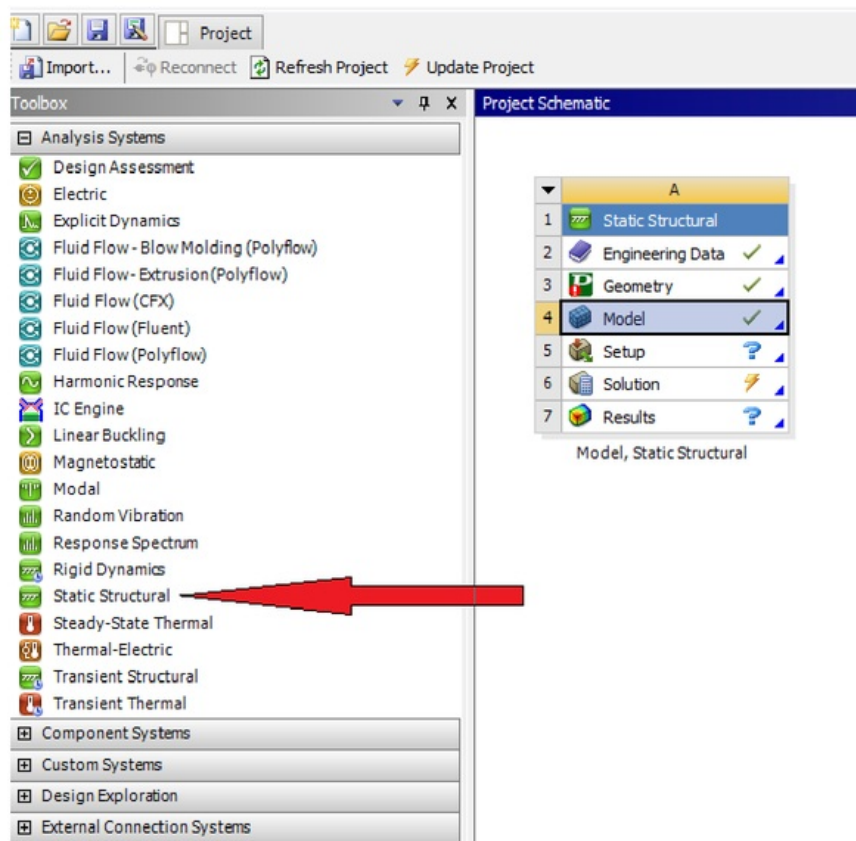


Figure 19: The main screen of ANSYS Workbench with the desired simulation highlighted

3.1.2.1 Engineering Data

In this section the necessary engineering data is prepared. The material is chosen along with options to edit the material properties are suggested.

As the bearings studied in this project are stainless steel bearings, stainless steel is selected as the material throughout the model with modifications as stated earlier under “Literature Review” -> “Bearings” -> “Project Bearings”.

3.1.2.2 Design Modeller

Double clicking on ‘Geometry’ opens Design Modeller and enables the CAD model to be imported into the simulation. To import the model, click on ‘File’, ‘Import external geometry file’, then choose the desired STP file and click ‘Generate’. From here, we can edit the parts of the case so the program knows which components are which.

3.1.2.3 Model Geometry

Exiting the Design Modeller, we proceed to open 'Model' (also by double clicking) where the simulation is run. In this part of the program the components are defined in terms of contact points, joints, loads, rotations as well as solutions such as deformation, stress and fatigue.

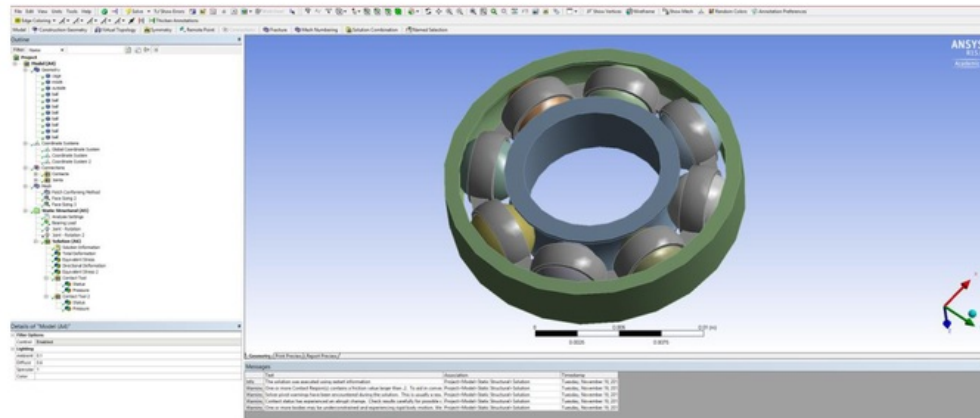


Figure 20: An overall look at the settings for preparing a simulation in FEA

Figure 14 displays the settings for this case. 'Geometry' lists all the components of the model, 'Coordinate Systems' are used for referencing rotation and movement to, 'Connections' is where contact points and joints are defined, 'Mesh' is where the mesh is generated and finally under 'Static Structural' the force and rotation parameters are defined along with the 'Solution' which contains the results of the case.

Under 'Model' there are options such as what material the component is made of and whether the component is flexible or rigid. As per the bearing used in the rollers (SKF 6306/2Z), the components are made to be flexible as to allow an attainable solution and the material of each component selected as stainless steel with some modifications shown in table 2.

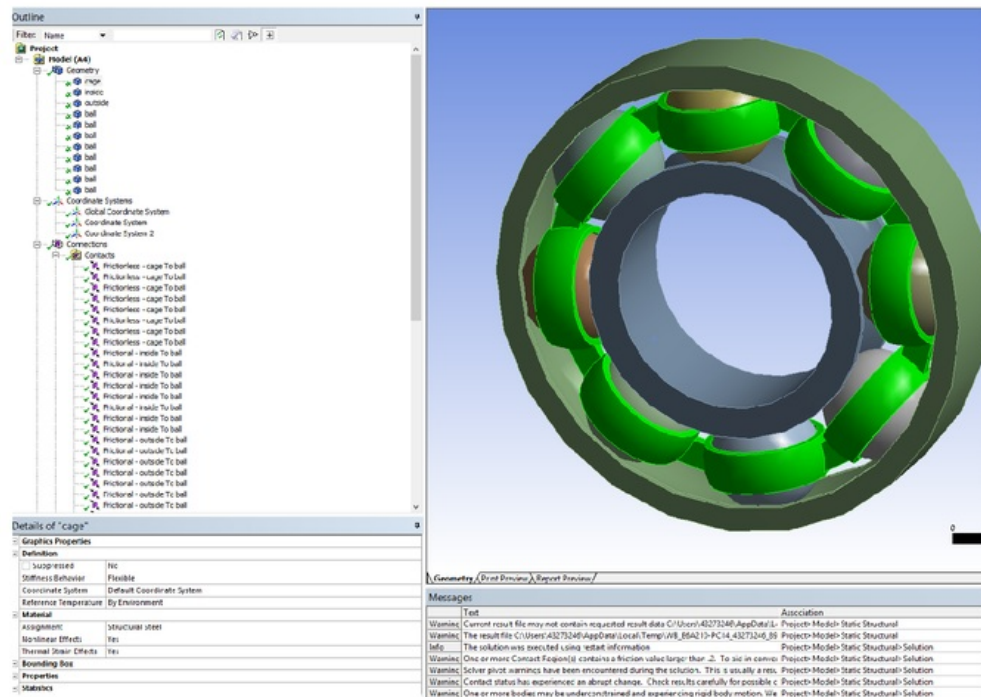


Figure 21: Cage (highlighted green) set to have flexible 'Stiffness Behaviour' and material Stainless Steel.

3.1.2.4 Coordinate Systems

Now, as the outer ring, the cage and subsequently the balls of the bearing will rotate, it is necessary to add in coordinate systems to reference these parts to. To keep things simple, the coordinate system was placed at the direct centre of the model. This one is used during the solution process when determining deformation and movement along the Cartesian planes, which is why its type was set to 'Cartesian'. Another coordinate system was added in, at the same coordinates, which will be used as part of the rotation aspect of the bearing. Making this type a 'Cylindrical' coordinate system enables the user to choose how the model will orient itself when subjected to a rotational parameter. In this case, due to the axis the bearing model was created on, the 'y' axis is the one which the bearing will rotate upon (and therefore the bearing will rotate around the 'z' axis). The two coordinate systems are displayed in the figures below.

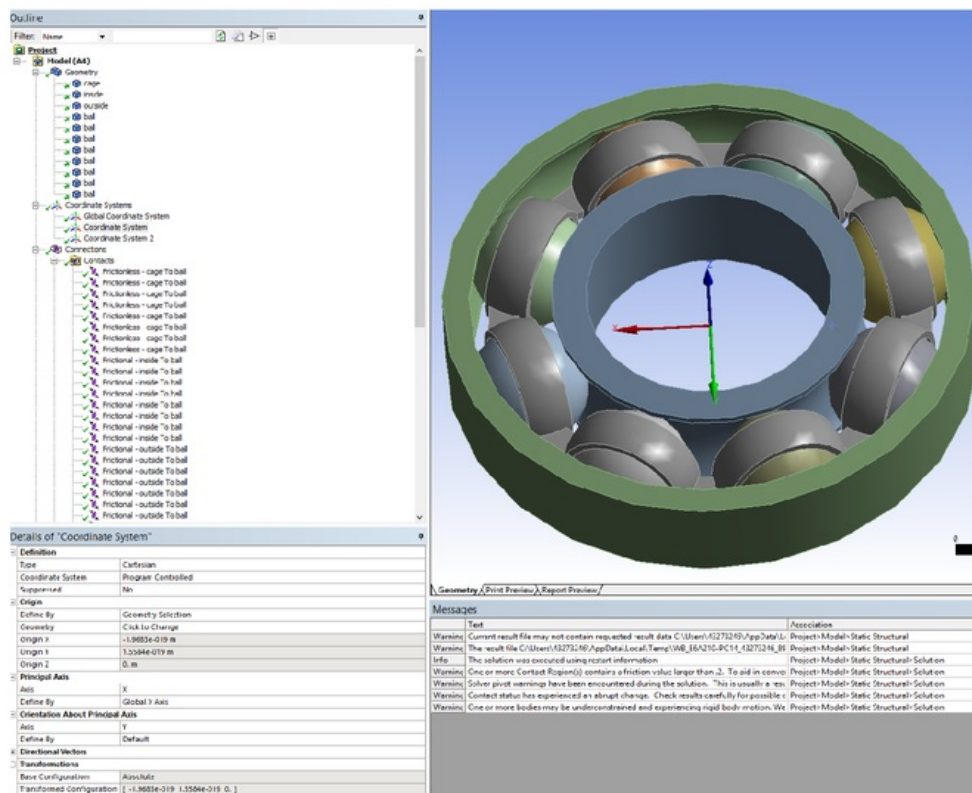


Figure 22: Cartesian coordinate system

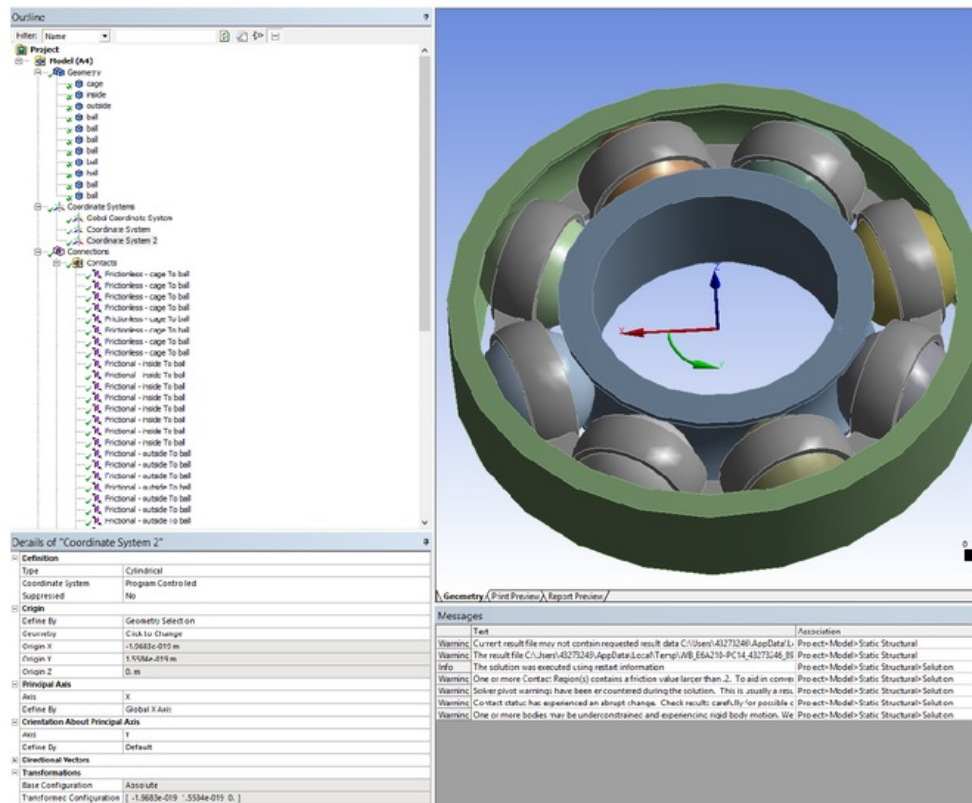


Figure 23: Cylindrical coordinate system

3.1.2.5 Frictional contacts

To run a lifelike simulation, frictional forces need to be taken into account during the setup process. As explained earlier, bearings attempt to eliminate friction between the shaft and rotating component using grease inside of the bearing. Without unnecessarily complicating the simulation, contact points are inserted along with friction coefficients.

Between the inside race and the ball, a frictional contact is made with a friction coefficient of 0.015 N. This value was taken from a table from the manufacturer of the bearings used in the experimental side of this project (SKF), found through their own analysis.

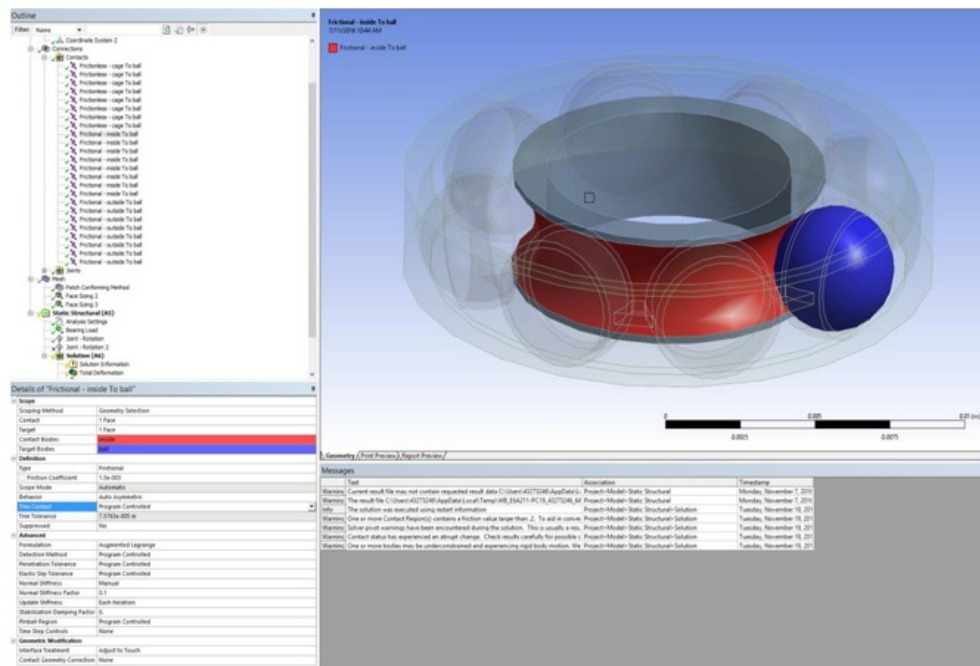


Figure 24: Frictional contact between the ball (blue) and the inside race (red)

The coefficient of friction of 0.0015 N for contact between outer race and the ball was observed under the conditions set by the manufacturer.

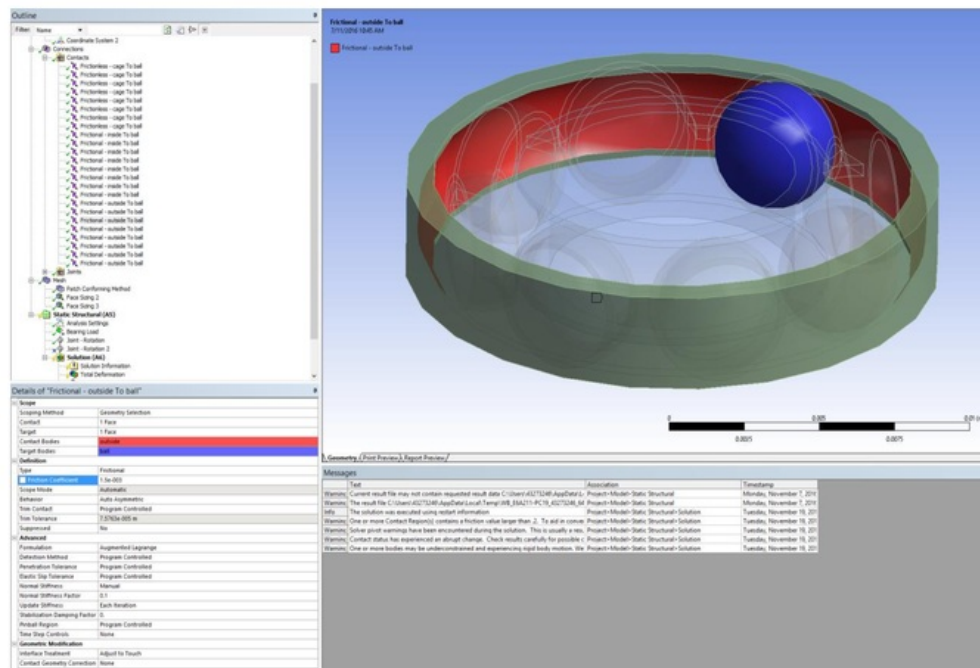


Figure 25: Frictional coefficient between the ball (blue) and the outside race (red)

Now, the cage is there to keep the balls in the correct formation and limit axial and radial movement. The contact between the balls and the inside ring of the cage should be a frictionless surface, as there is no relative loading between the two. Setting the contact to be frictionless causes the program to simulate zero friction, as shown below.

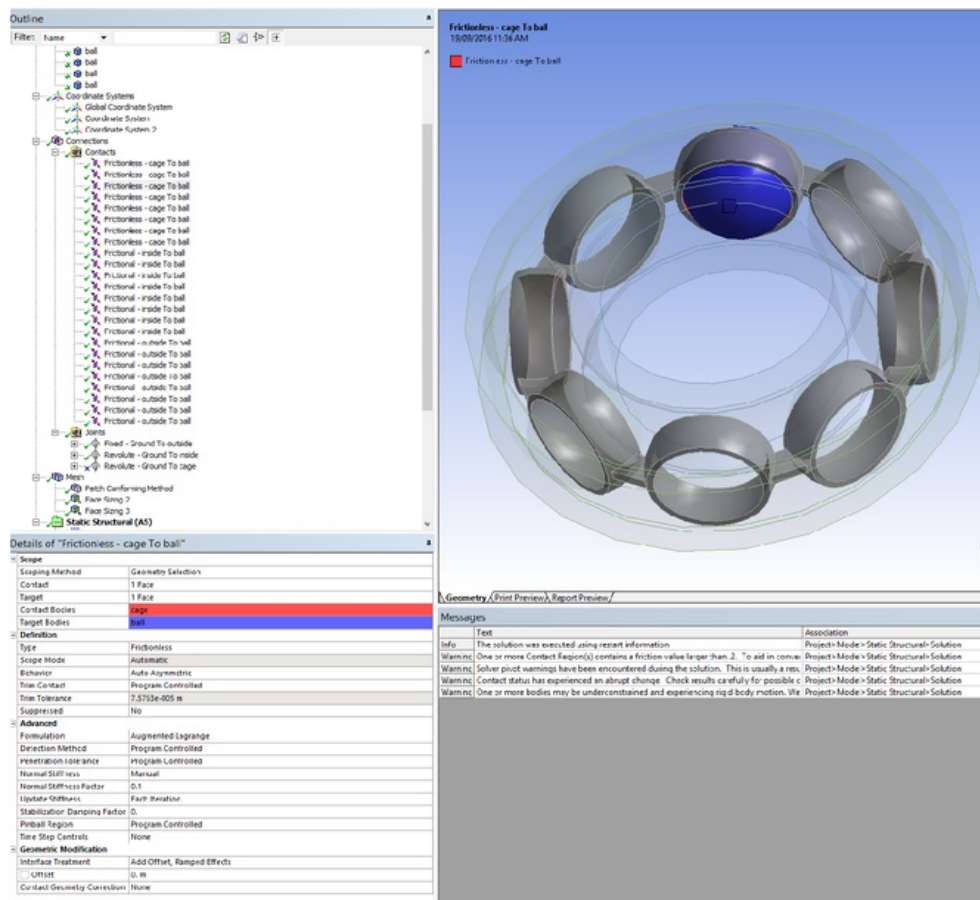


Figure 26: Frictionless contact between the ball (blue) and the inside ring of the cage (red)

3.1.2.6 Joints

To simulate rotation, 'Joints' must be added in for the inside ring, cage and outside ring, as all these components rotate in a bearing. The balls are designed to rotate on their axis and because they are reference to the cage, they do not need their own 'joints' parameter.

As the inside ring is fixed onto the shaft, which is held stationary on the belt conveyor, it is set as 'fixed' to the ground and the inner ring chosen as the body. This makes the component rigid.

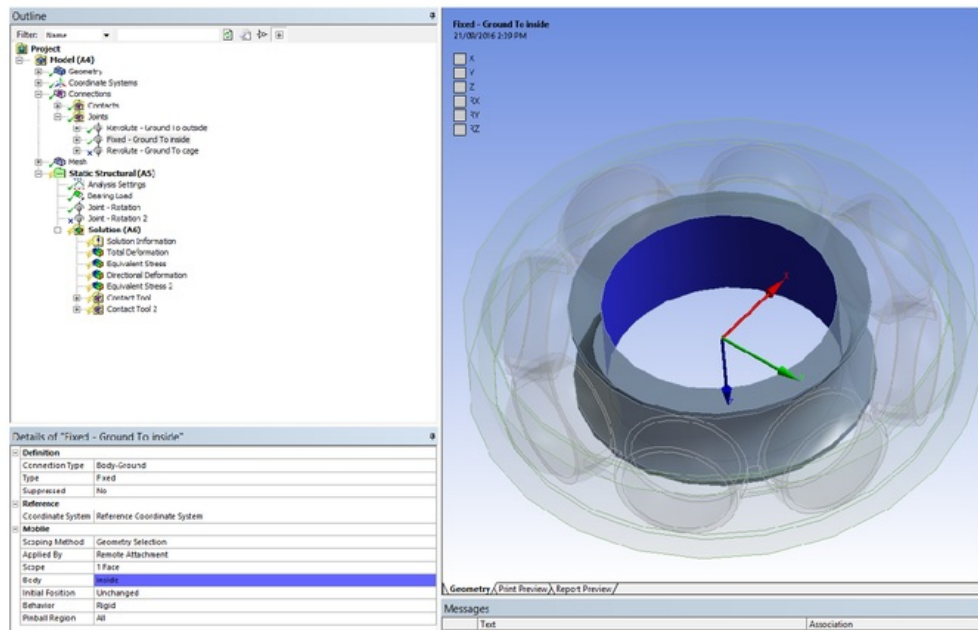


Figure 27: Fixed joint of the inner ring

In contrast to the fixed inner ring, the outer ring can rotate so a 'Revolute' function is set and the outer ring selected for the body.

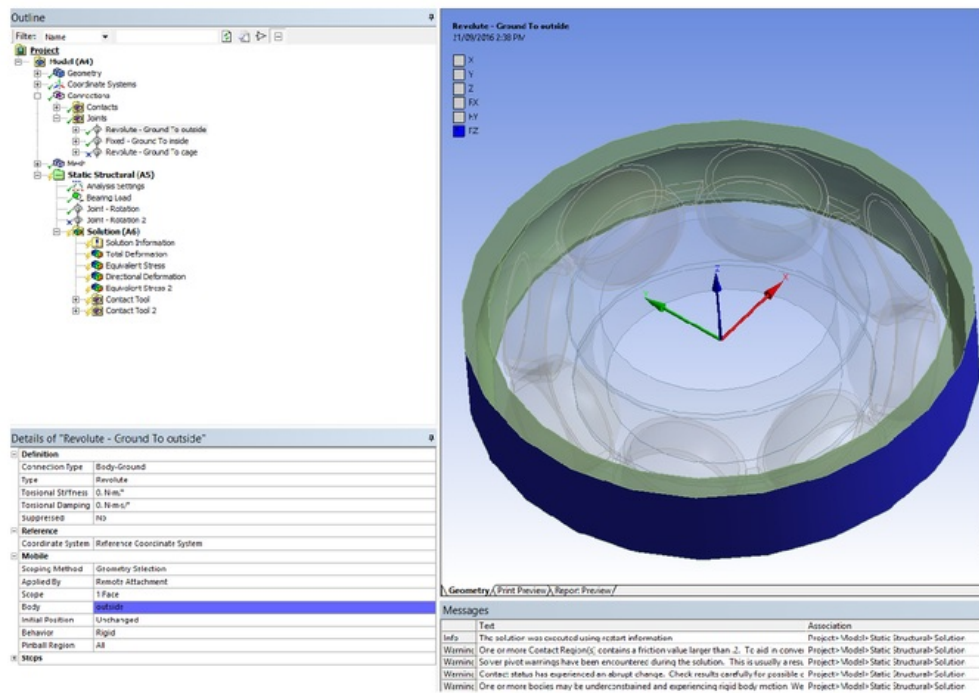


Figure 28: Revolute joint of outer ring

The cage is also set as a rotating component, 'Revolute' with the inside faces at the connecting points for each ring that holds a ball (the highlighted blue face)

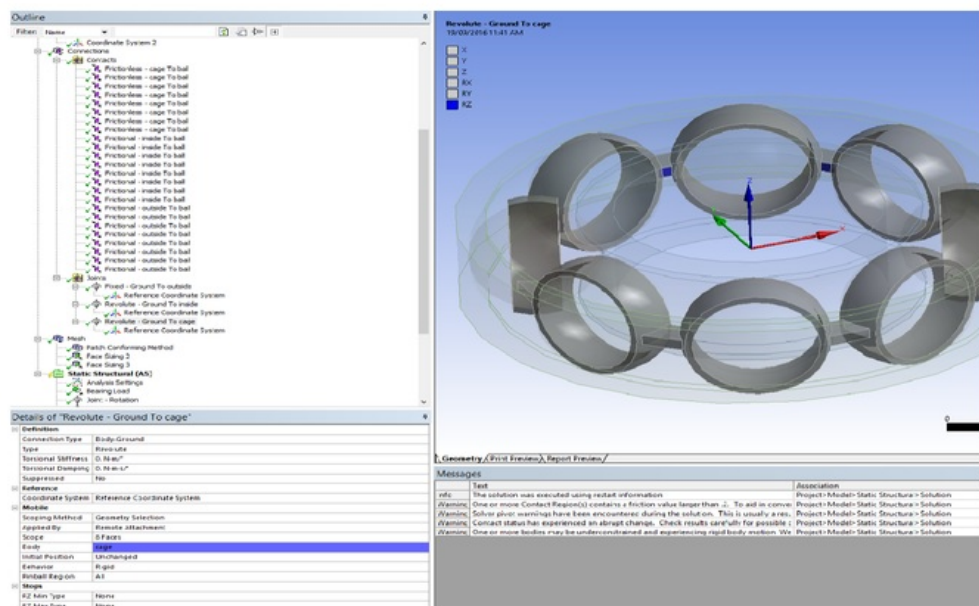


Figure 29: Revolute ground to cage

3.1.2.7 Mesh

The mesh is where all the calculations are done and how its set up will directly relate to the accuracy of the results. Essentially, the model is broken down into thousands of cells, or elements in which mathematical equations are solved. The results of each cell are then added up to produce a final result of the simulation [19].

Determining the faces of importance, the ones that interact with each other, is the next step. A 'Face Sizing' (shown below in figure 30) is inserted under the mesh to accommodate this with the inner race, outer race and each ball selected to be part of the reference 'Geometry'. An element size of 0.0005 m is chosen as a balance between accuracy and the time taken to solve the simulation. A soft behaviour allows the cells to vary in shape and size according to the surface of the model.

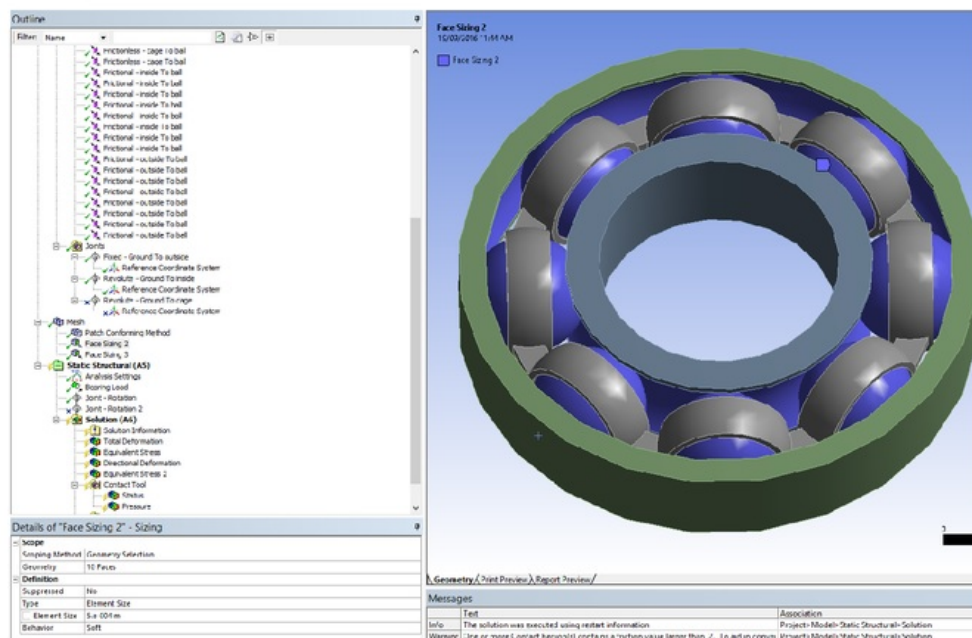


Figure 30: Face sizing of mesh (inner race, outer race balls)

Another 'Face Sizing' is inserted and the inner rings of the cage as well as the balls are selected as part of the 'Geometry' with an element size the same as before, 0.0005 m, refer to figure 30 below).

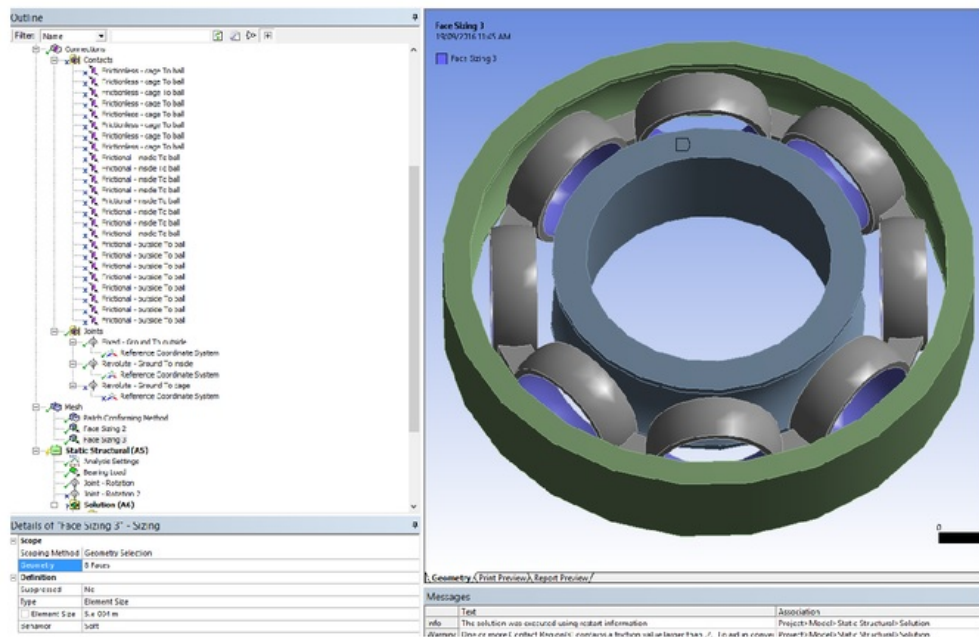


Figure 31: Face Sizing 3, cage and balls

Before generating a mesh over the model, the program must know how to form it. For a balance between accuracy of the results and the time taken to solve the simulation, a 'Patch Conforming Method' using Tetrahedrons is chosen. This means the mesh cells are triangular, allowing an accurate and consistent mesh throughout the model.

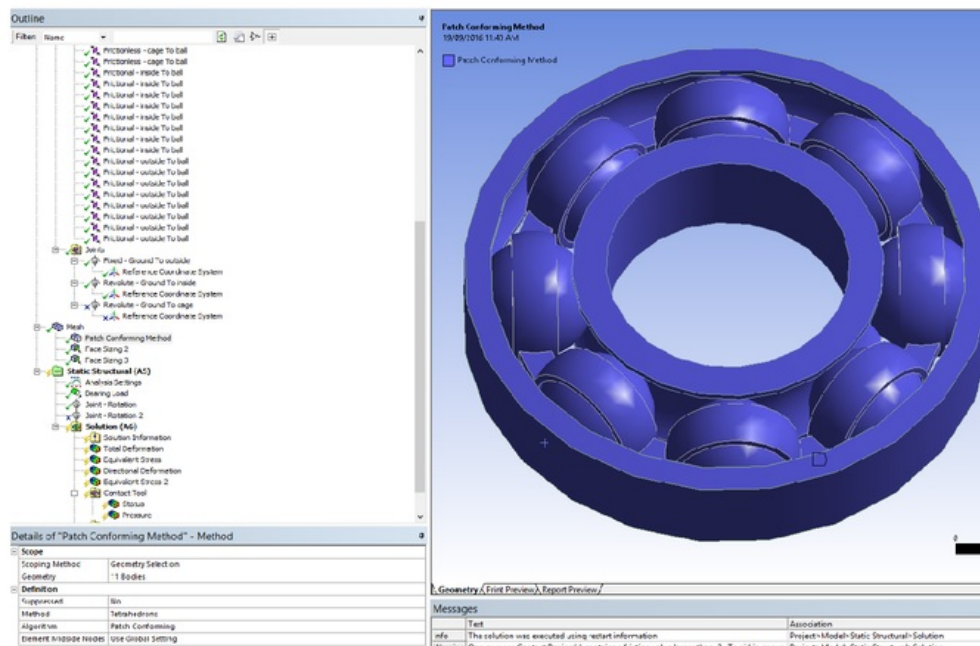


Figure 32: Patch Conforming Method of the mesh

Now the mesh is generated. In this case the maximum number of layers is 5, with a growth rate of 1.2, which means the cells adjacent to each other grow at a rate of 1.2 towards areas of less importance such as flat surfaces. For accuracy is it important for edges, curves and joints to have high concentration of cells.

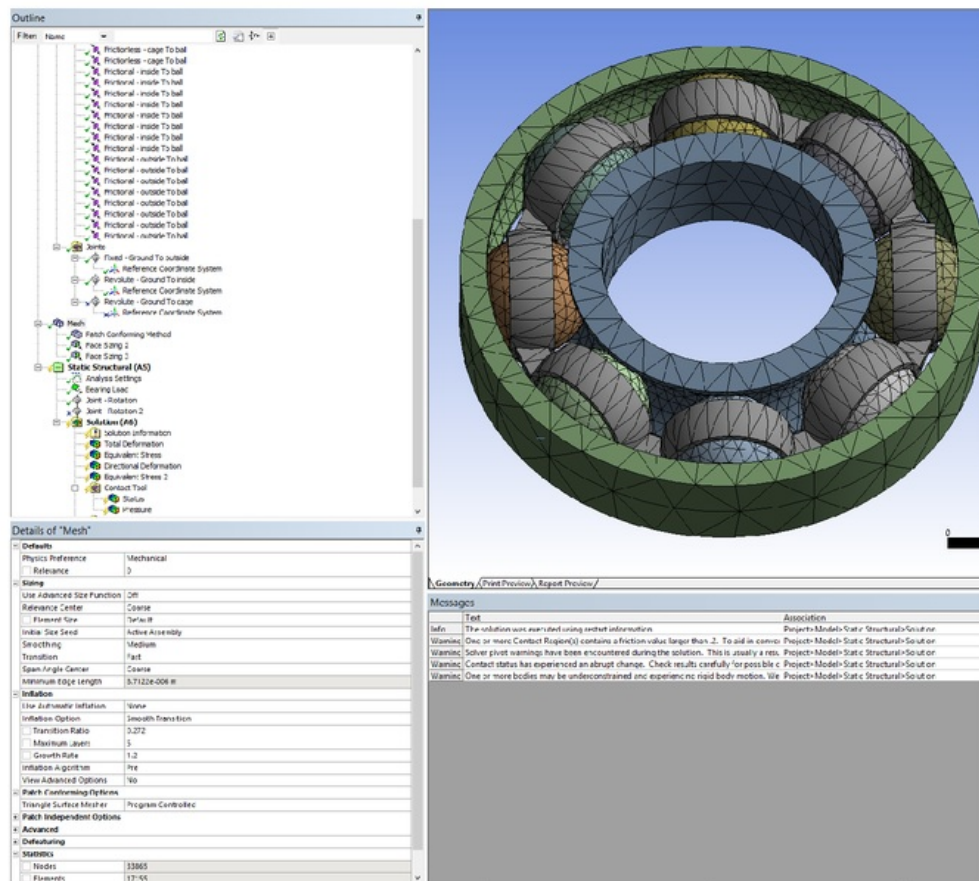


Figure 33: Mesh Details

3.1.2.8 Analysis Settings

In this section, the analysis settings will be setup to give the program loads, their direction and joint rotations. The number of steps is chosen, 5, with each step being 1-second-long and the minimum time step and maximum time step 0.01 seconds and 0.2 seconds respectively.

A 'Bearing Load' on the outer ring is inserted with increasing load in the 'x' axis direction.

Table 3: Bearing load values:

Steps	Time (seconds)	Force (N)
1	1	5000
2	2	10,000
3	3	15,000
4	4	20,000
5	5	29,600

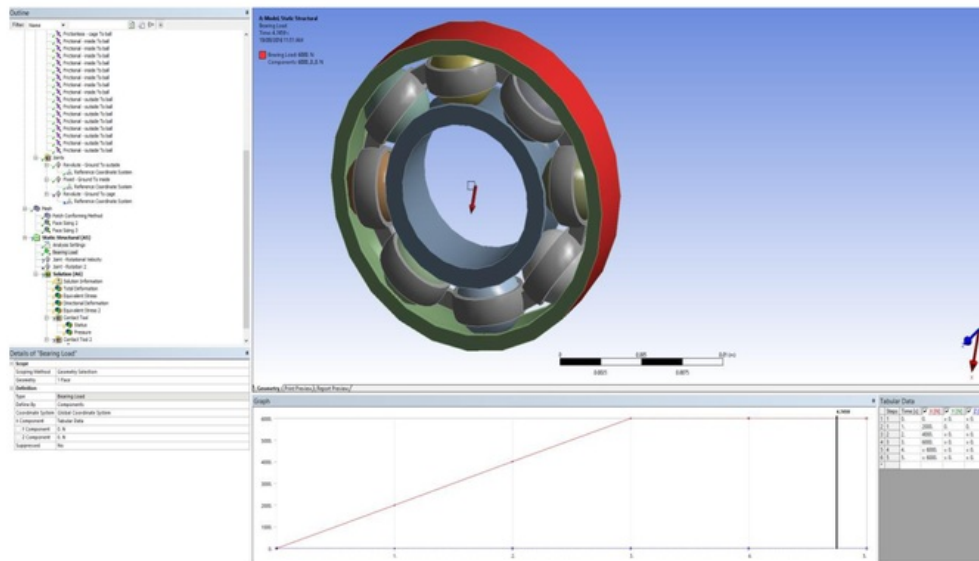


Figure 34: Bearing Load:

The joint 'Revolute – Ground to Outside' inserted earlier needs to be given either a rotational velocity or a value for degree of rotation. In this case the outer ring will be told how many degrees to rotate with each step as dictated in the table below.

Table 4: Degree of Rotation on outer ring

Steps	Time (seconds)	Rotation ($^{\circ}$)
1	1	20
2	2	50
3	3	90
4	4	140
5	5	200

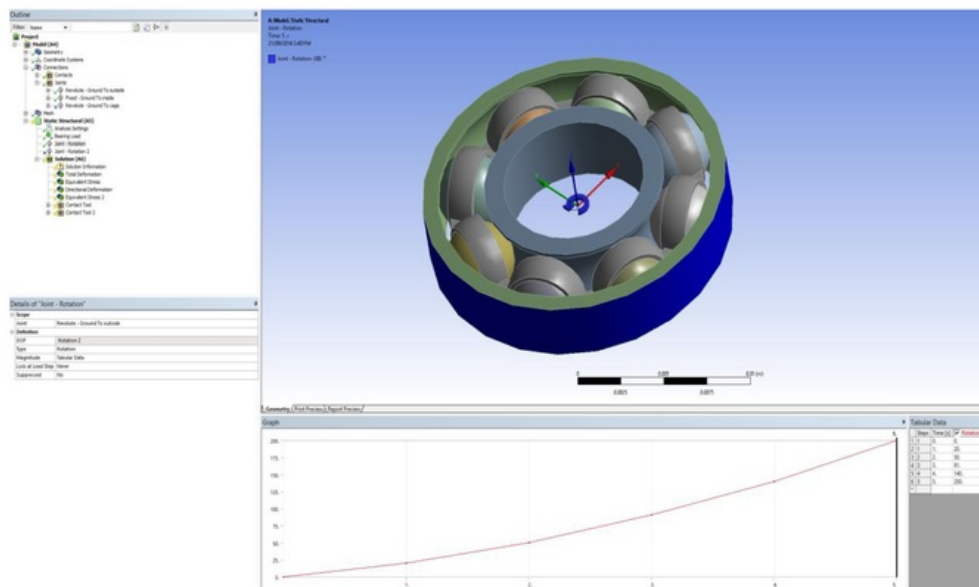


Figure 35: Joint Rotation of outside ring

3.1.2.9 Starting the Simulation

After preparing each aspect of the simulation it is time to run it. The program has all the required information to find a solution, presenting results in terms of 'Total Deformation', 'Equivalent Stress', 'Directional Deformation' and 'Thermal Strain'.

3.2 EXPERIMENTAL WORK

3.2.1 Removal of Bearings from Idler Rollers

The first stage is to remove the bearing assembly from the idler roller casing. This is so we can isolate the bearing from the rest of the components. The idler roller is not designed to be disassembled so machining and application of force is required.



Figure 36: Idler roller with aluminium shell before disassembly

As both bearings of the roller are needed we can throw away the centre section of the roller. At 150mm from one end of the casing a cut is made using an abrasive cutter. This cuts through the aluminium shell and the solid steel shaft. The same cut is made at the other end of the roller, leaving the two end cap sections containing the bearing, bearing housing, end cap and part of the shaft.



Figure 37: Cutting of idler roller in progress (150mm from end) in the abrasive cutter

A metal rod was inserted in the hole in the shaft to keep the shaft rigid as the blade cut through it.



Figure 38: The result of the first cutting process

The result of the cutting as shown above. A small section of shaft, rubber polymer end cap and part of the shell, containing the bearing.

The shaft has a small step in it just after the bearing housing which prevents the bearing sliding down the shaft. On the outside of the shaft before the bearing housing is a circlip which also prevents axial movement of the bearing housing. So the circlip can be seen, the rubber protector is pried off using a flat head screw driver. Now the circlip can be removed easily using a pair of pliers and a flat head screw driver.

As the bearing housing is press fitted onto the shaft using a large amount of force, the only way the housing can be removed is by applying force to the bearing housing so it slides off the end of the shaft. This is done using a hydraulic press, which presses the bearing out of the end cap section, breaking apart the polymer bearing housing in the process.



Figure 39: Hydraulic press in action, pressing the shaft through the bearing housing



Figure 40: Removed bearing housing from the shaft and bearing using a hydraulic press

In the end, we are left with the bearing, a broken polymer end cap, a shaft in multiple sections and a few small parts like the circlip and rubber seal. From here the damaged bearings will be easily accessible for cleaning and observing.



Figure 41: Small shaft section which the bearing and end cap are press fitted too



Figure 42: Two layers of press fitted sheet metal to prevent debris contamination to the bearing

These sheet metal layers are press fitted to the outside of the bearing to combat debris contamination. They also help eliminate friction as a secondary purpose. On top of these are rubber seals which seal off the components above as well as the bearing for the final layer of protection.



Figure 43: The bearing, isolated from all other components

This process is completed for each end of the roller to take out both bearings and for a total of six idler rollers.

During transportation around the work shop, one idler rollers polymer end cap disintegrated. This provided an opportunity to visualise the shaft and bearings with all the sealing components without the shell in the way.



Figure 44: The shaft, with bearings and seals



Figure 45: End of shaft with bearing, two sheets of metal, rubber seal (left to right)



Figure 46: Internal side of the bearing on the shaft

From the last picture, it can be seen there are no seals as on the inner side of the bearing. This may be due to the inability for any debris to reach the inside of the bearing, or a mechanism for heat to be released. It is obvious that the polymer has penetrated the bearing from the inside.



Figure 47: The aluminium shell from the shaft in figure 42

3.2.2 Bearing Preparation

Once the bearings are removed from their casing they must be prepared for photographing and further analysis. Each bearing is filled with grease (to a certain degree, depending on the state of the lubricant) to provide an efficient and frictionless environment in which the rolling elements can operate as designed.



Figure 48: Uncleaned bearing observations

While in this state the bearings are photographed to observe any problems within the lubricant such as foreign particles, breakdown and water contamination. To investigate further the grease from the bearings completely.

The method chosen to wash out the grease was to immerse the bearings in a small tub of petrol from the petrol station (unleaded 91). After leaving the bearings to soak for 10 minutes they were scrubbed with an old toothbrush to properly clean off the grease. This method proved efficient. Some larger chunks of grease, rubber were tricky to remove with a toothbrush so a small wire was used to poke out these larger parts.

After cleaning the bearings once over, the dirty, grease-petrol combination was disposed of and a clean tub of petrol set up. A second clean using a toothbrush would make sure all grease was drained out of the bearings (pictured below).



Figure 49: Scrubbing grease off bearings with a toothbrush



Figure 50: After the cleaning process

3.2.3 Cutting Bearings

For a detailed analysis to be taken it is necessary to study the races, balls and cage of the bearings from the inside. To do this, the bearings were cut in half along the axis shown below in figure.

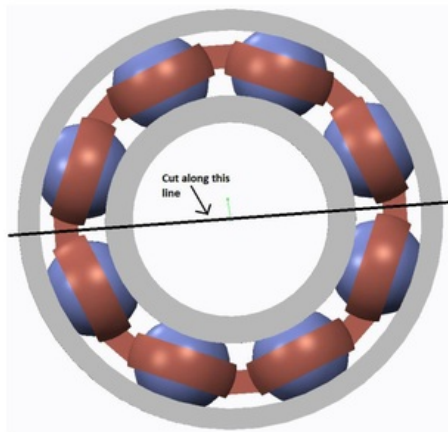


Figure 51: Diagram showing the line which bearings were cut

A cutting jig was made up (shown below in figure 52) to place the bearings in so that they were secure. This process was simple with each bearing part labelled and placed in their own separate bag to prevent mix ups of parts.

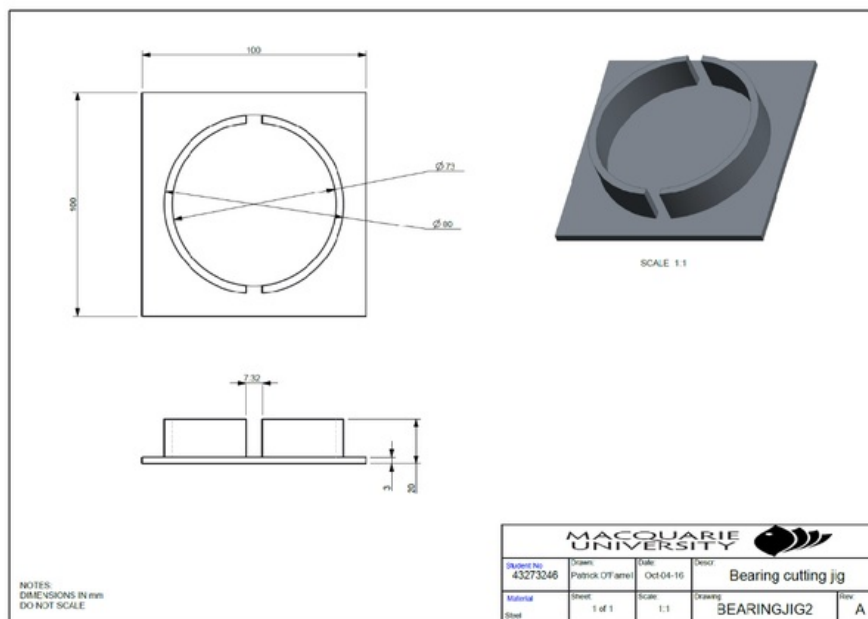


Figure 52: Jig used to cut bearings in half

During cutting of the bearings, small metal particles were left all over the components, therefore another clean in petrol (as per earlier in the cleaning section) was carried out to remove any small particles and dirt left over in previously inaccessible areas.

After progressing through these steps, the next stage is to analyse the balls, cage, inner race and outer race in detail, using an optical microscope. Various images at differing levels of magnification were taken so show detailed wear and anomalies.

3.2.4 Microscopic Images

Observing the races, balls and cage in detail requires a very high resolution, only possible with a microscope. An Olympus 3ZX18 Optical Microscope was used for this project shown in figure 53 below. A computer program allowed small scale focusing and magnification as well as for saving desired images.



Figure 53: Optical Microscope used for detailed images

3.2.5 Hardness Test

A hardness test of the bearing race was also undertaken of the outer race. To do this, a sample must be prepared.

Firstly, a small section of the outer race of a bearing was cut measuring 10 mm, using an abrasive cutting wheel as show below.

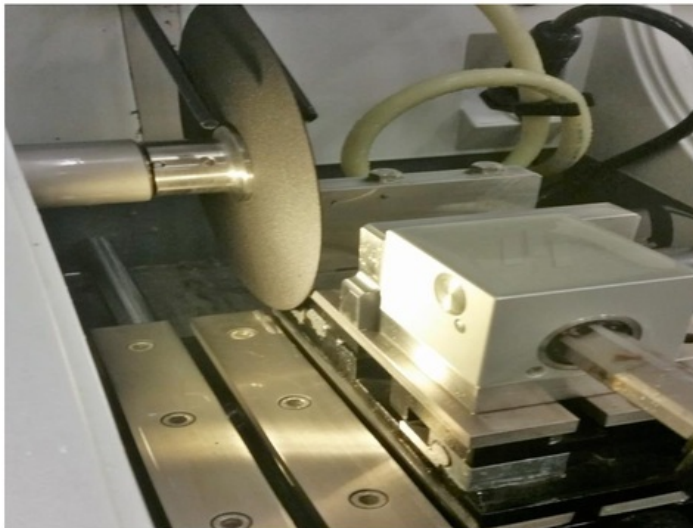


Figure 54: Struers Secotom-50 cutting tool

The cutting specifications for the process are displayed below.

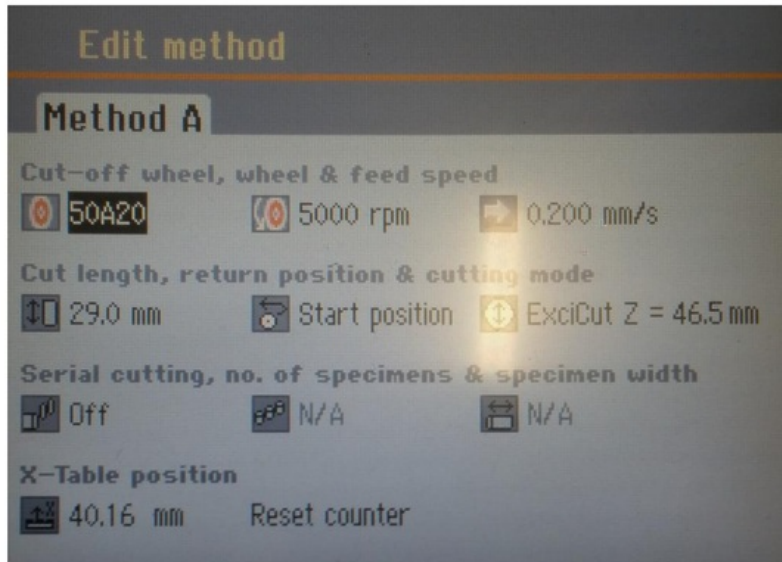


Figure 55: Abrasive cutting tool settings

The two small samples left over from this process need to be pressed into a mould so the hardness testing machine has a flat surface to indent.

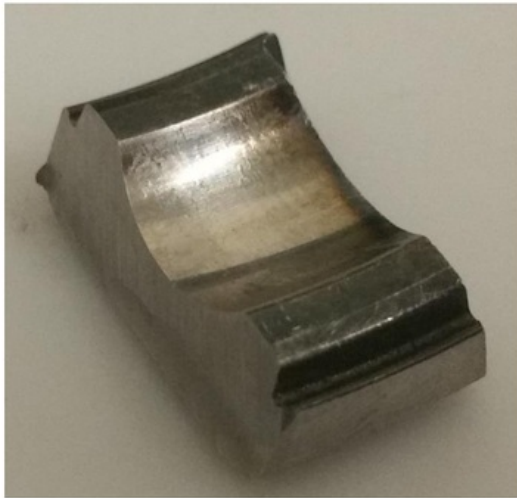


Figure 56: After first stage of cutting, this piece is cut in half horizontally

The sample needs to be polished for the hardness tester to have a smooth surface to indent so the results are more accurate. The polishing machine is used in two stages with the second pass providing a smoother finish on the sample.



Figure 57: Bearing pieces in the mould ready after being polished

The next step is to place the sample under the microscope in the hardness tester to determine the correct spot to indent. The program is run using Vickers hardness test which makes a diamond shape indent into the surface. The force applied is a HV5 which is a 5-kilogram force. The results are measured using the diagonals of the diamond, point to point as shown in figure 58 below.

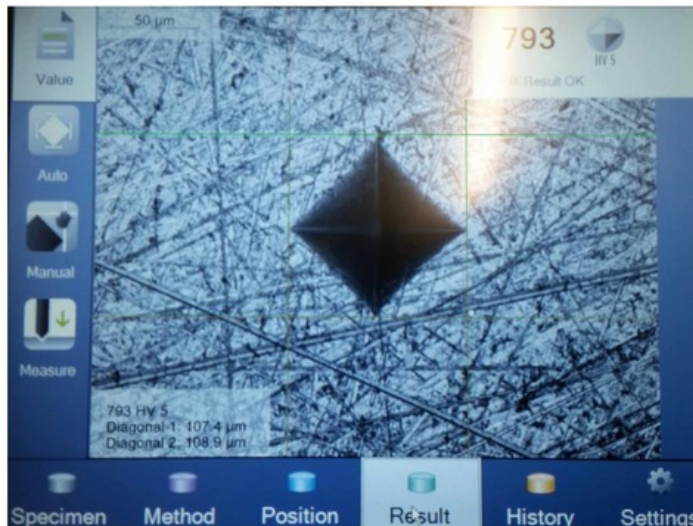


Figure 58: Hardness test result

4 RESULTS

4.1 FEA

In this section, the results from FEA simulations will be gathered with an analysis in the discussion.

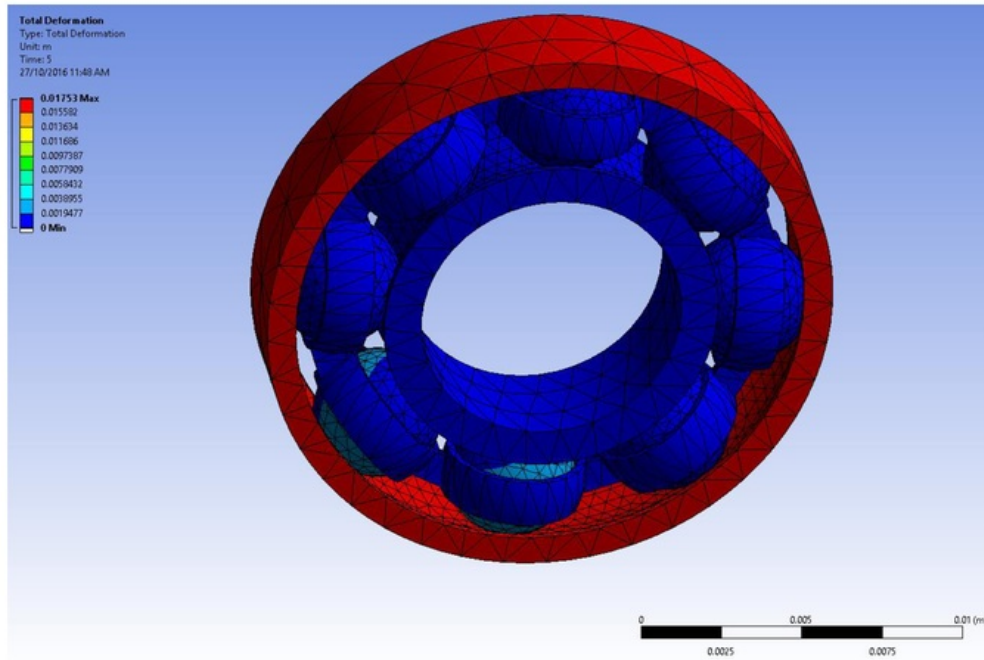


Figure 59: FEA Total Deformation of outer ring

Figure 59 above shows the total maximum deformation of the outer ring when subjected to bearing loads and rotation as stated in tables three and four respectively. The maximum load is 29,600 N and rotates to 200° over a period of five seconds. The maximum deformation of the outer ring is 0.0001753 meters.

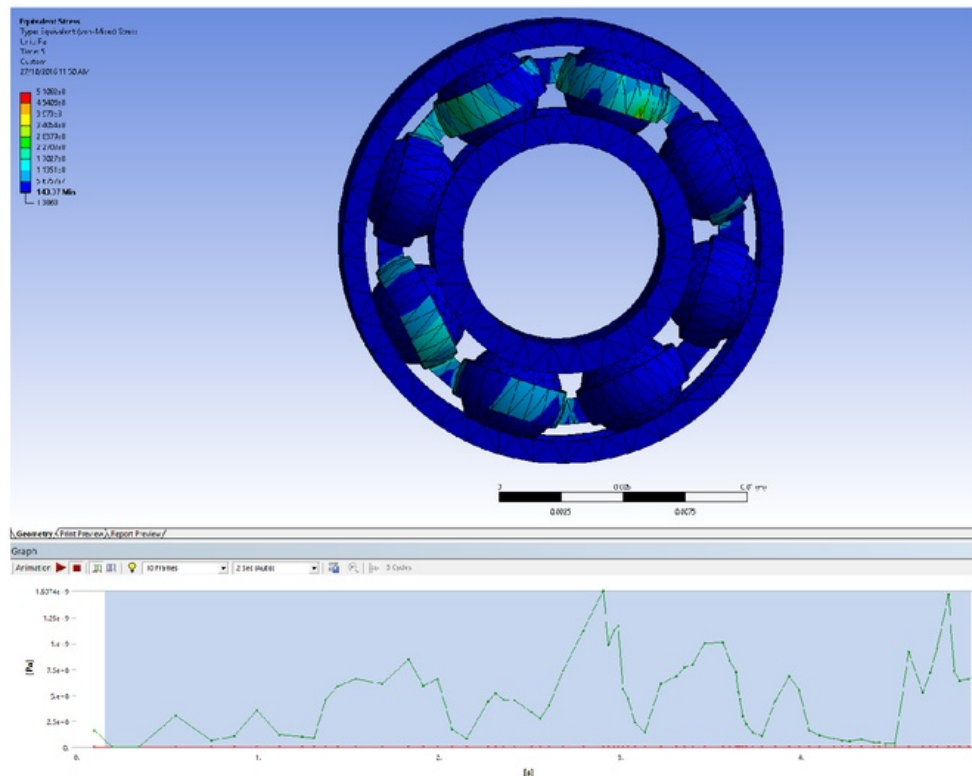


Figure 60: Equivalent stresses in a bearing

Equivalent stresses as shown above in figure 60 is a use of Von Mises stress which dictates when a material should fail due to high loads and stresses. It is measured in Pascals with the maximum stress reaching 510.82 MPa (mega Pascals) after approximately 2.9 seconds at the inner edge of the cage. The graph above depicts the increasing and decreasing levels of stress as the bearing load increases and the bearing rotates. This can be seen in figure 61 below with a high point of stress (highlighted red) on the inside edge of the cage next to the ball.

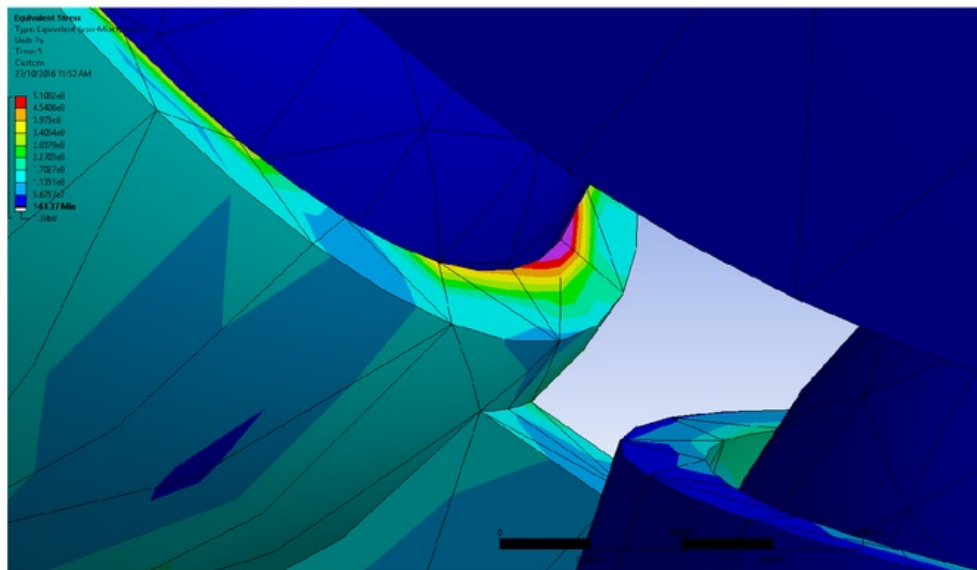


Figure 61: FEA Equivalent stress cage edge

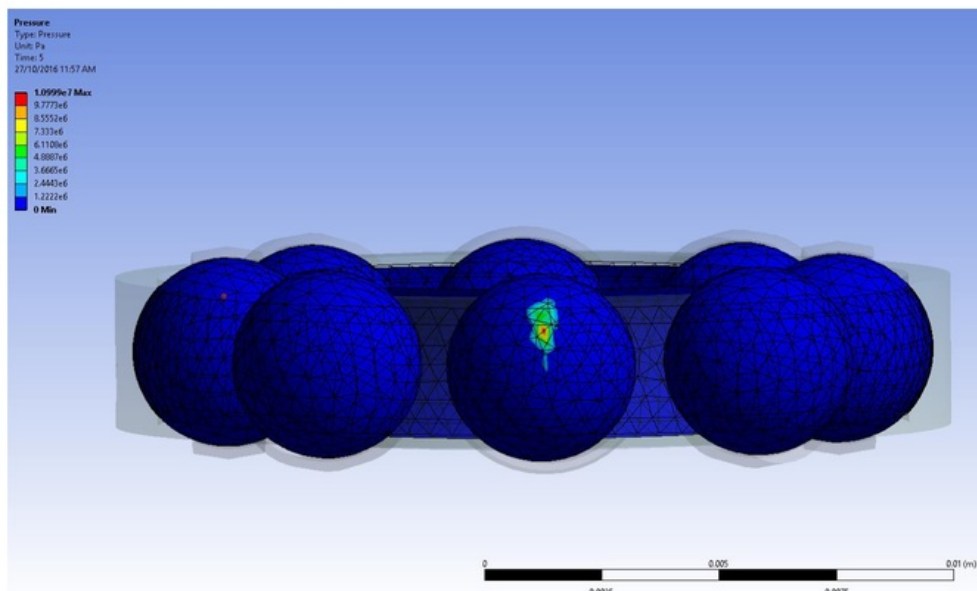


Figure 62: FEA pressure points on rolling elements

Figure 62 above also displays a reading in Pascals, in the form of pressure. The high point of pressure on the centre ball is applied by the bearing load and is transferred through the outer race to the ball. This is also after a period of five seconds and reaches a maximum value of 10.999 MPa.

4.2 EXPERIMENTAL RESULTS

In this section the results from each part of the practical experiment will be organised. This includes observations and pictures from just after the bearings were removed from their casing, from the post cleaning stage when the surfaces are visible to abnormalities and after the bearings were cut when the inside surfaces are clearly visible.

The images and results are in the following order:

1. Prior to cleaning (just after removal from idler roller)
2. A sample of lubrication grease from each bearing
3. Images of bearings after cleaning
4. Microscopic images of:
 - a. Surface Damage
 - b. Pitting/bruising
 - c. Fatigue Spalling
 - d. Chips
 - e. Surface Contamination
 - f. Heat Damage
 - g. Ball Damage
 - h. Cage Damage
5. Hardness Test

There are total of six idler rollers each with two bearings. For simplicity, each roller and subsequent bearing will be given a number. For example, a bearing from the first idler will be named "1.1", and the other "1.2". For the second roller, the bearings will be named "2.1" and "2.2", and so on for idler three to six.

4.2.1 Idler Roller 1

4.2.1.1 Bearing 1.1



Figure 63: Bearing 1.1



Figure 64: Bearing 1.1



Figure 65: Bearing 1.1 lubrication

This bearing rotated freely while lubrication was still sufficient with no apparent problems. There was minimal visible debris with the lubrication as depicted above in figure 65, with overflowing/leaking grease in a few areas. Although this could have occurred after disassembly. Spreading some of the grease out on a paper towel it was possible to detect some black particles (the polymer used for bearing housing) and a few silver particles believed to be from the balls or the races of the bearing inside.



Figure 66: Bearing 1.1 clean



Figure 67: Bearing 1.1 outside of outer ring

Observing a clean bearing 1.1, a 15 mm long wear patch on the outer edge of the outside ring can be seen. When rotated, there are audible noises which would appear to be the balls moving across indentations or gouges in the race or from surface imperfections on the race. Apart from this there is minimal damage visible to the naked eye other than a few scratches and discolouration's on the faces.

4.2.1.2 Bearing 1.2



Figure 68: Bearing 1.2



Figure 69: Bearing 1.2 lubrication

As with bearing 1.1, we can see the same black debris as well as more of the silver particles from the bearing housing and balls/races respectively. This bearing also rotates freely and smoothly.



Figure 70: Bear 1.2 clean

Like bearing 1.1, bearing 1.2 also has a noisy rotation, thought to be caused by the same factors, surface imperfections and interferences. Other than this, no other damage is observed in this state.

4.2.2 Idler Roller 2

4.2.2.1 Bearing 2.1



Figure 71: Bearing 2.1



Figure 72: Bearing 2.1



Figure 73: Bearing 2.1 lubrication

Bearing 2.1's grease is a slightly lighter colour, with a few dark areas, than the previous two bearings although it rotated smoothly and freely, with no obvious resistance. The lubrication also contains many small and large polymer particles, as well as a few small silver metal flakes.



Figure 74: Bearing 2.1 clean



Figure 75: Bearing 2.1 outer ring face

Like the previous two bearings, this bearing has the same symptoms judging from the noise level and feel when the bearing is rotated. The only other imperfections visible are on the outer surface of the outer race, small to medium specs of dirt which are stuck to the surface.

4.2.2.2 Bearing 2.2



Figure 76: Bearing 2.2



Figure 77: Bearing 2.2 lubrication

The lubricant in this bearing was a dark brown with small black polymer particles common throughout the grease along with minor amount of silver metal particles including a large flake of metal. The bearing still rotated freely and smoothly.



Figure 78: Bearing 2.2 clean



Figure 79: Bearing 2.2 outer ring face

Similarly, to bearing 2.1, bearing 2.2 has no visible damage apart from a series of lines on the outer face (shown above in figure 79) varying in size from 5 mm to 10 mm long with the same width, 1 mm. These lines cover roughly 50% of the circumference. At a few points during spinning there was a large resistance to rotation, clearly proving there are interferences in the race of balls.

4.2.3 Idler Roller 3

4.2.3.1 Bearing 3.1

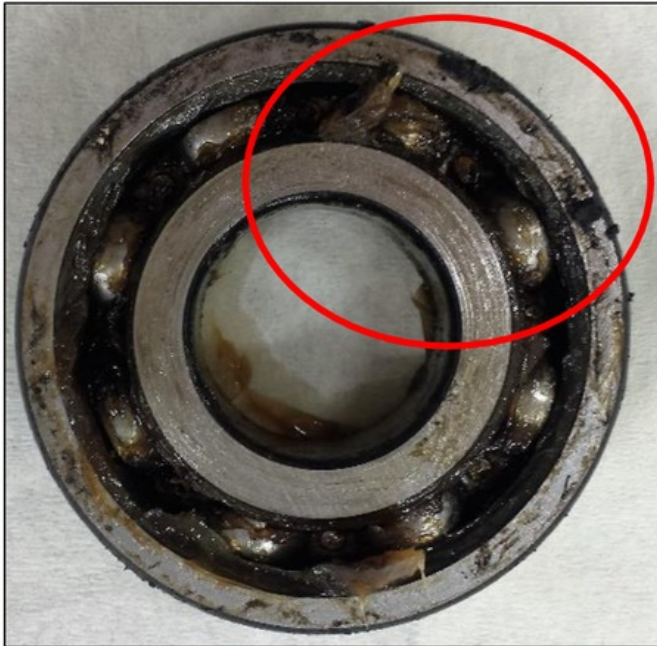


Figure 80: Bearing 3.1



Figure 81: Bearing 3.1



Figure 82: Bearing 3.1 lubrication

Bearing 3.1 required a little more force to rotate it but the action was smooth. There was a lack of lubricant in this bearing with multiple large black polymer particles inside and stuck to the various surfaces. There were two large silver metal flakes on the outer ring of the bearing as shown in figure 81 along with the same small black polymer particles throughout the grease.



Figure 83: Bearing 3.1 clean

Bearing 3.1 also has no visible forms of damage which would suggest failure, although it was extremely slow and labour some to rotate. Unlike the previous 4 bearings, this one was quiet when rotated.

4.2.3.2 Bearing 3.2



Figure 84: Bearing 3.2



Figure 85: Bearing 3.2 lubrication

Bearing 3.2 also had a lack of lubricant as with 3.1 and had multiple large black polymer particles common throughout the grease. The lubricant had leaked out to the edges bringing with it small metal flakes and small black particles. The bearing rotates freely but grinding/crunching was audible at various points around the bearing.



Figure 86: Bearing 3.2 clean



Figure 87: Bearing 3.2, inner edge of outer ring



Figure 88: Bearing 3.2 outer ring face

As with bearing 3.1, bearing 3.2 also has a large resistance to rotation, expected as they are both from the same idler roller, with relatively quiet noises coming from inside the bearing due to imperfections. Figure 87 above shows a small (1 mm) chip on the inner edge of the outer ring. In Figure 88 small scuffs can be observed on the outer edge of the outer ring.

4.2.4 Idler Roller 4

4.2.4.1 Bearing 4.1



Figure 89: Bearing 4.1

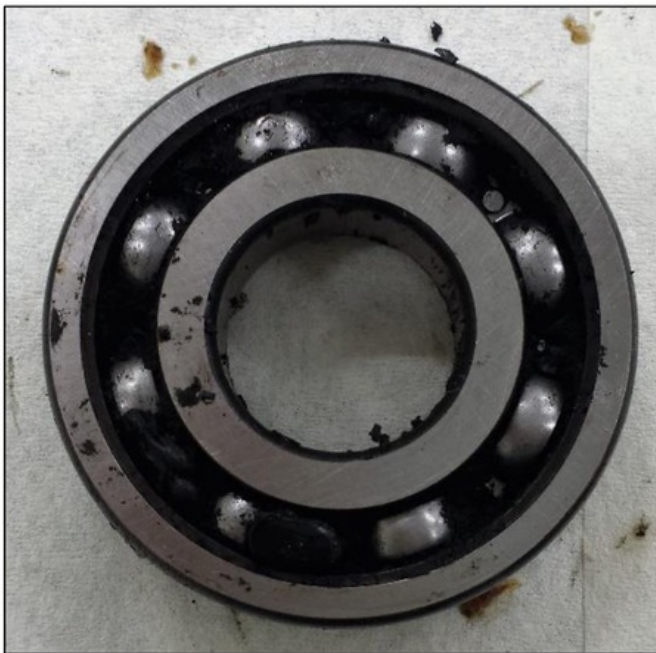


Figure 90: Bearing 4.1



Figure 91: Bearing 4.1 clean, outer ring face

This bearing is completely seized with no rotation possible. The polymer bearing housing has melted into the bearing internals as well as the outside of the outer ring, taking the place of the lubrication, restricting movement in either direction. Small orange splotches on the outer face (roughly 0.5 mm to 2 mm in diameter) are common.

4.2.4.2 Bearing 4.2



Figure 92: Bearing 4.2



Figure 93: Bearing 4.2 clean, outer ring face

The same result as bearing 4.1, the rubber polymer bearing housing has melted into the bearing and seized it, although allowing approximately 20° of rotation. There was a miniscule amount of lubrication inside the bearing as shown in figure 92. As with the previous bearing on the same roller the same orange splotches are found on the outer rings surface.

4.2.5 Idler Roller 5

4.2.5.1 Bearing 5.1



Figure 94: Bearing 5.1



Figure 95: Bearing 5.1 Lubrication



Figure 96: Bearing 5.1 lubrication

Bearing 5.1 also rotated smoothly prior to cleaning, although at first try some crunching was heard but disappeared after repeated rotation. Lubricant filled roughly 70% of the bearing and contained a few large particles of black rubber polymer (approximately 4x2x1mm) as well as some small metal particles. These can be seen in figures 95 and 96.



Figure 97: Bearing 5.1 clean



Figure 98: Bearing 5.1 outer ring face

Bearing 5.1 has low resistance to rotation and is quiet when spinning, although some imperfections on the race mean there are audible noises during rotation. On the outer rings face, large discolourations all the way around the bearing are visible as shown above in figure 98.

4.2.5.2 Bearing 5.2



Figure 99: Bearing 5.2



Figure 100: Bearing 5.2 lubrication

There was a lack of lubricant in bearing 5.2 for roughly one quarter of the bearing and was chunky, as if stuck together in clumps. It rotated smoothly with no audible crunching or grinding and very few polymer debris nor were metal particles visible. However, the debris found was predominantly on the larger side.



Figure 101: Bearing 5.2 clean



Figure 102: Bearing 5.2 outer ring face



Figure 103: Bearing 5.2 inner ring edge

4.2.6 Idler Roller 6

4.2.6.1 Bearing 6.1



Figure 104: Bearing 6.1



Figure 105: Bearing 6.1



Figure 106: Bearing 6.1 lubrication

Bearing 6.1 also rotated smoothly while grease was still contained, albeit roughly 60% of lubricant remaining. There were 2 long thin strands of metal (7 mm long and much less than a fifth of a millimetre in diameter) on the edges of the outer rings race. As with the previous bearings the same small and large polymer particles and small metal particles were found within the grease.



Figure 107: Bearing 6.1 clean



Figure 108: Bearing 6.1 outer ring face

4.2.6.2 Bearing 6.2



Figure 109: Bearing 6.2



Figure 110: Bearing 6.2 lubrication

This bearing had by far the dirtiest lubrication of all bearings. 6.2's grease was filled with fine polymer particles as well as a small number of metal flakes. The bearing rotated smoothly except for slight grinding in one area.



Figure 111: Bearing 6.2 clean



Figure 112: Bearing 6.2 outer ring face

4.3 MICROGRAPHS

4.3.1 Surface damage

4.3.1.1 Scratches

The following images are micrographs of a selection of bearing race surfaces, both inner and outer races. They depict abrasion in the form of three body and two body abrasive wear, both causing surface damage such as scratches, scoring and grooves.



Figure 113: Bearing 1.1 outer ring scratches



Figure 114: Bearing 2.1 outer race scratches



Figure 115: Bearing 2.2 outer race scratches

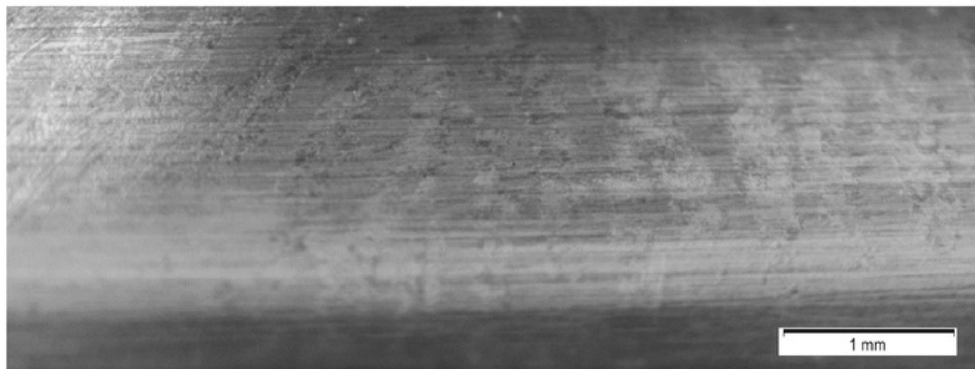


Figure 116: Bearing 2.1 outer race



Figure 117: Bearing 3.1 inner race scratches

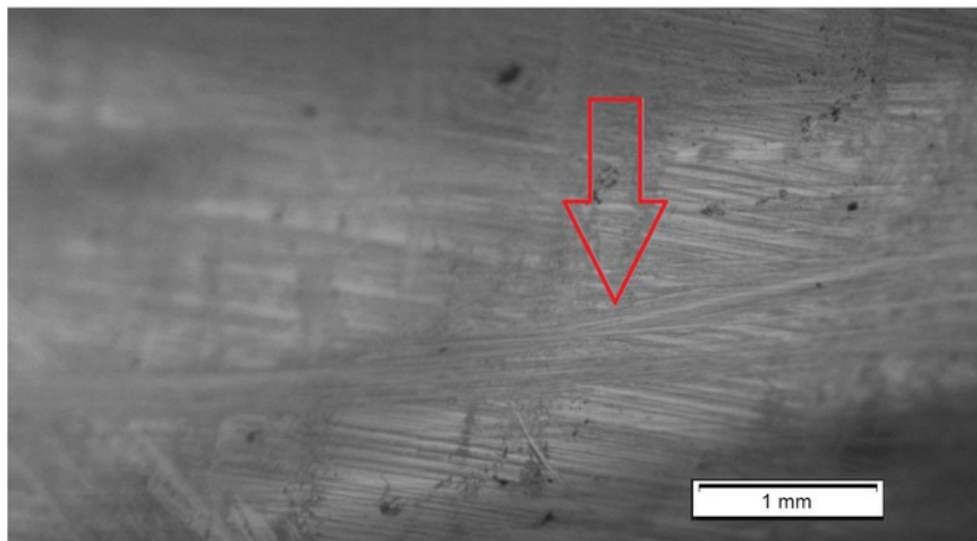


Figure 118: Bearing 3.2 outer race scratches



Figure 119: Bearing 3.2 outer race scratches



Figure 120: Bearing 4.2 outer race scratches



Figure 121: Bearing 5.1 inner race scratches

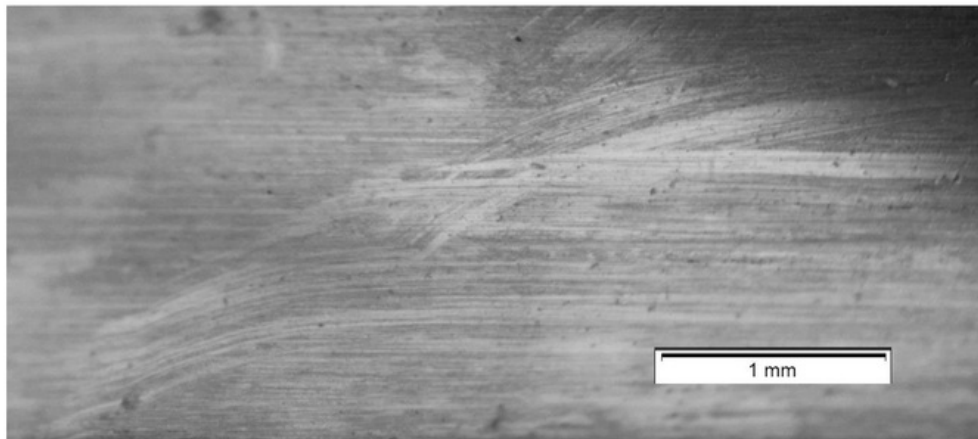


Figure 122: Bearing 5.2 inner race scratches

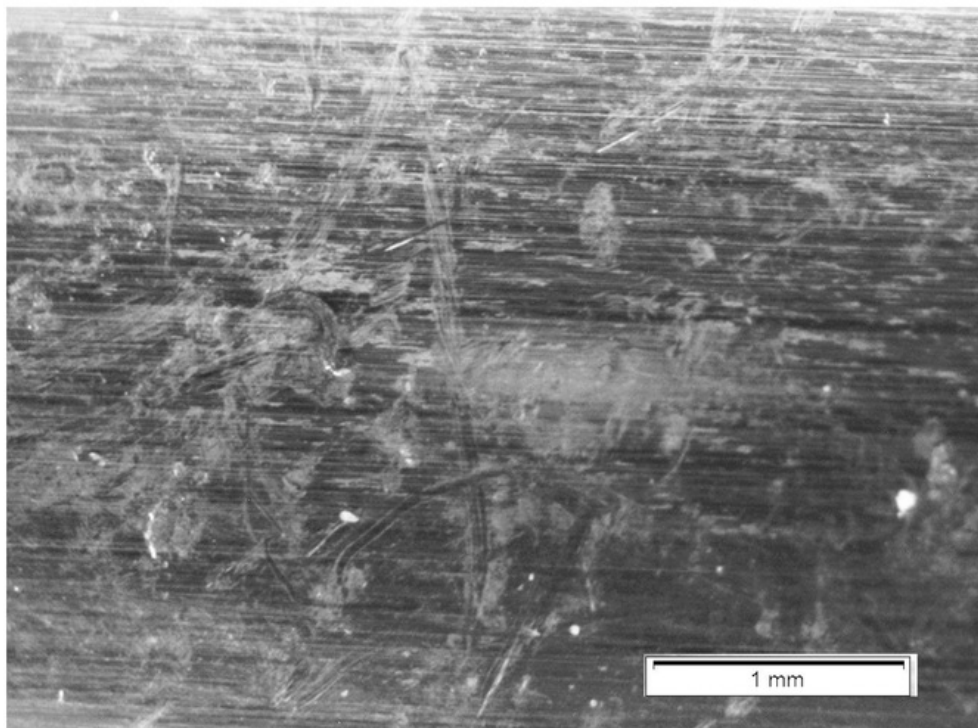


Figure 123: Bearing 6.1 outer race scratches

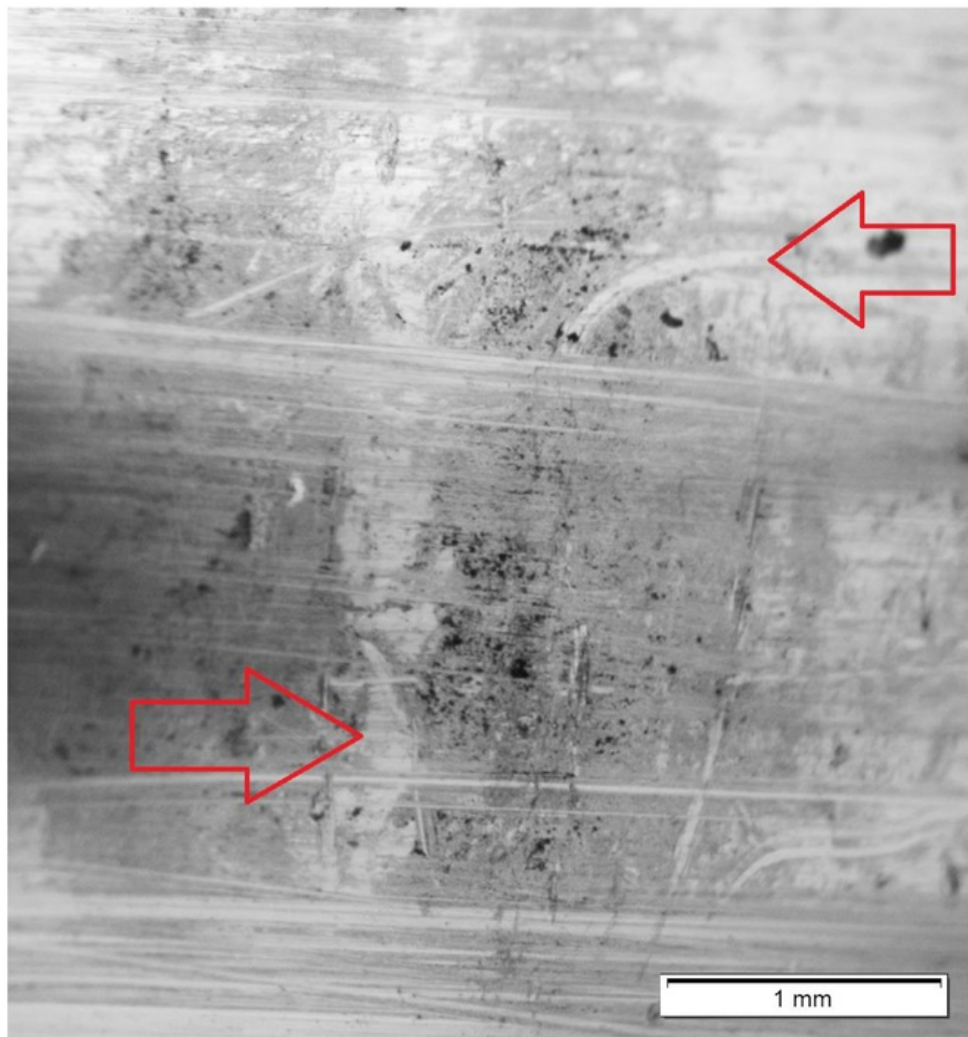


Figure 124: Bearing 6.1 outer race scratches

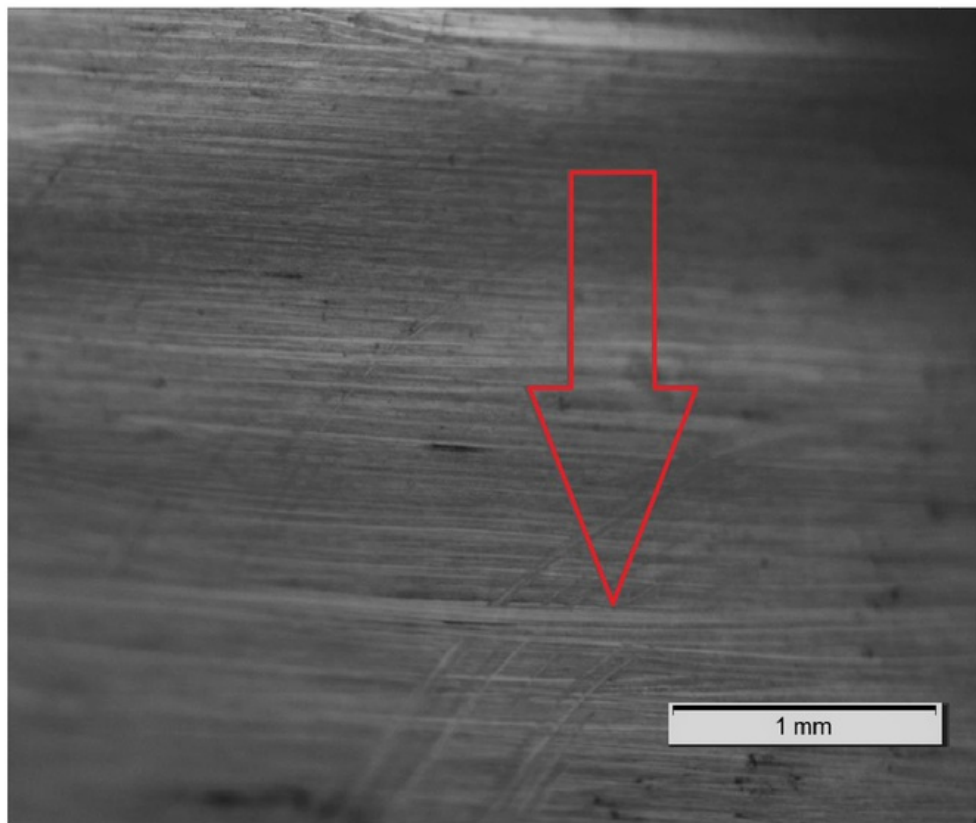


Figure 125: Bearing 6.2 outer race scratches

4.3.1.2 Gouges and Deep Scratches

Gouges and deep scratches are the result of three body abrasion and are the next stage on from surface scratches. These were also found on the inner and outer races of multiple bearings in multiple places, making them relatively common.

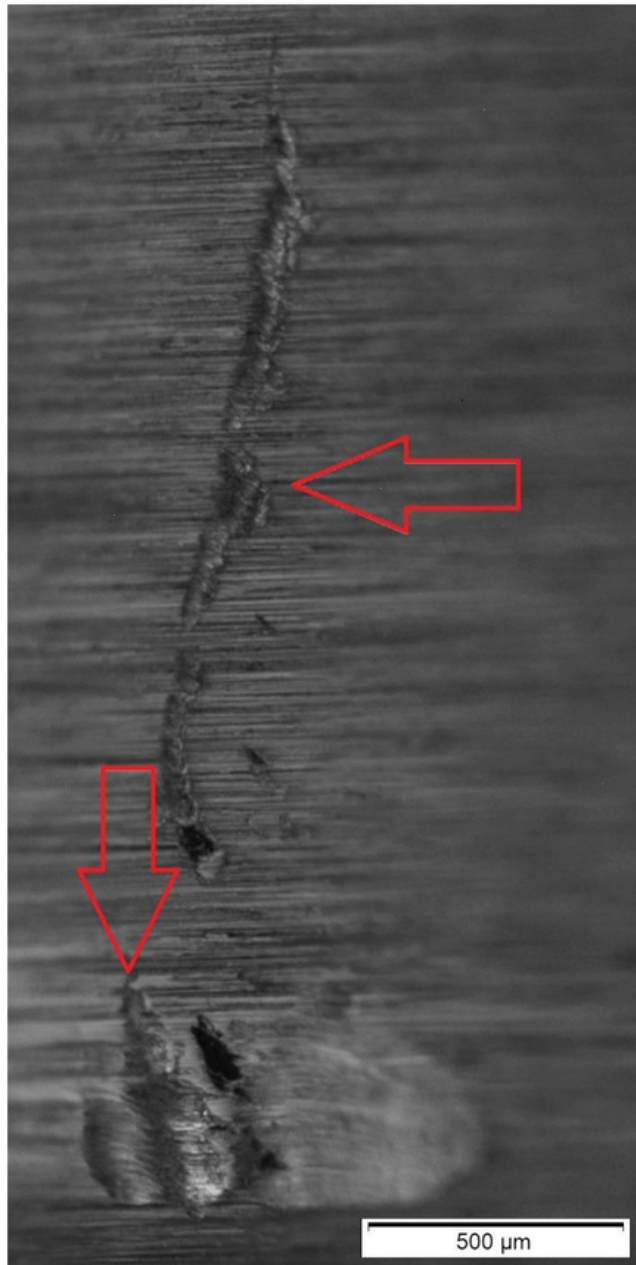


Figure 126: Bearing 1.1 inner race edge

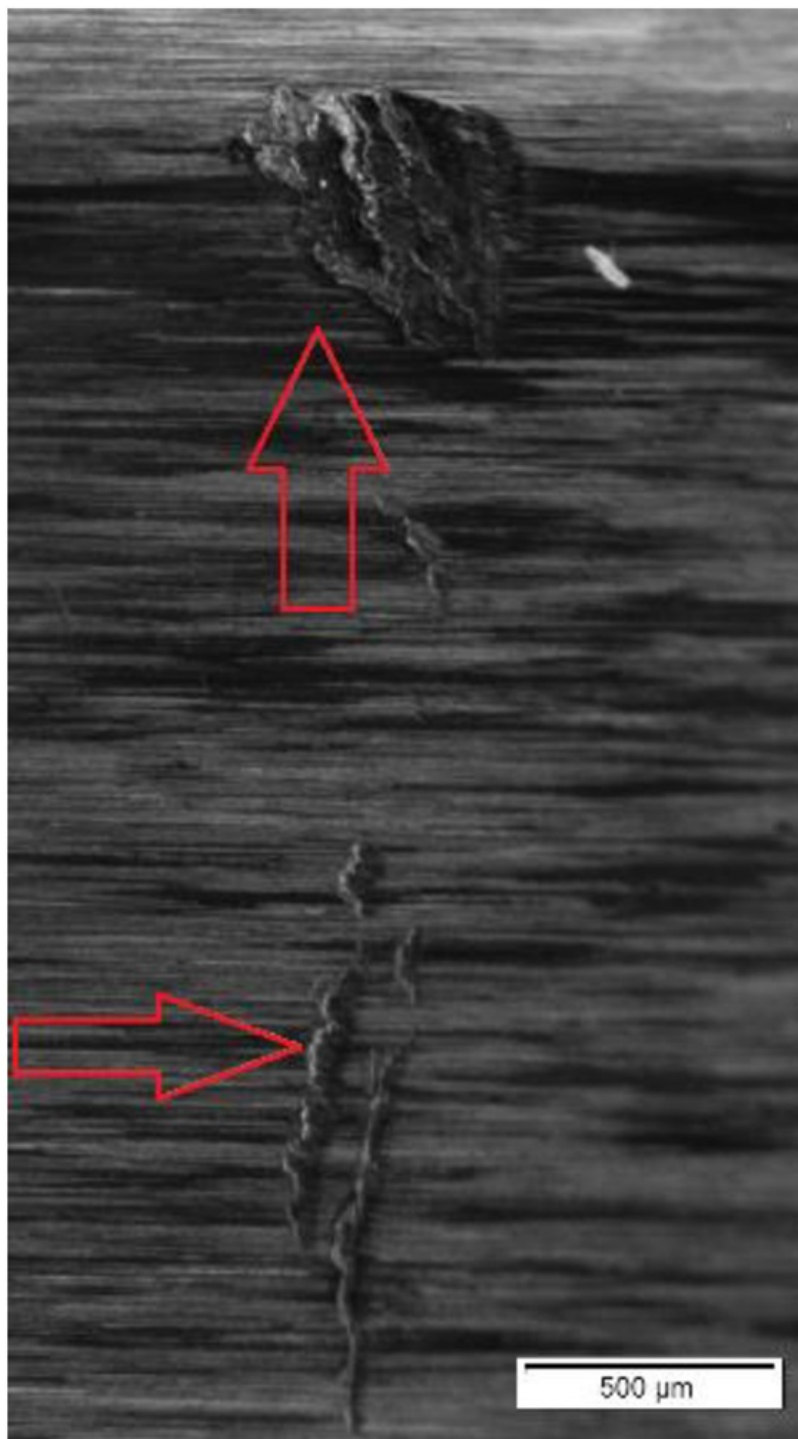


Figure 127: Bearing 2.1 outer race gouges near edge of race

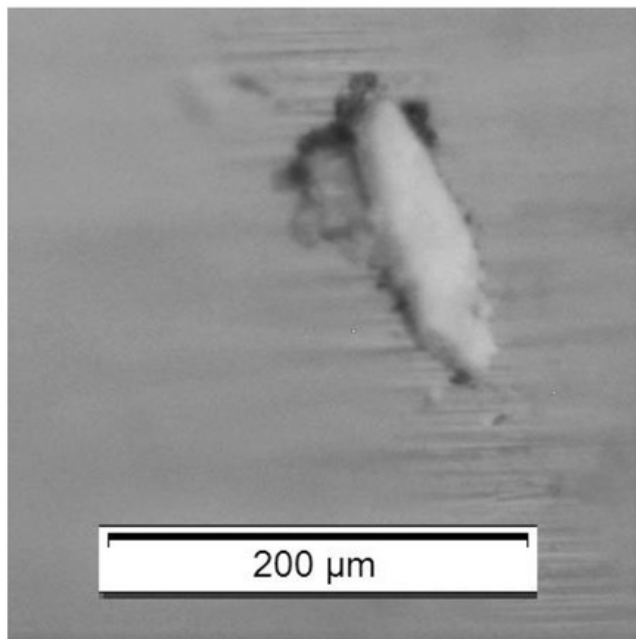


Figure 128: Bearing 4.1 inner race gouge

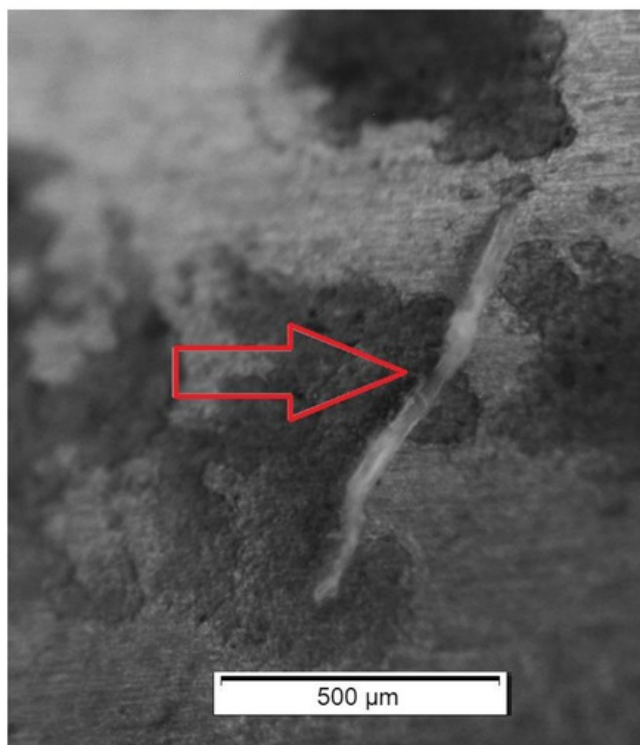


Figure 129: Bearing 4.2 outer race gouge and surface contamination

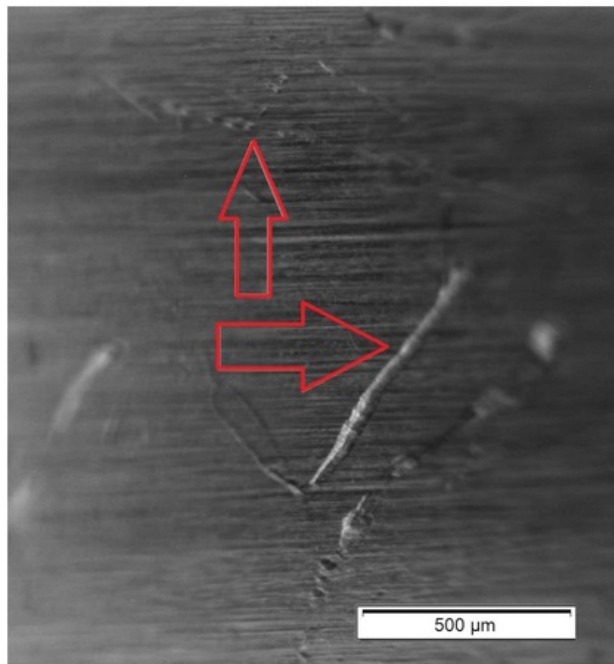


Figure 130: Bearing 5.1 outer race gouges and pitting

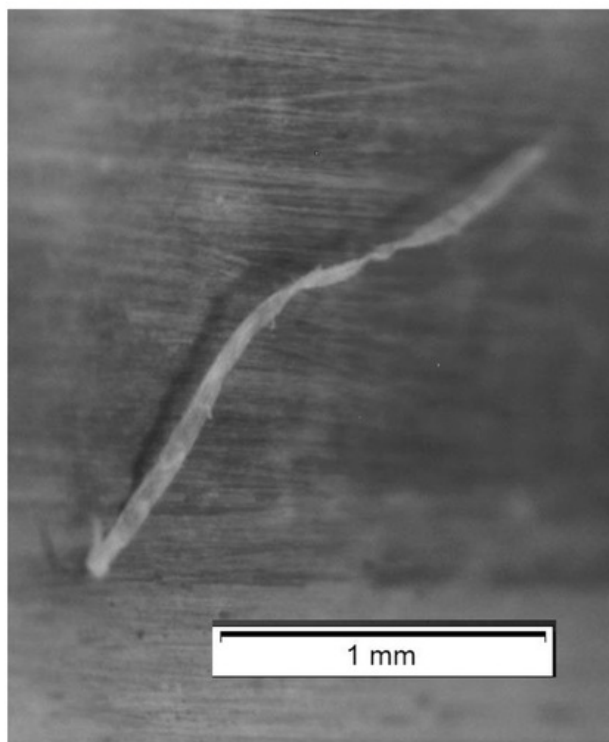


Figure 131: Bearing 5.2 inner race gouge

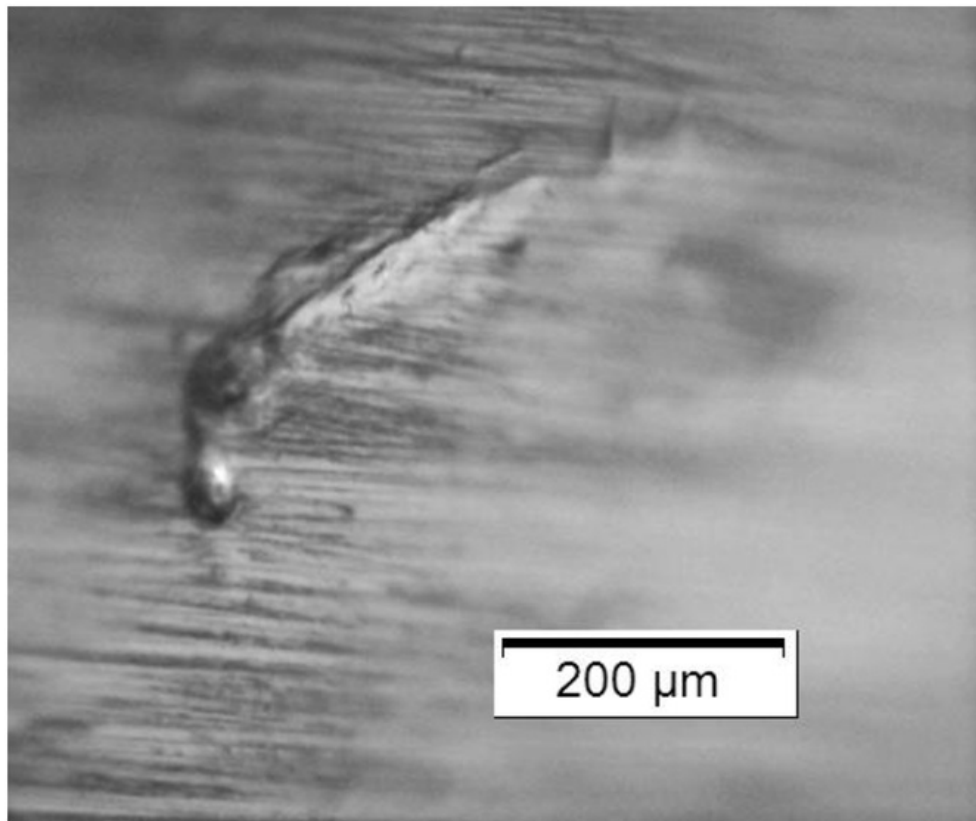


Figure 132: Bearing 6.1 outer race gouge

4.3.1.3 Grooves

Grooves like the ones shown below are also a result of three body abrasion and are relatively long, measuring from approximately 2 mm to 10 mm in length and approximately 5 microns in diameter.

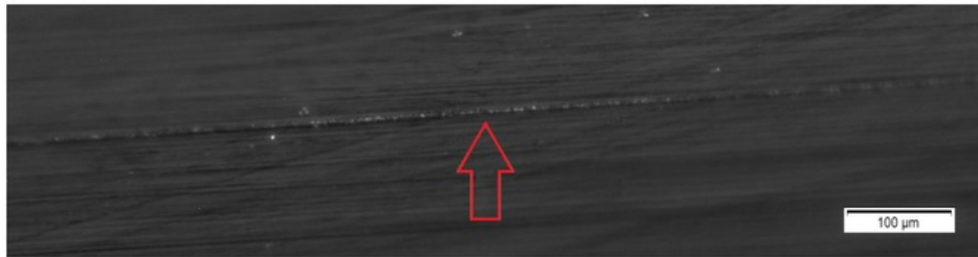


Figure 133: Bearing 3.1 outer race groove

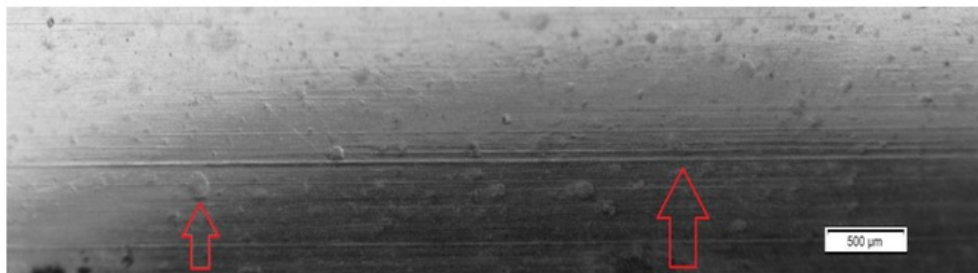


Figure 134: Bearing 4.1 inner race groove and bruising



Figure 135: Bearing 5.1 outer race groove

4.3.2 Pitting/Bruising

Pitting and bruising are like each other in the fact that the surface is indented irregularly due to a third body. This form of damage is known as a fatigue failure as the surfaces are plastically deformed. Examples of pitting and bruising can be found in the following figures.

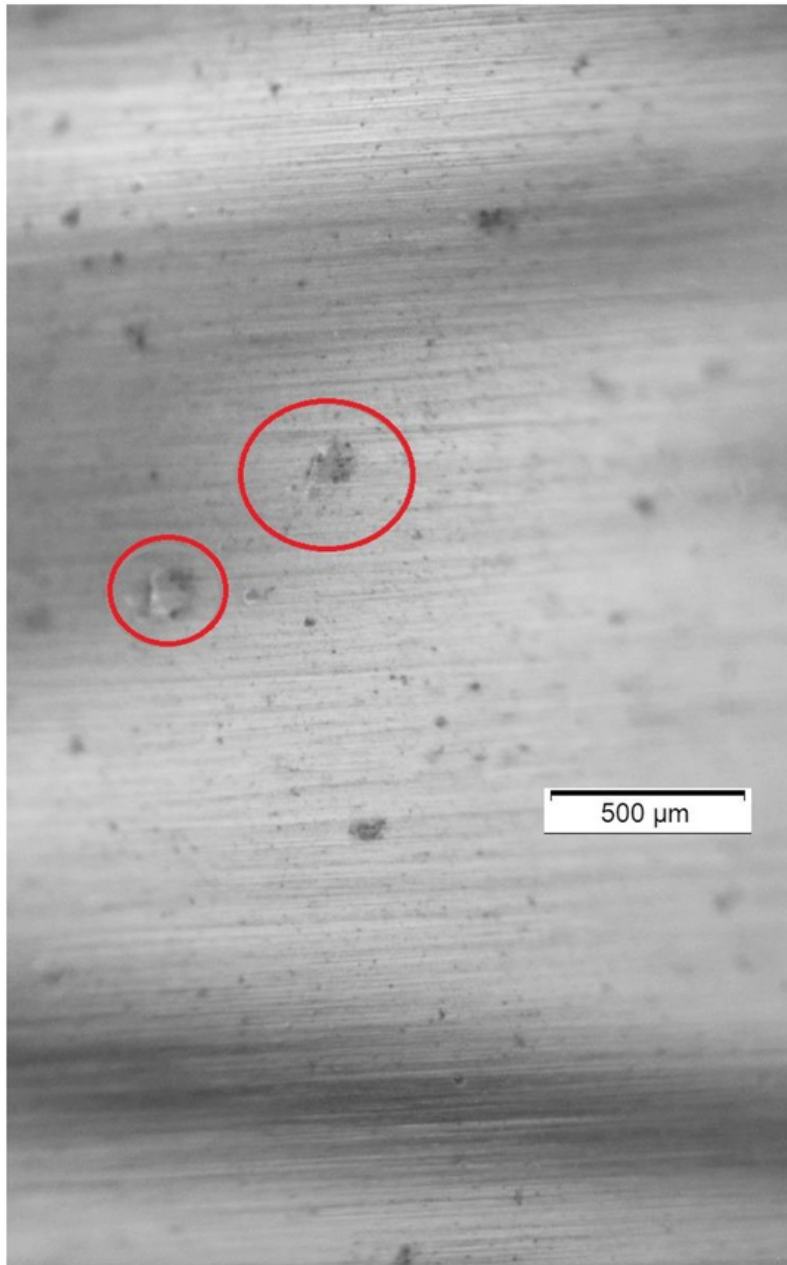


Figure 136: Bearing 1.1 inner ring pitting

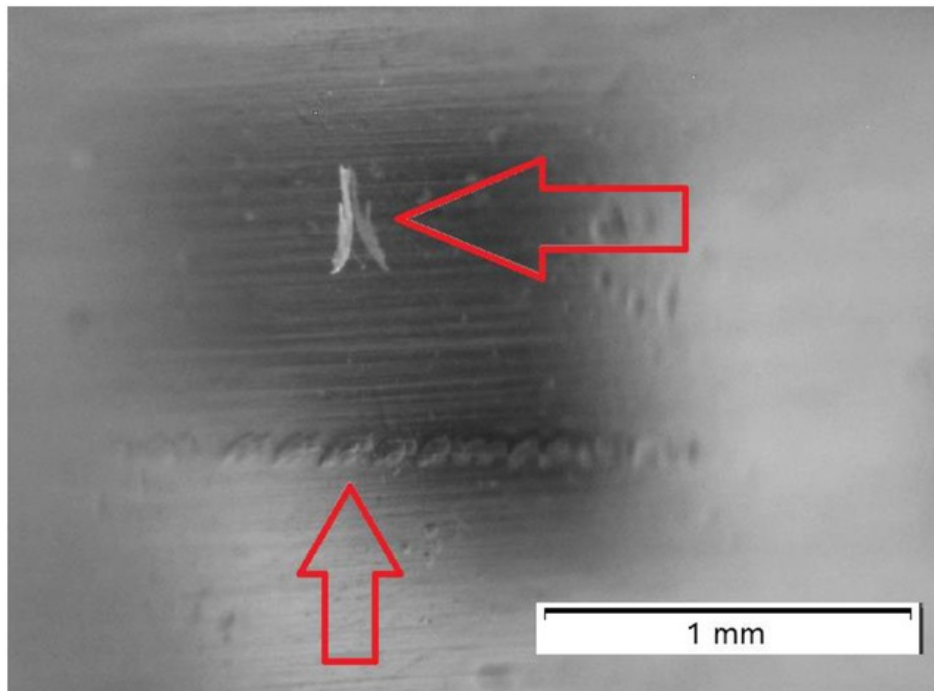


Figure 137: Bearing 3.1 inner race bruising

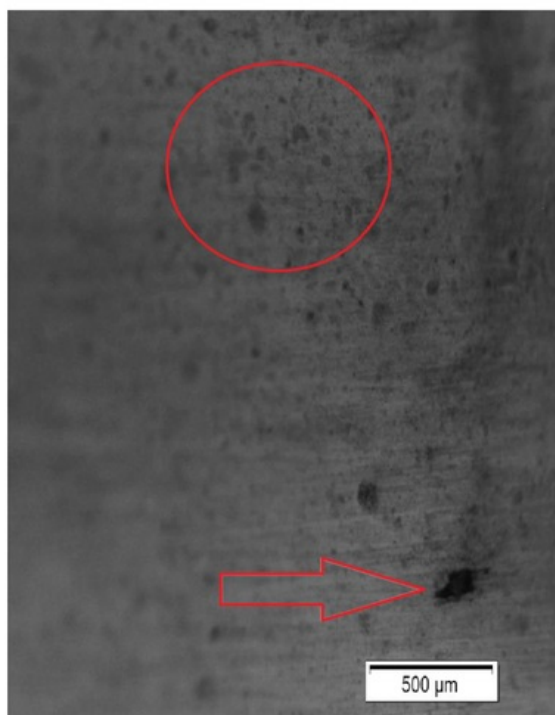


Figure 138: Bearing 4.1 outer race pitting

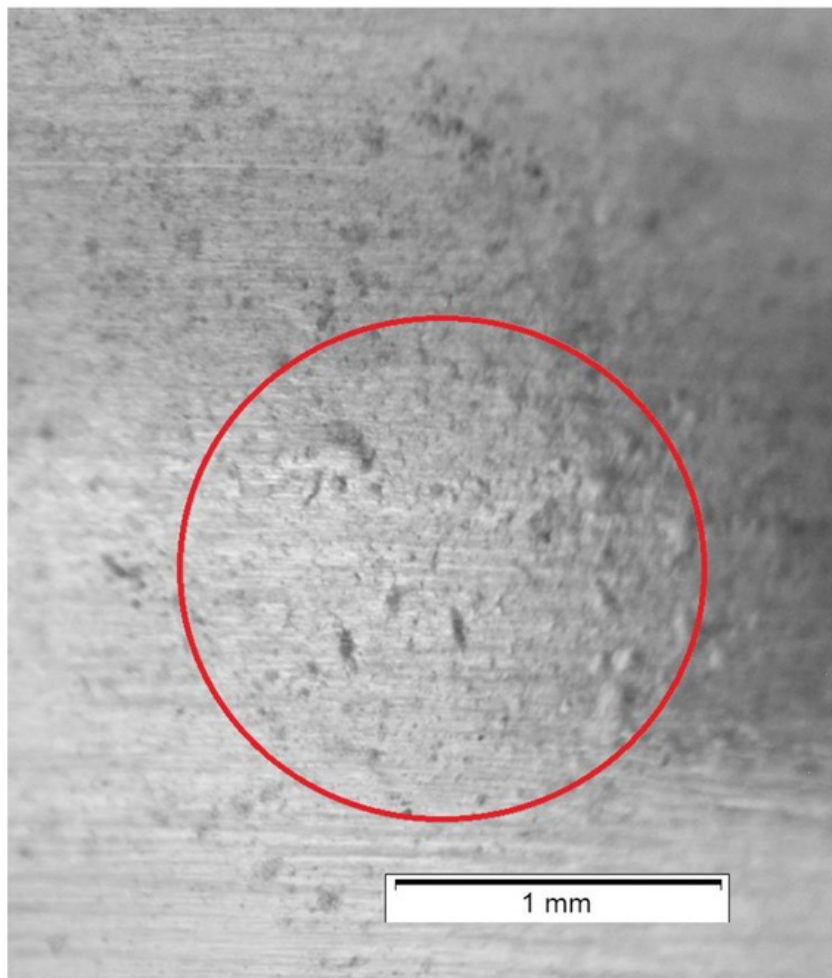


Figure 139: Bearing 4.2 outer race pitting

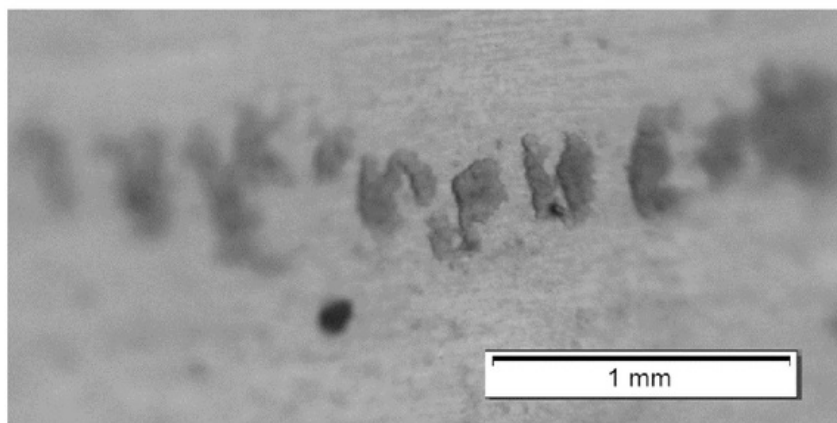


Figure 140: Bearing 4.2 inner race series of chips

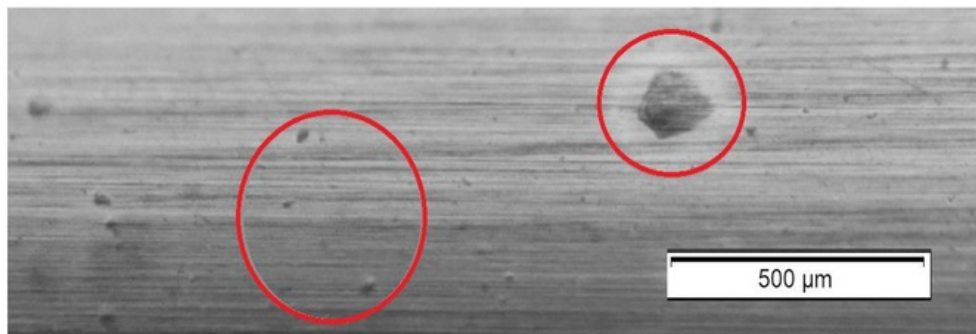


Figure 141: Bearing 5.1 outer race bruising

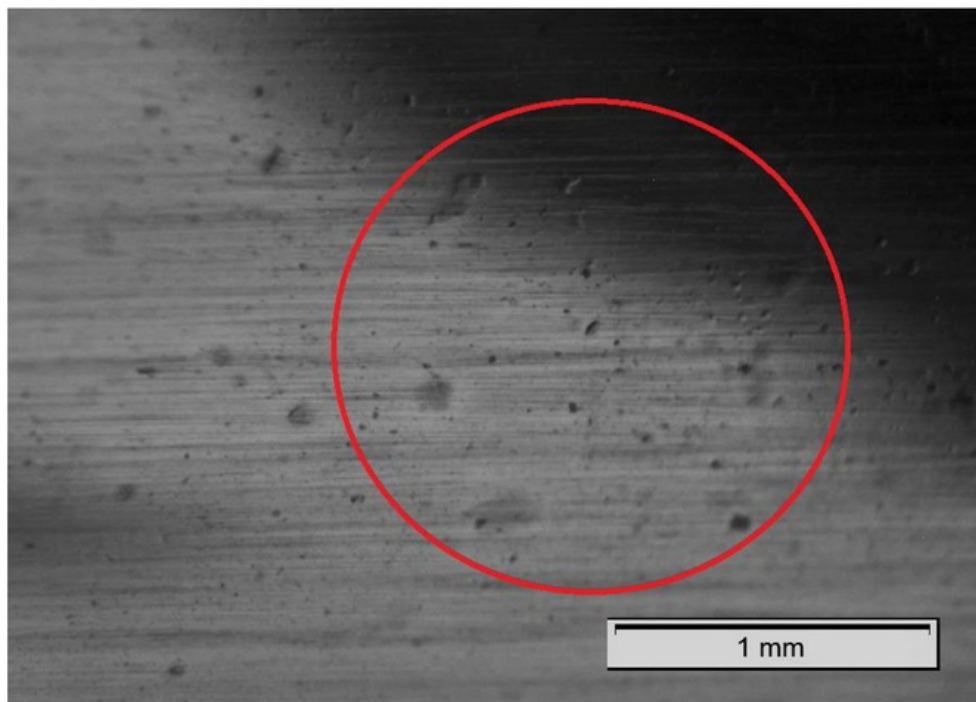


Figure 142: Bearing 6.2 inner race pitting and bruising

4.3.3 Fatigue Spalling

As explained earlier in “Bearing Damage Analysis” -> “Wear” -> “Fatigue Spalling” under in the section of this document, Spalling is the fatigue wear of a surface under repeated loading. Examples of fatigue spalling are seen in the figures below.

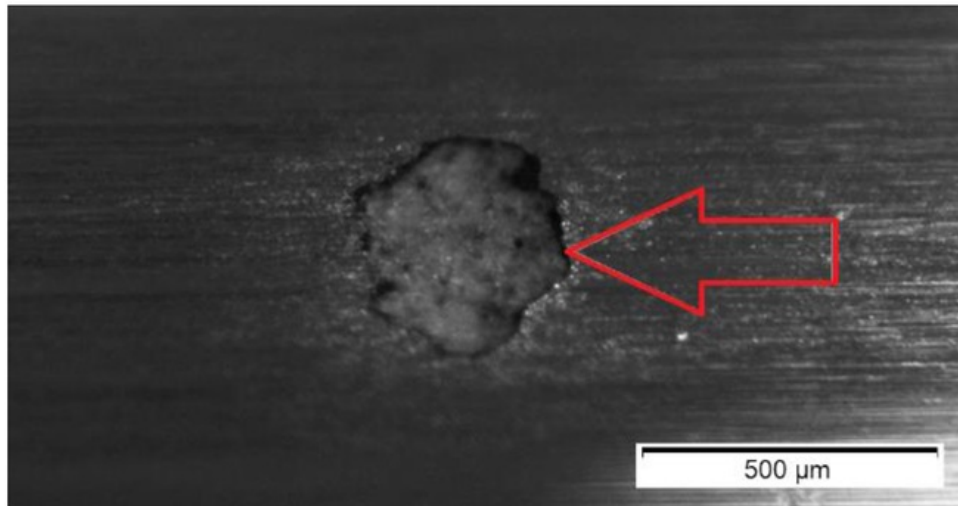


Figure 143: Bearing 1.1 outer ring spalling

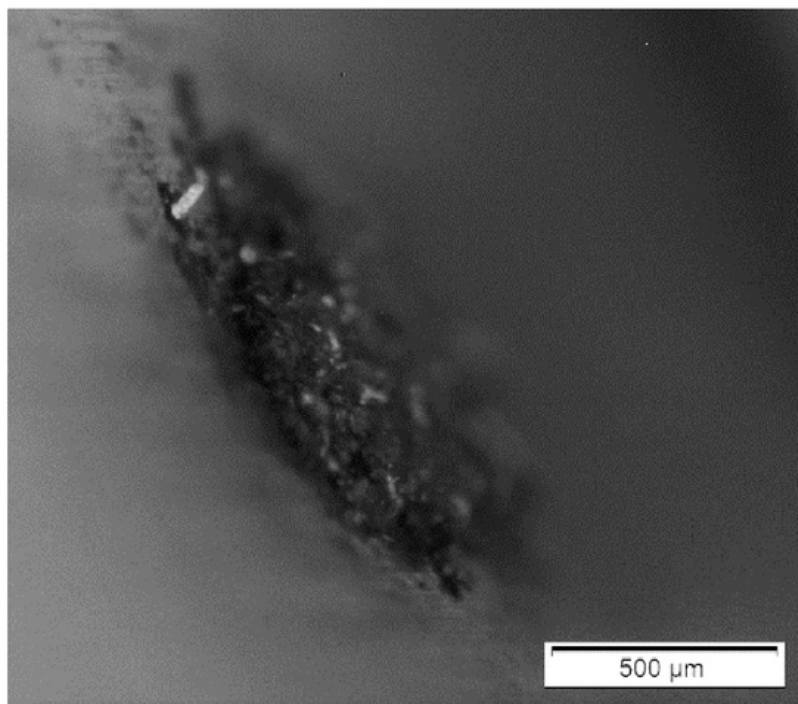


Figure 144: Bearing 2.1 inner race spalling

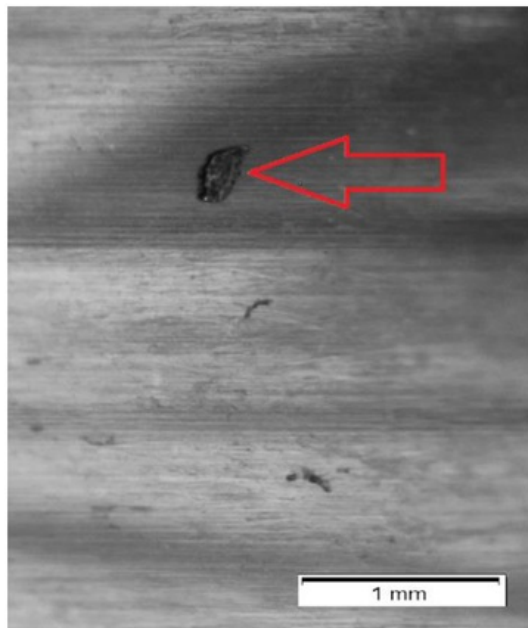


Figure 145: Bearing 3.2 inner race spalling

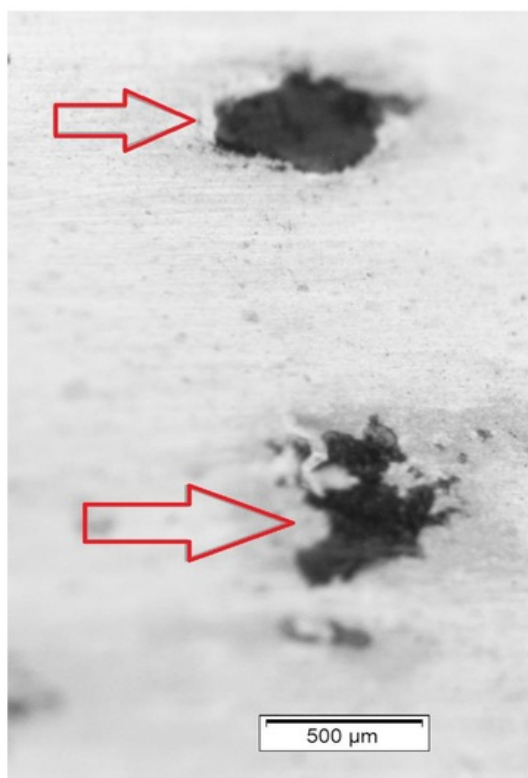


Figure 146: Bearing 4.1 inner race spalling

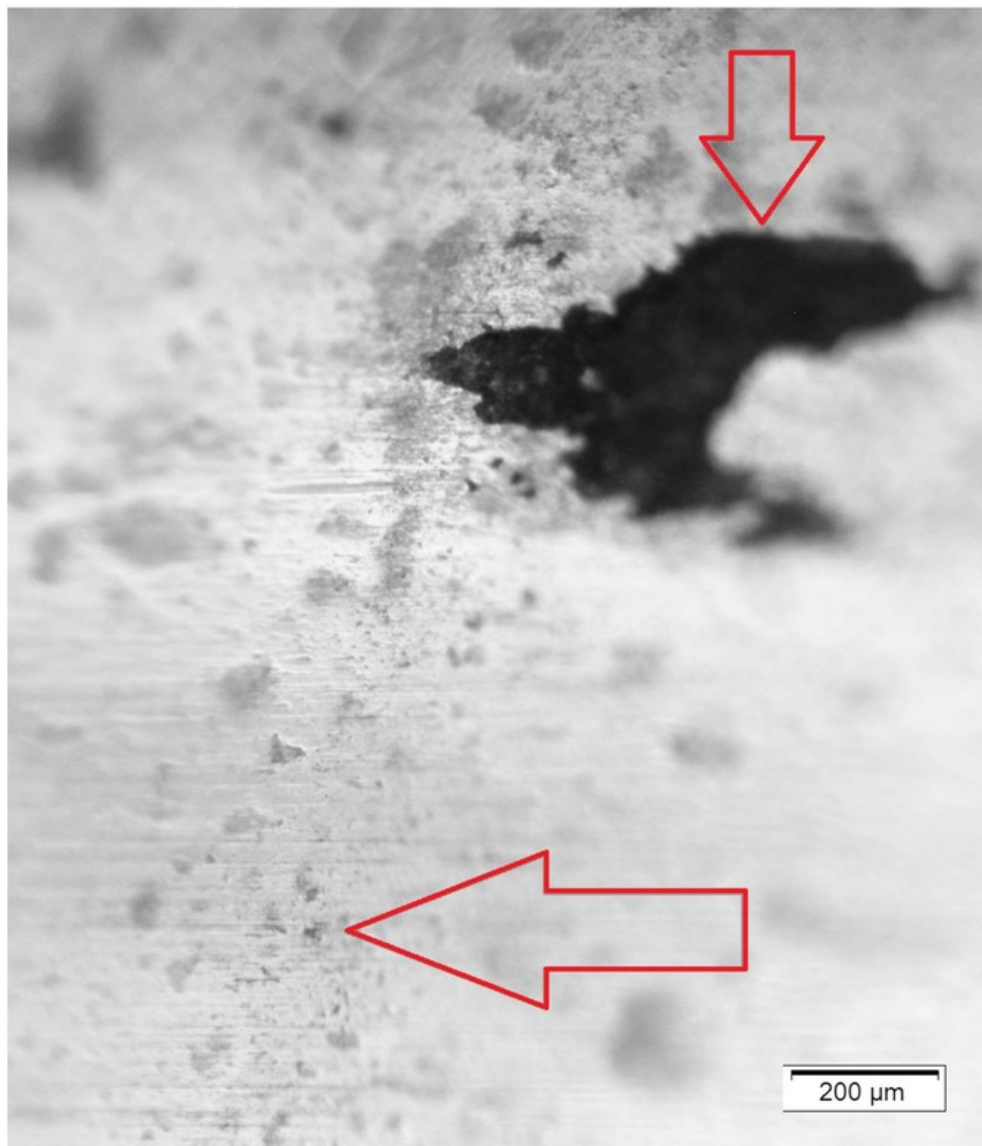


Figure 147: Bearing 4.2 inner race PSO spalling

4.3.4 Chips

Chips like those shown in figure 150 were not too common during for the bearings used in this project. This example, as well as 3 others, were all located on the edges of the outer races.

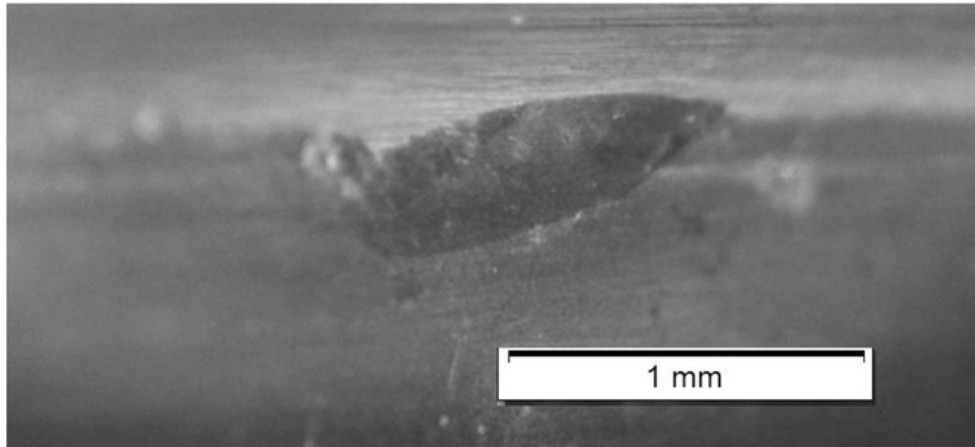


Figure 148: Bearing 6.1 outer race chip on edge

4.3.5 Surface Contamination

Surface contamination refers to any substance, either originally part of the bearing or from an outside source that alters the consistency of the original surface. The following images all display a form of surface contamination that has remained after the cleaning process.

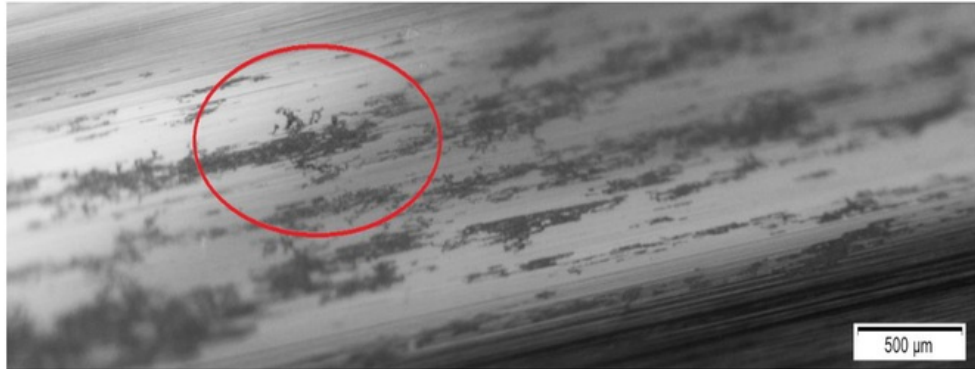


Figure 149: Bearing 1.2 outer race surface contamination



Figure 150: Bearing 2.2 inner race surface contamination by polymer of bearing housing



Figure 151: Bearing 5.1 outer race surface contamination

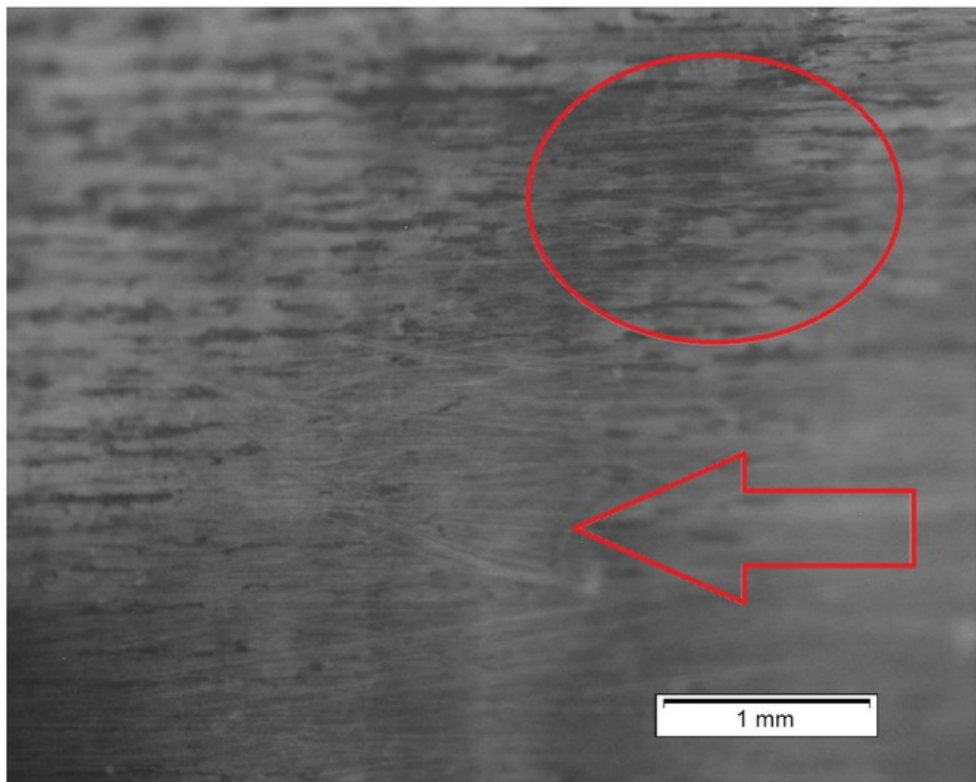


Figure 152: Bearing 5.2 inner race surface contamination

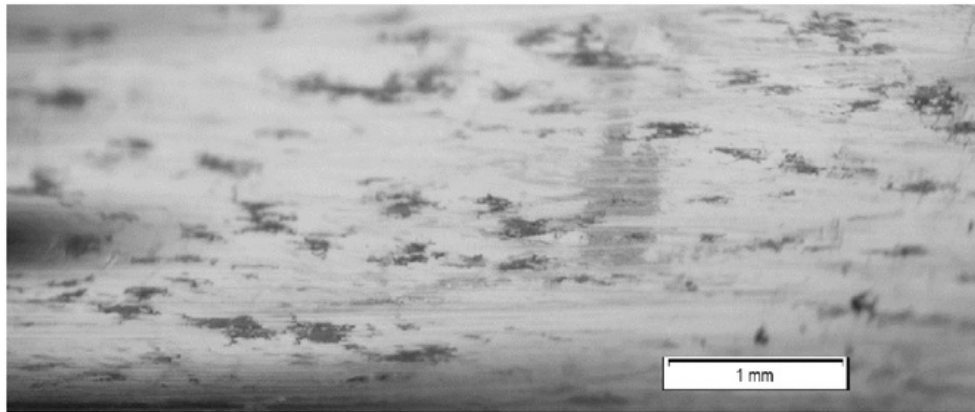


Figure 153: Bearing 6.1 outer race surface contamination

Surface Contamination may result in etching or corrosion.

4.3.6 Corrosion/Etching

Corrosion or etching is explained under “Bearing Damage Analysis” -> “Wear” -> “Corrosion/Etching” and is where contaminants as water penetrate the bearing, wearing away the surface and increasing friction due to the uneven surface. It can be identified by wear patterns shown in figure 154.

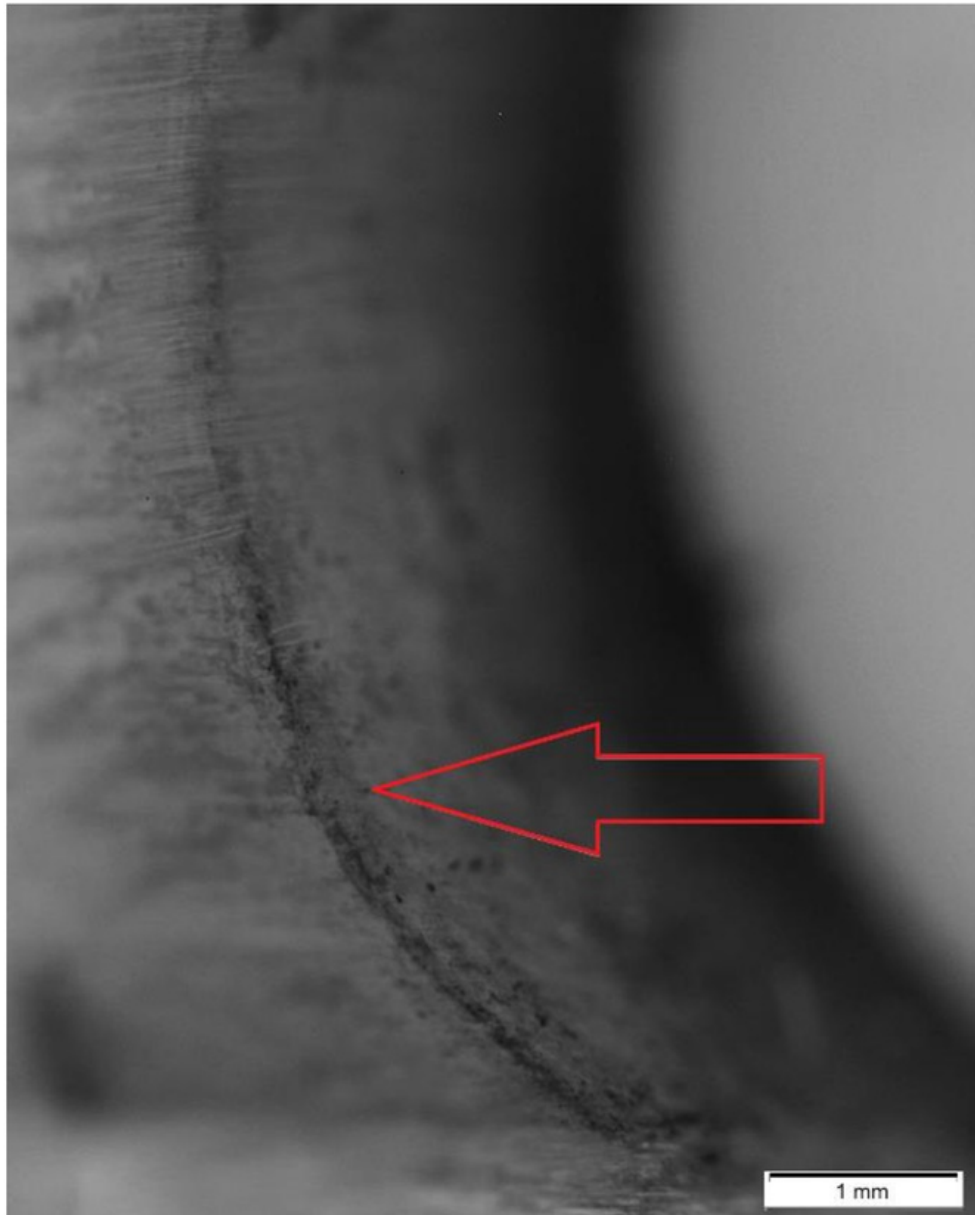


Figure 154: Bearing 2.2 inner race corrosion/etching

4.3.7 Heat Damage

Heat Damage is the result of high friction due to various reasons explained in detail later such as lubrication breakdown, imperfect surfaces from pitting or corrosion. The surface is usually discoloured as depicted in figure 155.

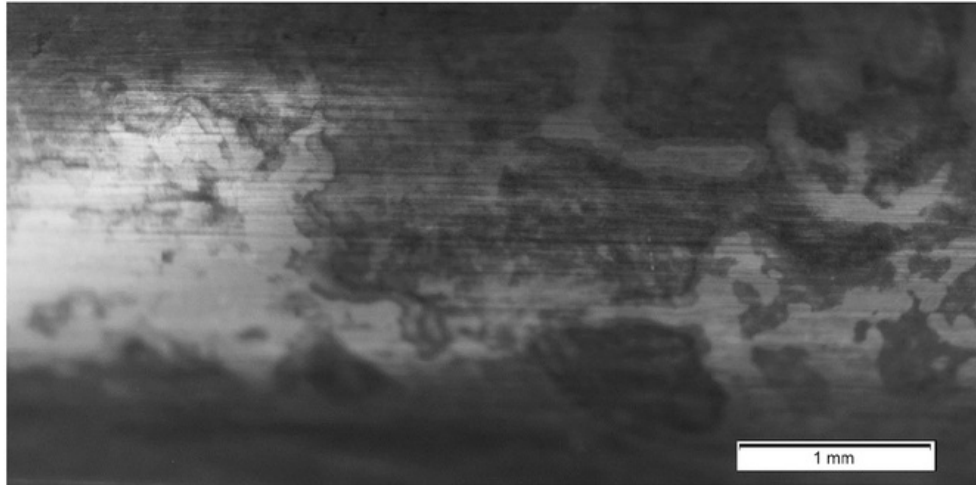


Figure 155: Bearing 4.1 outer race surface breakdown due to heat

4.3.8 Ball damage

This section specifically looks at the damage to the balls of the bearing. The wear is a mix of surface scratches, gouges, pitting and bruising as well as surface contamination. All of which a result of third body abrasion, bar surface contaminations in figure 164 highlighted by the red circle.



Figure 156: Bearing 1.1 ball surface scratches

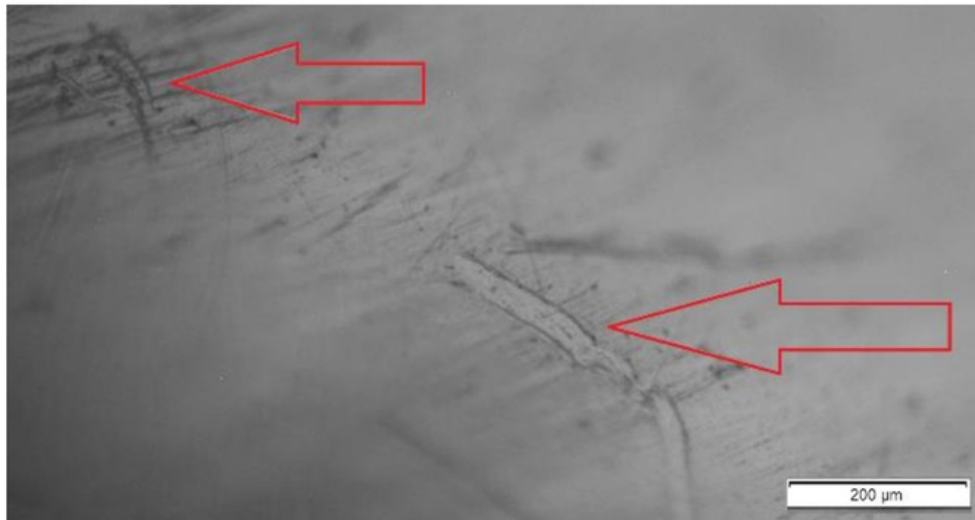


Figure 157: Bearing 2.2 ball surface scratches and pitting

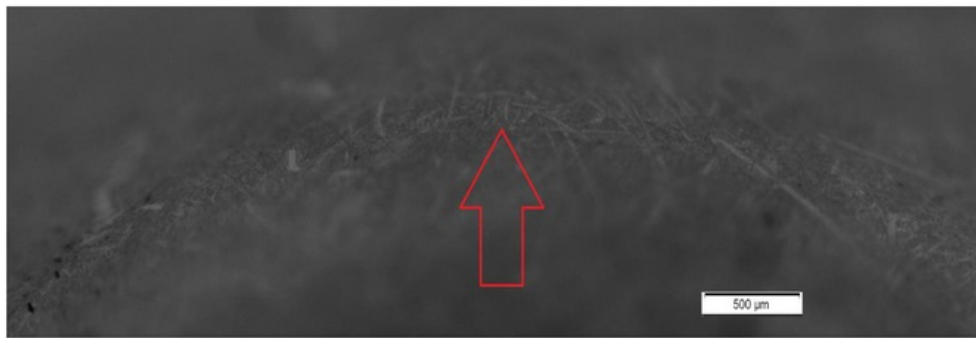


Figure 158: Bearing 3.1 ball surface scratches



Figure 159: Bearing 3.2 ball scratches

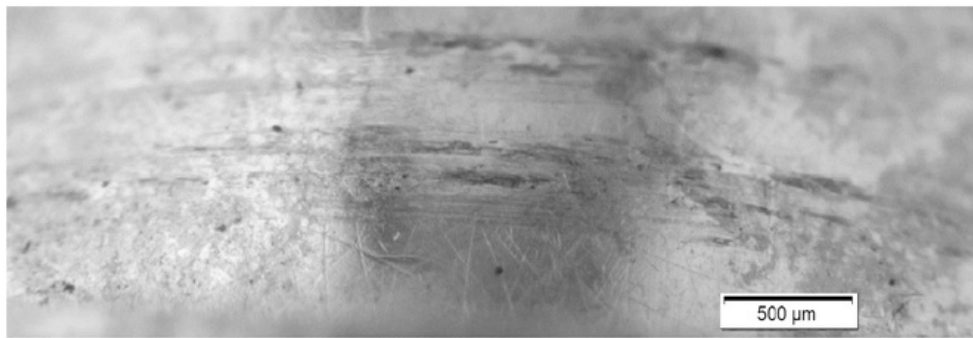


Figure 160: Bearing 4.1 ball surface scratches and wear

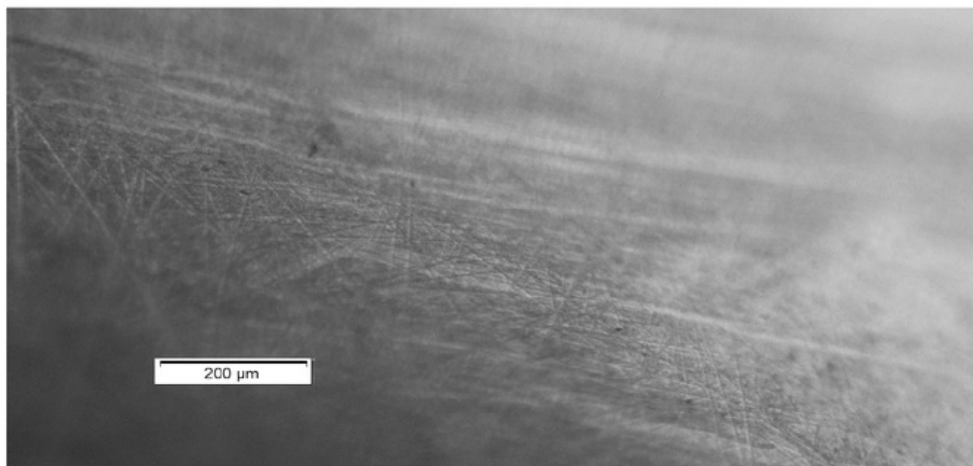


Figure 161: Bearing 5.1 ball scratches

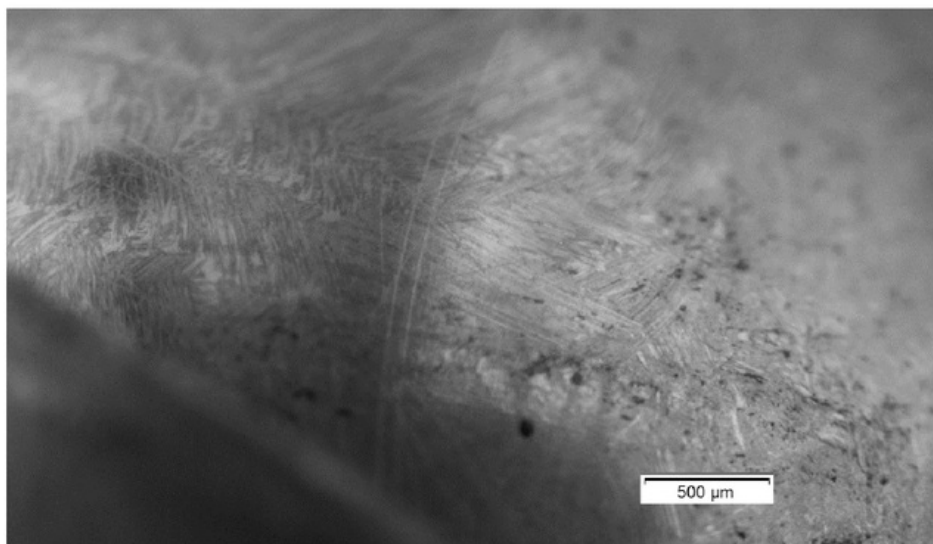


Figure 162: Bearing 5.2 ball scratches and pitting

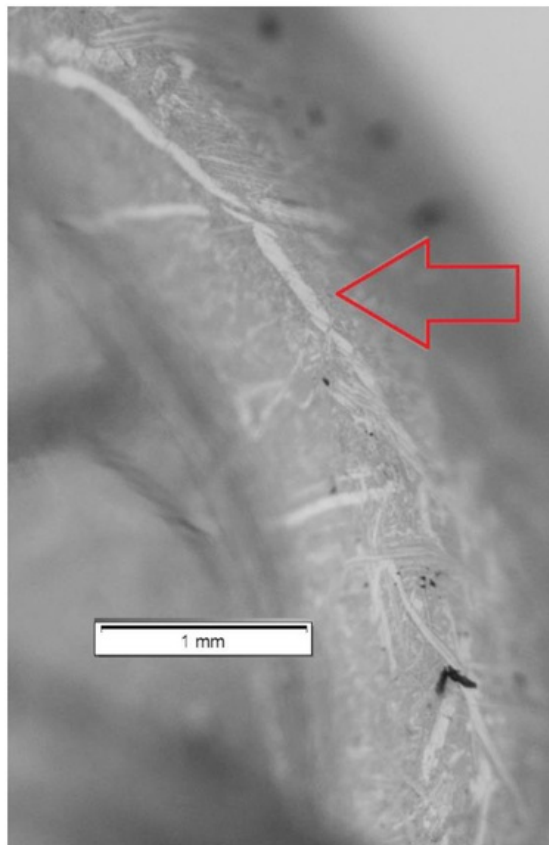


Figure 163: Bearing 6.1 ball scratches

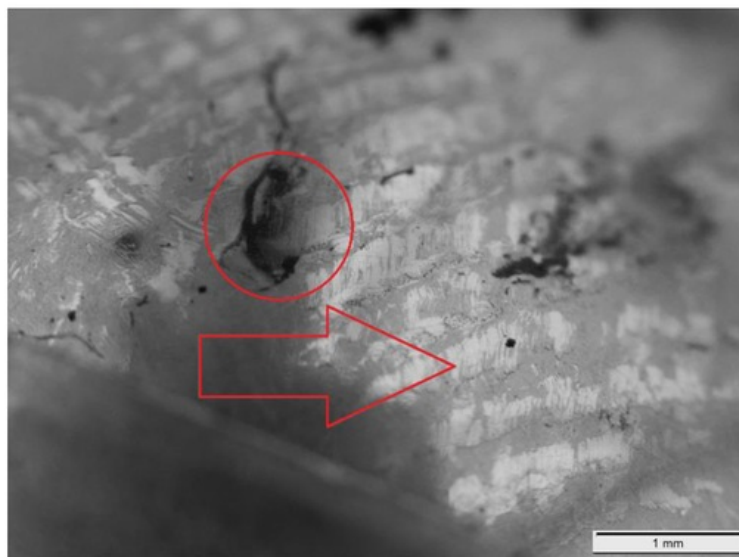


Figure 164: Bearing 6.2 ball scratches (arrow) and surface contamination (red circle)

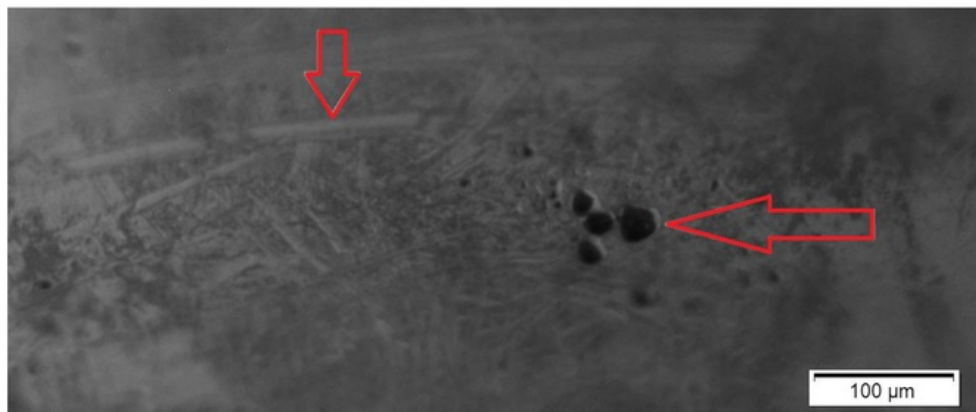


Figure 165: Bearing 2.1 ball scratches and pitting

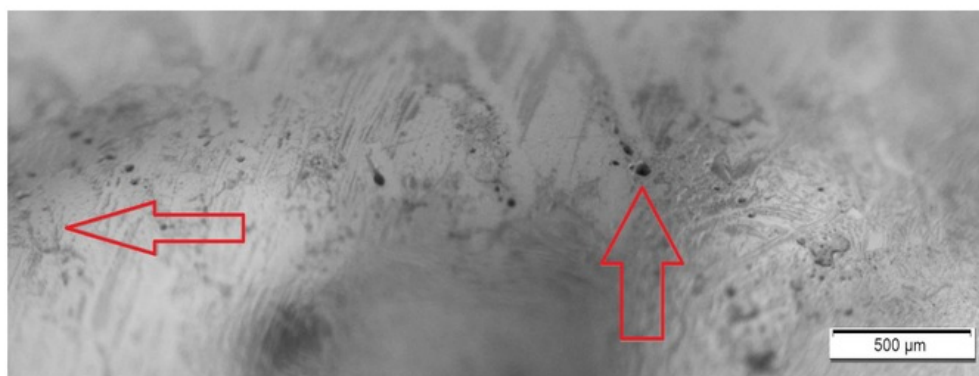


Figure 166: Bearing 3.2 ball pitting with surface wear

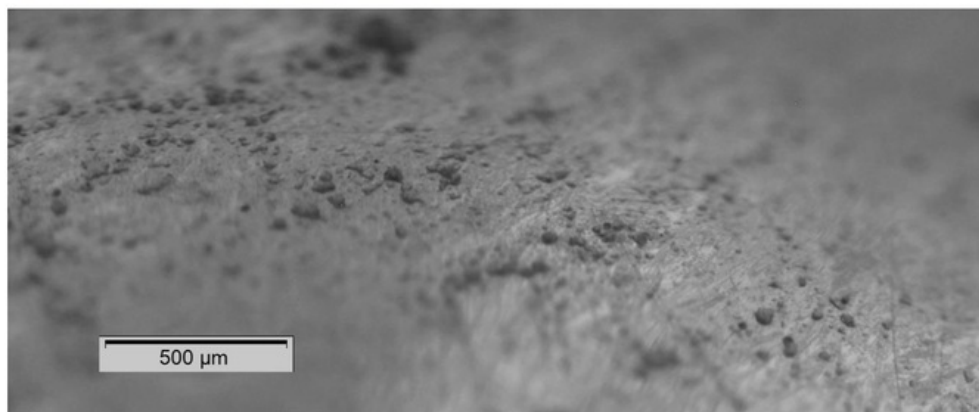


Figure 167: Bearing 4.2 ball pitting

4.3.9 Cage Damage

The following figures display wear to the cages of the ball bearings. All damage is at the cage edge and varies from abrasive wear (such as figures 168, 169 and 175) to heat damage like in figures 170, 172 and 174.

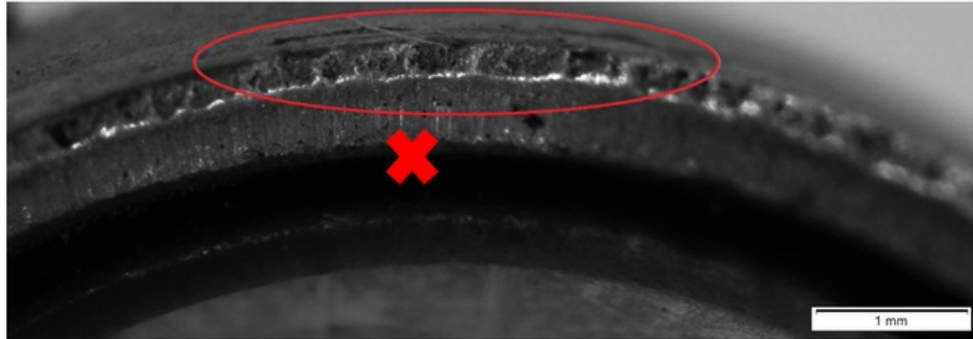


Figure 168: Bearing 1.1 cage edge wear

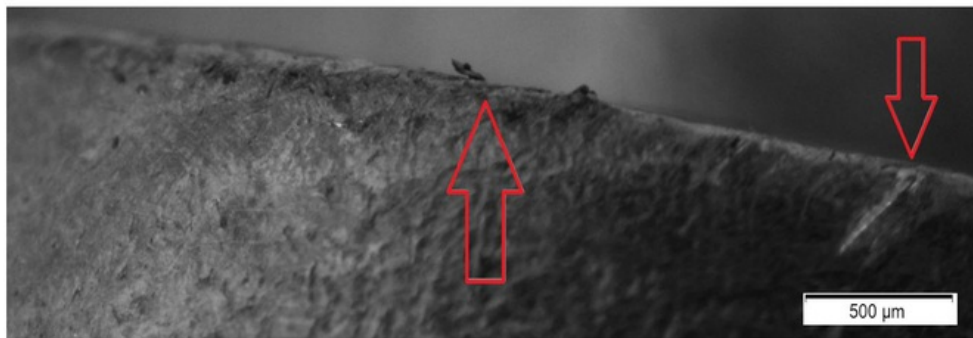


Figure 169: Bearing 3.1 cage edge wear

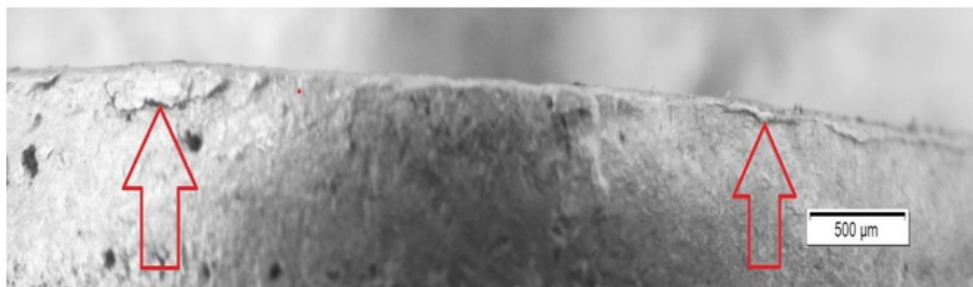


Figure 170: Bearing 4.1 melted cage edge

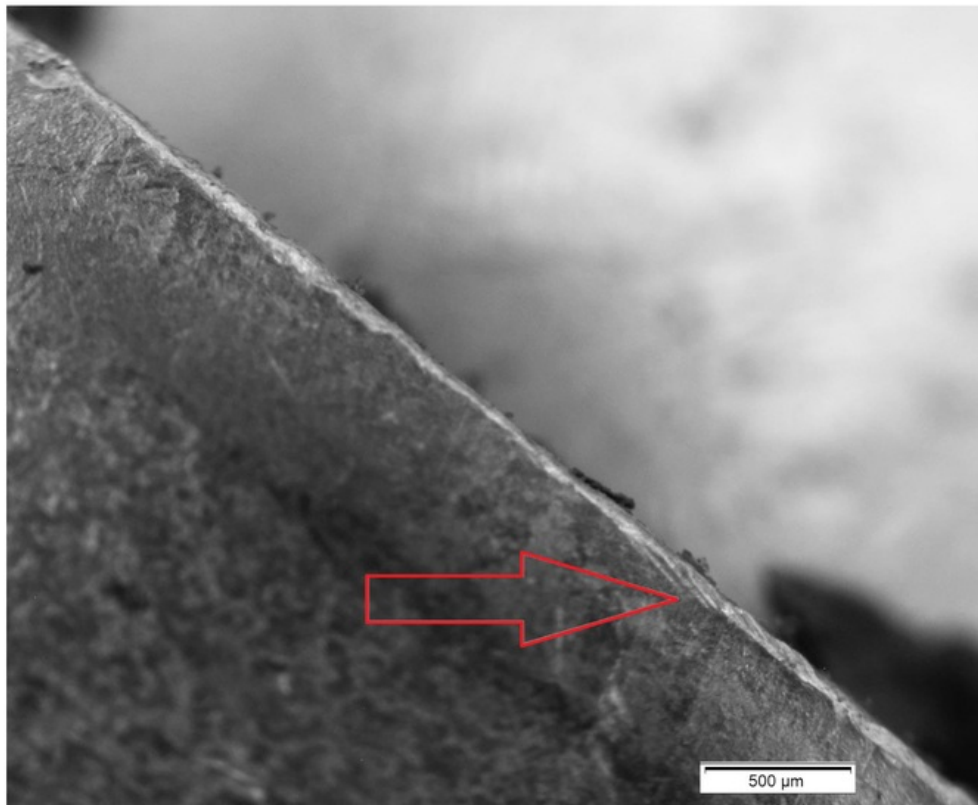


Figure 171: Bearing 4.2 melted cage edge and wear



Figure 172: Bearing 5.1 melted cage edge and wear

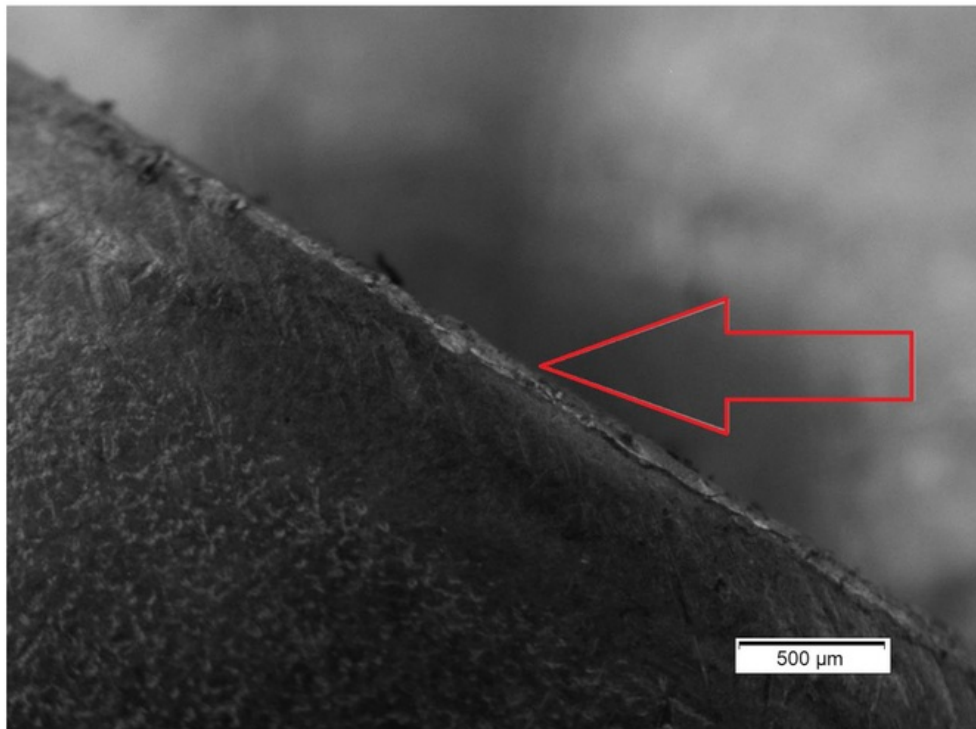


Figure 173: Bearing 5.2 cage edge wear

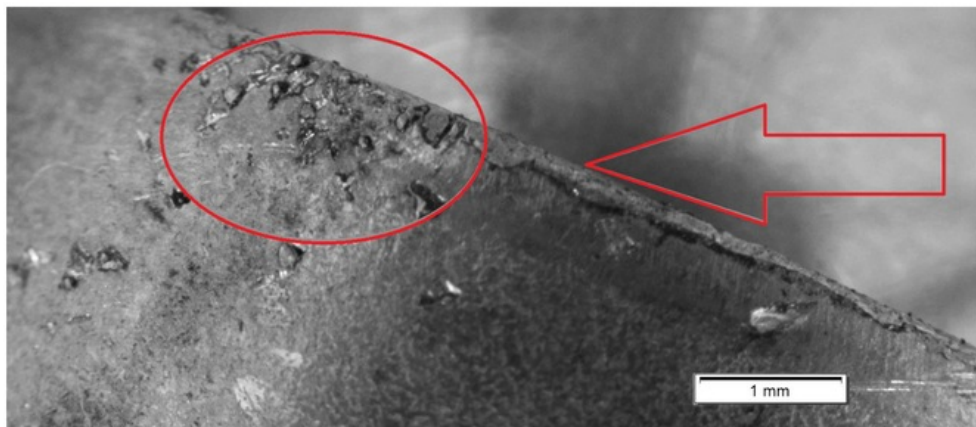


Figure 174: Bearing 6.1 cage edge wear

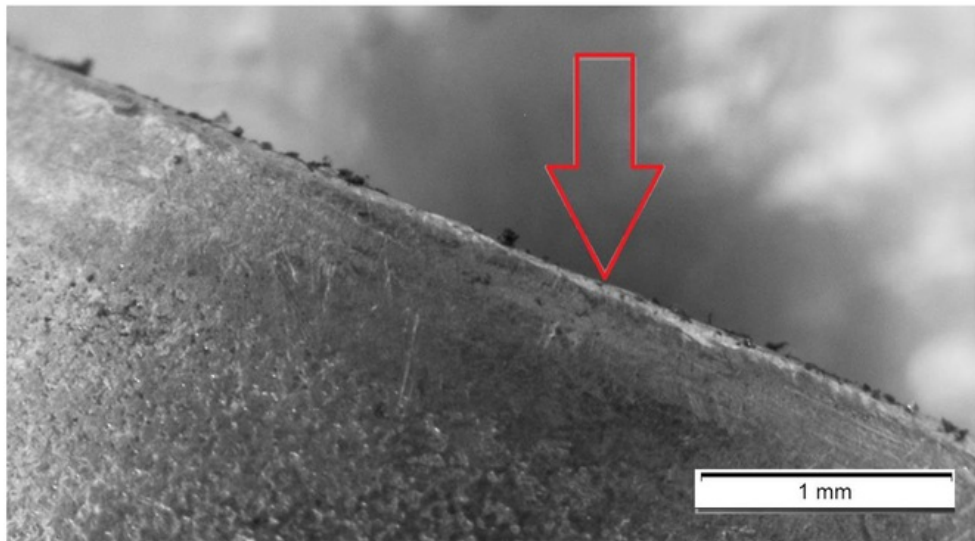


Figure 175: Bearing 6.2 cage wear

4.4 HARDNESS TEST

A hardness test was carried out on a sample of one of the bearings (6.2 to be exact) to investigate whether any plastic deformation had occurred on the race. A Vickers hardness test was used which basically applies a HV5 force (a 5-kilogram force) to the sample. A table below shows the value attained from the hardness test at points on the outer race top to bottom.

Table 5: Hardness Test results

Point	HV5 Value
1	793
2	802
3	812
4	798
5	801

The specifications sheet for the bearing has a hardness test value measured in HV10, meaning this test cannot be justifiably used in discussion.

5 DISCUSSION

In this section the results of the project will be discussed in relation to previously known information about bearing failure and how well the hypothesis match the results. The findings of the FEA simulation will be analysed to determine whether the bearing design is flawed and if it requires to be redesigned, which parts need attention. The simulation has been run using the specifications from the manufacturer including dimensions, rated loads and material choice so a realistic model can be attained.

Following this, the results from physically observing the bearings before and after cleaning and cutting will be discussed in detail. This also includes micrographs from the optical microscope focusing on surface wear, pitting/bruising, fatigue spalling, surface contamination, corrosion/etching and ball and cage damage. The cause and effect of each of these damage modes will be analysed.

5.1 FEA COMPONENT

Running a FEA on a bearing design which has been tried and tested in detail by the manufacturer may appear to be pointless. The idea is to verify the design with the rated load, speeds and specifications as stated by the manufacture (SKF) and compiled in table 2 (page 22), and determine whether the design of the bearing meets the requirements with minimal deformation to support an ideal life time.

As shown in the Theoretical Work in Experimental Procedures earlier, various measurements will be taken, a total deformation of the bearing, the stresses in both the inner and outer races as well as the balls and cage and finally a pressure measurement on just the rolling elements and cage. These are the most looked at results of any bearing design as well as thermal loads, which in this case is disregarded as on site temperatures are not known for a meaningful result to be found.

From table 2, the material is known to be bearing steel 100Cr6, so for this case the selected material is stainless steel as the properties were most similar. This material was modified, changing the density, hardness, modulus of elasticity and thermal expansion making the material for this case very like the steel used in real bearings.

5.1.1 Total Deformation

In our case, the inner ring is stationary with the outside ring rotating with the roller (refer to figure 59). This means the load is applied to the outer rings face and rotates. When subjected to a bearing load of 29,600 N over a 200° rotation over five seconds, the total maximum deformation of the bearing is on the outer ring, with a value of 0.0001753 m. Considering the bearing is rotating at the time of applied load, the deformation is spread out over the entire area of the outer ring. In millimetres this is 0.1753 mm, a miniscule deformity. Judging from these results it can be shown that, as the total deformation is minimal, the bearing design is unrelated to the causes of premature failure.

5.1.2 Stress

The stress subjected to the bearing is measured using Von Mises stress which helps dictate when a material will fail due to high loads and stresses. It is measured in Pascals with the maximum stress of 510.82 MPa occurring on the inner edge of the cage as shown in figure 60. Basically, this means that this point will be the first to fail, undergoing elastic then plastic deformation. We can see from the graph in figure 60 the increasing and decreasing stresses as the bearing rotates. As the modulus of elasticity is 210 GPa (table 2) we can observe the stresses subjected to the bearing are 0.2432% of the maximum value before plastic deformation. This verifies that the bearing has zero problem with the stresses and is unrelated to the premature failure of the bearing.

5.1.3 Pressure

Figure 62 displays the pressures on the rolling elements (balls) and cage. While this does not validate any hypothesis, it is useful to detect the point on the balls that are subjected the highest amount of load and stresses. It is unusual that the point of highest pressure, 10.999 MPa is not directly in the centre of the balls axis (in terms of z axis, up). This could be due to the location of the coordinate system the bearing load is applied on or because the balls are free to rotate. However, this result is not significant to whether the bearing design is flawed, although is useful when examining the race and balls under a microscope to detect whether there is a pattern. It is possible more wear will occur along that plane on the race. The same cannot be said of the balls as they are free to rotate so even wear should be observed.

Therefore, as the total deformation and stresses on the bearing are nowhere near large enough to cause plastic deformation during the five second, 200⁰ rotation with a load of 29,600 N applied, it is safe to say the design of the bearing itself is sufficient to suggest premature failure. Any structure, tool, component must have a factor of safety that well exceeds the loads it is designed to undergo. This bearing design meets and exceeds these under the conditions set in the simulation for this project. Drawing on this knowledge, premature failure must be caused by other means.

Prior to cleaning the bearings of muck, dirt and lubrication it is possible to take samples of the grease and observe it for any abnormalities such as water, dirt and other particles that could be the cause of premature failure. As discussed earlier, the most common cause of premature bearing failure is the contamination of the bearing by foreign particles which then cause the breakdown of the bearing races, balls and cage, all of which increase friction and in turn, overheat the bearing.

Figures 64, 68, 72, 76, 81, 84, 94, 99, 105 and 109 show bearings 1.1, 1.2 to 6.2 respectively (excluding bearings 4.1 and 4.2). The interesting part they all have in common are foreign particles present in the bearing grease. As the grease is still present in the bearing, we can assume these particles would travel around the bearing as it rotated, increasing friction and damaging the balls, cage, inner race and outer race. The extent of this damage will be discussed later using micrographs under "Discussion" -> "Micrographs".

Much of the visible debris in the lubrication are black particles ranging from small to long large particles. Upon further observation, it was found they are a black rubber polymer of the same material as the bearing housing. The bearing housing is designed to prevent contaminants from penetrating the bearing and getting mixed into the grease inside the bearing. Also present within the bearing are smaller, silver particles found to be metal of the same material as the bearing. At this point, it is assumed that these metal particles are fragments of the races, balls or cage or a combination of all three. The metal particles are a sign that significant damage has already been done to the bearing, resulting in large interferences, high friction coefficient and vibrations. The origins and result of the metal debris will be discussed later through micrographs under "Discussion" -> "Micrographs".

5.2 LUBRICATION SAMPLES

From each bearing, a sample of lubrication grease was removed and spread out over a surface. Doing so would allow a more in depth observation of what the grease contains. While not all the contaminated lubrication could be extracted, it can be assumed the remaining grease inside the bearing is roughly the same. This can be justified as during operation lubrication will travel around the bearing moving with it particles and debris. The samples of grease can be examined in figures 65, 69, 73, 77, 82, 85, 95, 96, 100, 106 and 110 with red circles highlighting the foreign particles. Coherent with observations made earlier of the bearings before cleaning, much of debris are the black polymer particles from the bearing housing as well as containing many small metal particles with some larger ones. Polymer particles ranged in sizes and shapes, from 0.5 mm to 15 mm in length with 90% being no more than 2 mm in width and height. Metal particles were nearly all 1 mm by 1 mm in area with miniscule height. While it is highly possible other particles of material from an outside system are present in the bearings, especially lubrication, it was not possible during this project to extend to further detail in terms of debris.

It is thought, that as the rubber casing is directly adjacent to all faces of the bearing, throughout the lifetime of the roller the casing is more likely to break down and have particles break free. The rubber casing can be worn down or broken apart for multiple reasons. The most likely causes are high temperatures caused by a bearing running with high friction and vibrations within the bearing as it spins. If a bearing rotates under load with a higher friction coefficient than designed for, the heat generated will increase up to a point where the rubber polymer will break apart more easily or in worst case scenario, melt down. At higher temperature, small particles are more likely to break off in a vibrating bearing and will make their way into the internals of the bearing. From figure 89 and figure 92 it is evident that bearing seizure has been caused by the rubber polymer casing melting into the bearing. The root cause of high heat can be found when looking at the inner race, outer race and balls of the bearing in detail, look under "Results" -> "Micrographs".

Each sample of grease was very similar in colour and composition, suggesting each bearing would have similar failure modes from the same cause. These particles move at high speeds as the bearing rotates, increasing friction, and causing vibrations and therefore wear. As discussed earlier in "Literature Review" -> "Wear Mechanisms" -> "Lubricant Related Abrasive Wear", the film thickness for the lubrication is much thinner than the thickness of many particles

present in the grease. The small particles that come in between the contact points cause three body abrasion which at this point is the suspected cause of premature failure.

It is not certain whether the initial cause of three body abrasion is foreign particles from a separate system in the environment or from the bearing itself (polymer casing or races, ball or cage). The severity of three body abrasion cumulates with the increase in particles. This means that three body abrasion will create more particles which themselves will cause more three body abrasion, and so on, until the bearing is deemed failed. During this process, the friction of internal components will increase due to imperfect surfaces, particles creating interferences and dirty surfaces of the balls and/or races. The imperfect surfaces because of three body abrasion will also be discussed later using the micrographs.

5.3 MICROGRAPHS

It is suspected that three body abrasion is the root cause for causing premature failure of a bearing. Symptoms such as bearing metal particles and polymer bearing casing particles frequently found throughout the lubrication (as discussed earlier) point to the fact that there must be material removal inside the bearing. This is also highlighted when spinning the bearings after they have been cleaned. Rotating the clean bearings reveals audible grinding of the balls over the races. It was possible to feel the rolling balls travel over uneven surfaces which ideally should be smooth and frictionless.

Therefore, in order to validate this theory a close detailed look at the bearing races, balls and cages is needed to study the surfaces. A series of micrographs have been grouped together in "Results"-> "Micrographs" based on the mode of damage as well as where the damage is, either the inner or outer race, balls or cage. These vary both in severity, stage of wear and root cause. The micrograph groupings are surface damage, pitting/bruising, fatigue spalling, chips, surface contamination, corrosion/etching, heat damage, ball damage and cage damage.

5.3.1 Surface Damage

Surface damage as depicted in figure 113 through to figure 125 all show surface damage in the form of scratches. This is the first stage of three body abrasion as material has not been removed at this point. As explained earlier in this document a particle, whether it be dirt, dust, bearing metal, polymer particles from the bearing housing come between the contact points, in this case the ball and either inside or outside race. Under load and rotation, the particle scratches the two surfaces. Taking figure 118 (the outer race of bearing 3.2) and figure 159 (the ball surface of the same bearing, 3.2) we can see scratches on both surfaces. This would suggest that a third body has become stuck between the two components and as the two bodies are moving against each other the particle causes the surfaces to be scratched. More examples of surface scratches can be seen in figures 113 to 125.

Sometimes it is possible for a particle to penetrate one of the two surfaces, most of the time the softer material as it is more malleable. A hardness test was undertaken on the outer race of a bearing (see "Results" -> "Experimental Results" -> "Hardness Test") for the results. Due to the varying results compared with the specifications stated by the manufacturer, the test will be disregarded as a consistent result could not be found. This means that it is not known whether the ball or the race material is a harder substance, however, by looking at the various micrographs we can see that the wear is more severe on the races than the balls. This is assumed as wear involving plastic deformation and material removal is much more common on the races than the rolling elements.

Following this, figures like 165, 166 and 167 depict small pits in the balls surface. These would be formed when a hard particle like metal comes between the contact point with the race under high load. The particle is pressed into the balls surface and become lodged there, creating an uneven surface. As the ball rotates with the particle sticking out it will gouge out the surface of the race and plastically deforming it. The result are deep scratches and long grooves as per the next two sections.

5.3.1.1 Gouges and Deep Scratches

Scratches on the surfaces as shown are the initial stages of wear in bearings. Damage that progresses from here are gouges, deeper scratches and grooves all of which involve material removal and plastic deformation of the material around the edges of the damage. The removed material is then likely to initiate or cause more gouges and grooves. Third body abrasion utilising metal rather than dust, dirt or polymer as the third body is far more severe. The result of this is what can be seen in the next two sections of “Surface Damage”, Gouges and Deep Scratches” and “Grooves”.

Figures 126 through to 132 all show large material removal on the bearing races. Deep gouges like these are the next step on from surface scratches seen in figures 113 to 125 and have far more severe impacts on the efficiency of the bearing. As explained earlier in “Bearing Damage Analysis” -> “Wear” -> “Abrasive Wear” as well as in “Literature Review” -> “Wear Mechanisms” -> “Lubricant Related Abrasive Wear”, material removal creates high spots around the edges of the deformation. These high spots increase the friction of the bearing as the balls pass over the high, low and high places. This also allows the ball to move in the radial direction slightly which means at high speeds this will cause vibrations within the bearing.

5.3.1.2 Grooves

Grooves are similar to gouges and deep scratches from earlier, except that these grooves are linear. They follow a straight line and are up to 10mm long and only a few microns wide. Examples can be seen in figures 133, 134 and 135.

For such a linear gouge to form there can only be one rotating body and it must be the race. If the ball was free to rotate on any axis the groove would be look something like what can be seen in figure 131. For the groove to form the ball is seized, most likely due to a particle lodging itself in between the cage and the ball (location signified by the red ‘x’ in figure 168) This initial three body abrasion is now two body abrasion, with the seized ball and particle acting as the cutting tool. During this process, there is a large amount of material removal and plastic deformation like that of three body abrasion.

In some areas of the balls surface there are pits that would have been formed by hard particle indentation. Figures 165, 166 and 167 highlight the pits in the surface. The red arrow on the right in figure 165 points to large holes in the surface in which hard particles would be lodged.

5.3.2 Pitting/Bruising

Pitting or bruising is plastic deformation of the surface at points of high stress. The high stress points are a result of particles between the area of contact becoming a point of focus and high spots caused by material removal from third body abrasion.

The result of pitting is an indentation in the surface of the race or ball. Examples can be found in every bearing showing that it is a common problem with premature failure of bearings used on mine sites. Figures 136 to 142 are all examples of pitting or bruising to the inner or outer race. The shape of the pits are generally similar to that of the particle that caused it.

Figure 139 is a clear example of the extent of the damage caused by bruising. The red circle is the area of focus in this micrograph. It is littered with bruises caused by high loading on free particles onto the outer race. Each pit is extremely small but is significant as they cause miniscule vibrations as the balls rapidly rotate over the surface.

Looking at figure 137 the inside race, the lower red arrow points to a series of bruises in a linear path, each the same shape indent. This would suggest the same particle has created these in quick succession. The damage is roughly 1 mm long with each pit approximately 83.3 microns in width. The particle must be extremely resistant to deformation and not brittle in any way to consistently create the same profile pits. The suspected method of pit formation of this type is a hard particle become lodged or stuck to the ball. At high speeds and under high loads, as the part of the ball with the particle rotates on the race it indents the surface. This is similar to how a groove is formed but in this case the ball is not seized and free to rotate. The same mode of damage can be seen in figure 140.

Pitting or bruising is a significant issue as it creates an uneven surface that when balls pass over it, they undergo small periods of low and high loading. This, coupled with the miniscule vibrations as the balls roll over the race, amplifies the internal friction of the bearing. An increase in friction results in a decrease in efficiency and therefore life of the bearing, increasing the likelihood of premature failure of the bearing. It is another form of damage due to free particles moving around the internals of the bearing.

5.3.3 Fatigue Spalling

Fatigue spalling is yet another result of debris causing damage to the races of the bearing. It is not three body abrasion as discussed earlier but is closely related to it. Examples of fatigue spalling can be seen in figures 143 to 147. The material on the surface appears to flake away and can grow to cover a reasonably large area such as figure 147 which is approximately 500 microns by 600 microns. Like pitting, spalling is also caused by high localised stress which is often the result of plastic deformation during the process of material removal as discussed earlier under "Discussion" -> "Micrographs" -> "Fatigue Spalling".

Point Surface Origin (PSO) spalling as shown in figure 147 is the most common form of spalling, a result of very high localised stress. It is often in the shape of an arrowhead pointing in the direction of bearing rotation.

Wear in the form of spalling grows over time. With repeated fatigue, small flakes of material will be chipped away and move around the lubricant as the bearing spins, adding to the material creating three body abrasion.

5.3.4 Chips

Chips like that shown in figure 148 were not a common appearance in the bearings studied. A chip like this has no signs of wear in the close vicinity, suggesting that it was not caused by three body abrasion or another form of wear. The chip in figure 148 was similar to other chips in 2 other bearings in both location and size, approximately 1 mm in length.

There is little or no force or stress subjected to the edge on the races meaning that this damage could not have occurred during the operation of the bearing. In "Literature Review" -> "Bearing Damage Analysis" -> "Installation", it was said that it was common for damage to take place during installation or transportation of the idler roller. A roller can be dropped, knocked around or installed using improper tools which can lead to a chip like in figure 148 being created.

Damage of this type is a significant problem as there is already debris ready to initiate three body abrasion inside the bearing. Once wear has started it very quickly gets out of hand, as each impairment cumulates, resulting in the failure of the bearing.

5.3.5 Surface Contamination

Surface contamination is basically the surface of the race of rolling element being covered with a substance reducing the efficiency of the bearing. As explained earlier a micron thin film covers the race and ball, creating a frictionless contact between the two. All the above forms of wear increase the coefficient of friction within the bearing by deforming the surface in some way, whether it be by gouges, pitting, plastic deformation (high spots) or fatigue spalling. All of these actions generate more heat and increase the wear of the components.

From figure 149 to figure 153, we can see that the surfaces of the bearing race are not affected much by three body abrasion and have no pits, spalling or gouges in them. The main issue here is the surface being covered by foreign material, with a higher friction coefficient than bearing metal. As the material is stuck to the race, it adds a small layer of thickness to the race, resulting in a slightly tighter fit for the ball to travel past (between the inner and outer races) meaning more friction and therefore more heat. An added issue of a different surface is that the lubrication was not designed to be in contact with other material. It is no longer possible for a thin film to be formed over the contaminated surface, also increasing the friction.

Looking at figure 150, a large patch of material (approximately 7 mm²) has melted onto the inner race. Upon close examination, it was found the material was the same as the bearing housing, the black rubber polymer. A piece would have found its way into the bearing and due to the high heat generated by the bearing melted onto the race and become part of the surface. It is not known at what point during the bearing's life this occurred, but for the polymer particles to melt to this extent a large amount of heat would need to have been generated. This heat could have been because of high friction inside the bearing possibly due to one or a combination of reasons such as surface damage in the form of gouges, grooves, pitting/bruising or fatigue spalling.

In figure 164, the surface of the ball has also had some of the polymer melted onto the surface. The layer appears to be rather thick and on top of some surface wear. Therefore, it is likely in this case the damage to the bearing had already been done, and that the high heat caused by the damage bearing allowed the bearing housing to be broken down and penetrate the internal components of the bearing.

Another example of dirty surfaces of a different variety are found in figure 149 where the ball passing over the contaminated surface has worn away some of the contaminant (also suspected to be the same rubber polymer as the bearing housing).

5.3.6 Corrosion/Etching

Corrosion or etching takes place when foreign, oxidising particles such as water sit inside the bearing and erode the surface away. There are varying degrees of severity ranging from surface stains to water spalling as shown in figure 9. Etching occurs at the contact points between the ball and race where the particles can aid wear, acting as a catalyst for two body abrasion and spalling.

An example of the initial stages of corrosion can be seen in figure 154. The surface has become stained as pointed out by the red arrow.

5.3.7 Heat Damage

Heat is a factor of many of the forms of damage above and is also a product of these many forms of damage. Essentially surface wear, pitting/bruising, fatigue spalling, surface contamination and corrosion/etching all generate heat due to friction. That heat then amplifies that wear as the components become hot and more malleable, allowing three body abrasion as well as pitting to be a more frequent occurrence and more effective.

As discussed earlier in "Surface Contamination" the higher heat takes its toll on the bearing housing, giving way to polymer particles to melt onto the race. A severe example of this can be seen in figures 89 and 92 where a large amount of the rubber bearing housing has melted into the bearing itself, seizing it and rendering it useless.

Another factor to consider is that the lubrication inside these bearings is designed to work at. At extreme heats the molecules that make up the lubricant break down and fail to keep the thin film on the surfaces intact, leading to increased friction, two body abrasion and assisting three body abrasion further. Two body abrasion occurs as the ball no longer has a frictionless surface to roll against (the race).

Heat damage on the races usually results in discolourations or stains on the metal as can be seen in figure 155. The effects of heat also translate to the softer metal of the cage containing the rolling elements. We can see the result on the edges of the cage in figures 170, 172 and 174 looking at the red arrows. While the melted outside edges are not an issue, the same heat damage to the inside edge of the ball (shown by the red 'x' in figure 168) can interfere with the rotation of the ball, possibly causing two body abrasion.

5.3.8 Frequency of Various Damage Types

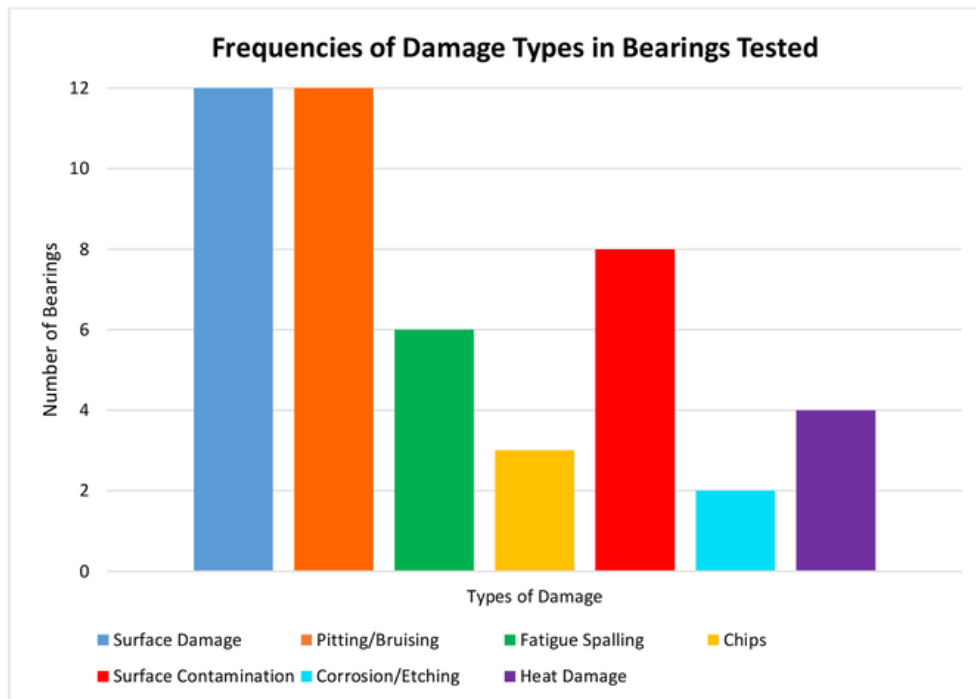


Figure 176: Frequency of various damage types

The graph above displays how common each type of damage is relative to the others. We can see that “Surface Damage” and “Pitting/Bruising” occurred in all twelve bearings meaning that three body abrasion is a common root cause of failure. Fatigue spalling is also a result of three body abrasion but is a more severe form and so is less common. Surface contamination is also common result with corrosion/etching happening only once in the batch of bearings studied.

From these results, it can be assumed that three body abrasion is the most likely cause of premature bearing failure of any idler roller used on mine sites.

6 CONCLUSIONS

The goal of this project was to perform a failure analysis on bearings used in idler rollers on mine sites. The rollers had failed well before their estimated life span so a detailed analysis on the cause of failure was performed. It was found through research that the most common failure on idler rollers in a mining environment was the bearing, so that was the area of focus.

A literature review was conducted to understand the fundamentals of a belt conveyor system including the belt, the idler rollers and narrowing it down to the components of the roller (bearings, bearing housing, shaft and seals). As this report focuses on the bearings of the idler rollers, information about how bearings work and the features specific to the bearings studied in this project are explained.

Following this, an overview on known causes and effects of failure was given to provide the reader information on how and why bearings can fail. An analysis on abrasive wear, fatigue spalling, overheating, excessive loads and other modes of damage was provided. It was found during this research the most common cause for premature failure is three body abrasion due to the high number of foreign particles in the environment. Three body abrasion also has many side effects which can lead to other forms of failure. It is suspected (from the information gathered so far) the root cause for premature bearing failure is three body abrasion. While each mode of failure is not a direct result of three body abrasion, it is a significant factor in many types of damage to these bearings.

To verify that this is the case an FEA on a bearing model was simulated to test whether the bearing design is sufficient to support the rated loads and speeds set by the manufacturer. It was found that there was very little deformation or stress on any components of the bearing, which would suggest that the structural design alone has very little to do with premature failure.

Further detailed analysis of failed bearings shipped from a mine site was conducted to determine the cause and effect of premature failure. This was done using both macro and micro photographs. Macro photographs of bearings shortly after they were removed from their bearing housing were especially useful to observe the result of failure. Samples of lubrication from each bearing were studied to verify that debris was common throughout the grease (and the nature of the debris) suggesting three body abrasion had taken place.

Cutting each bearing in half would permit the internal structure to be examined meaning the inside and outside races, balls and cage of the bearing. Using an optical microscope, close-up pictures could be taken to properly study the state of the surfaces.

From the discussion and research, it is evident that most damage was related to three body abrasion. It does not mean that the only reason of failure is three body abrasion but as it occurs, it gives way to other forms of damage which in turn lead to further damage.

Essentially, a snowballing effect which cannot be reversed once begun.

7 FUTURE WORK

Based on the results of this project, three body abrasion is the root cause of premature bearing failure. It is however, unclear which particle initiates this type of abrasion and from where it came from. Research would suggest that dust, dirt or similar penetrate the bearing housing and start off the process but it was difficult to trace this during this project.

Future work could look at how particles manage to work their way into the internals of the bearing through the bearing housing. This points to the quality of the sealing methods for bearings used in such hostile environments. Computer simulations can be run on various types and configurations of sealing mechanisms as well as experiments of the same to validate results. It would be interesting to see the percentage of failed idler rollers that are set up on an angle as opposed to being flat (refer to figure 2). It was also interesting to see that no seals existed on the inside face of the bearing and the reason for this design choice is not known.

Therefore future work should investigate the design, quality and efficiency of the sealing methods for idler rollers used on mine sites.

REFERENCES

- [1] A. M. Dr, "Condition monitoring of belt Condition monitoring of belt," in *Sydney : IQPC Mining*, Perth, 2011.
- [2] A. V. Reicks, "Belt Conveyor Idler Roll Behaviours," Overland Conveyor Co.
- [3] Lorbrand, "Lorbrand products," Lorbrand, [Online]. Available: http://www.lorbrand.com/images/content/steel_roller03.gif. [Accessed 19 7 2016].
- [4] V. L. International, "Technical Data," Valley Longwall International, 5 August 2016. [Online]. Available: <http://www.valleylongwall.com.au/bulk-materials-handling-technology/technology/idlers-frames/>. [Accessed 5 August 2016].
- [5] E. Toolbox, "Modulus of Elasticity or Young's Modulus - and Tensile Modulus for common Materials," Engineering Toolbox, [Online]. Available: http://www.engineeringtoolbox.com/young-modulus-d_417.html. [Accessed 31 8 2016].
- [6] GMN, "Labyrinth SEal Design and Technology," GMN, [Online]. Available: <http://www.gmnbt.com/labyrinth-seals-technical-guide.htm>. [Accessed 31 8 2016].
- [7] "Static," [Online]. Available: http://static.wixstatic.com/media/dad14e_9d030bcf6433ae61b8628d9b199b5afa.jpg/v1/fill/w_640,h_480,al_c,q_90/dad14e_9d030bcf6433ae61b8628d9b199b5afa.jpg. [Accessed 8 31 2016].
- [8] "iecltd," [Online]. Available: <http://www.iecltd.co.uk/Uploads/Image/ball%20bearing%20structure.gif>. [Accessed 2 9 2016].
- [9] Timken, *Deep Groove Ball Bearing Catalog*, Timken, 2015.
- [10] SKF, "Single Row Deep Groove Ball Bearing Designation," [Online]. Available: <http://www.skf.com/au/products/bearings-units-housings/ball-bearings/deep-groove-ball-bearings/single-row-deep-groove-ball-bearings/designation-system/index.html>. [Accessed 28 9 2016].
- [11] B. King, "Bearing King," [Online]. Available: <https://www.bearing-king.co.uk/bearing/6306-c3-skf/4357>. [Accessed 28 9 2016].
- [12] SKF, "Materials for bearing rings and rolling elements," SKF, [Online]. Available: <http://www.skf.com/au/products/bearings-units-housings/super-precision-bearings/principles/bearing-specifics/materials/materials-for-bearing-rings-and-rolling-elements/index.html>. [Accessed 27 10 2016].
- [13] Timken, *Timken Bearing Damage Analysis with Lubrication Reference Guide*, The Timken Company, 2011.
- [14] B. Precision, "Bearing Failure: Causes and Cures," Barden Precision Bearings.
- [15] K. Kato and K. Adachi, "Wear Mechanisms," Tohoku University, Sendai, Japan, 2001.

- [16] M. J. Murray, P. J. Mutton and J. D. Watson, "Abrasive Wear Mechanisms in Steels," *Journal of Lubrication Technology*, vol. 1, no. 1, pp. 9-16, 2009.
- [17] elsevier, "elsevier," [Online]. Available: http://www.elsevier.es/ficheros/publicaciones/22387854/0000000400000002/v3_201505310059/S2238785414000969/v3_201505310059/en/main.assets/gr1.jpeg. [Accessed 2016 10 27].
- [18] R. S. Dwyer-Joyce, "Wear," *Predicting the abrasive wear of ball bearings by lubricant debris*, Vols. 233-235, no. 1, pp. 692-701, 1999.
- [19] AutoDesk, "Finite Element Analysis," AutoDesk, [Online]. Available: <http://www.autodesk.com/solutions/finite-element-analysis>. [Accessed 20 9 2016].
- [20] SKF, "Deep Groove Ball Bearings Catalogue," SKF, [Online]. Available: <http://www.skf.com/au/products/bearings-units-housings/ball-bearings/deep-groove-ball-bearings/single-row-deep-groove-ball-bearings/single-row/index.html?designation=6306-2Z&unit=metricUnit>. [Accessed 17 9 2016].
- [21] SKF, "Estimating the frictional moment," SKF, [Online]. Available: <http://www.skf.com/group/products/bearings-units-housings/ball-bearings/principles/friction/estimating-frictional-moment/index.html>. [Accessed 20 9 2016].
- [22] L. Zhao and Y. Lin, "Typical failure analysis and processing of belt conveyor," *Elsevier*, pp. 942-946, 2011.
- [23] T. J. Walker, "Idler Roller Bearings: Living the Good Long Life?," *Paper, Film and Foil Converter*, vol. 1, no. 82.7, p. 12, 2008.
- [24] Roltech, "Manufacturing Process and QAP for Idler Rollers," [Online]. Available: <http://roltechindia.com/>. [Accessed May 2016].
- [25] P. O'Farrell, "Project Scope Document," Macquarie University, Sydney, 2016.
- [26] P. O'Farrell, "Initial Literature Review," Macquarie University, Sydney, 2016.
- [27] P. O'Farrell, "Draft Project Plan," Macquarie University, Sydney, 2016.
- [28] P. Nel, "Conveyor idler configuration optimization in overland," *Conveyors, Belt Scrapers, Ancillaries*.
- [29] W. Michael, "Lubrication of Rolling Bearings - Technical Solutions for Critical Running Conditions," *Machinery Lubrication*, 2006. [Online]. Available: <http://www.machinerylubrication.com/Read/844/lubrication-rolling-bearings>. [Accessed May 2016].
- [30] A. Mahbub, "The aerodynamics of a cylinder submerged in the wake," *Journal of Fluids and Structures*, vol. 51, pp. 393-400, 2014.
- [31] T. Abbey, "Technology for Optimal Design Engineering," 1 6 2013. [Online]. Available: <http://www.deskeng.com/de/conduct-fatigue-analysis-using-fea/>. [Accessed 24 8 2016].
- [32] P. O'Farrell, "Final Project Plan," Macquarie University, Sydney, 2016.

APPENDICES

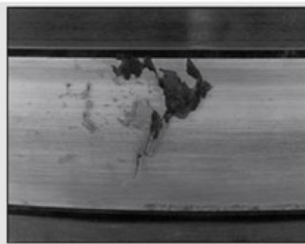


Fig. 6. A tapered roller bearing inner race (cone) with spalling from debris contamination bruises.

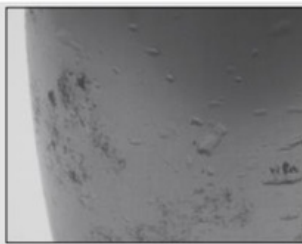


Fig. 7. Hard particles caused contamination bruising on this spherical roller bearing.

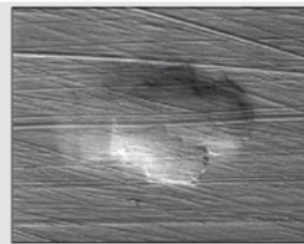


Fig. 8. This photo, taken with a microscope, shows a debris contamination bruise on a bearing race. A corresponding surface map of the dent is shown below in Fig. 10.



Fig. 9. Debris from other fatigued parts, inadequate sealing or poor maintenance caused bruising on this tapered roller bearing race.

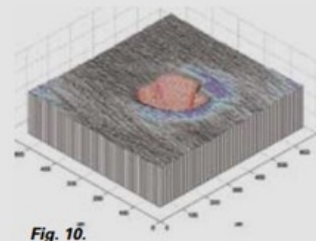


Fig. 10.

Figure 177: Fine particle contamination examples [9]



Figure 178: Heat Damage at roller ends [13]

Fig. 19. Level 3 – Heat damage on these tapered rollers was caused by metal-to-metal contact.

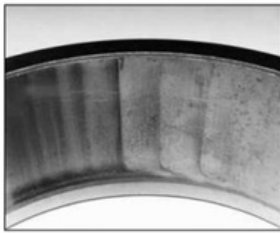


Fig. 31. Scalloping marks in the cup are common with excessive endplay. Unloaded rollers enter the small load zone and are suddenly exposed to heavy loads.



Fig. 32. Cage pocket damage from excessive roller movement.



Fig. 33. Heavy wear in the small end of the cage pockets is typical of excessive endplay.

Figure 179: Example of excessive end play damage [13]

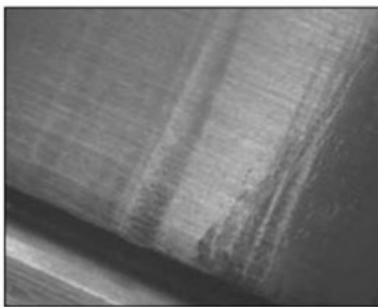


Fig. 55. This inner ring of a spherical roller bearing shows roller impact damage from shock loading.

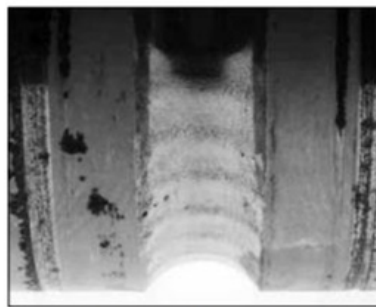


Fig. 56. Shock loading caused brinell damage on this ball bearing inner ring.

Figure 180: Example of impact damage to the races of the bearing [13]

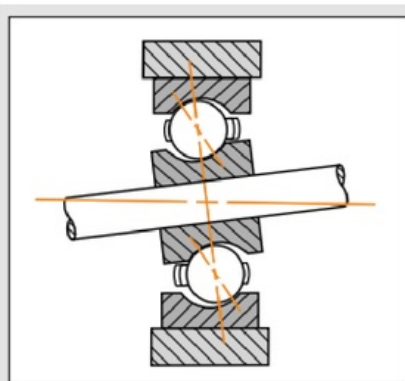


Fig. 34A. Shaft misalignment

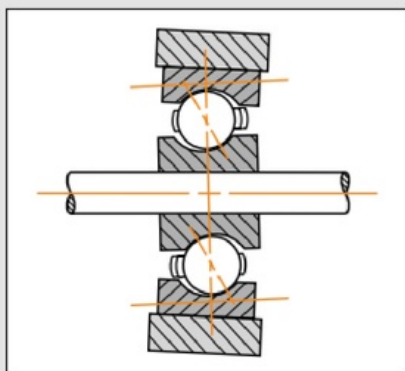


Fig. 34B. Housing misalignment

Figure 181: Shaft misalignment and bearing housing misalignment [13]



Fig. 35. Deflection, inaccurate machining or wear of bearing seats caused an irregular roller path on this tapered roller bearing outer ring.

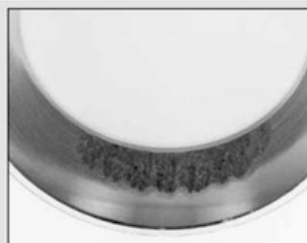


Fig. 36. This irregular roller path is 180 degrees opposite of Fig. 35.



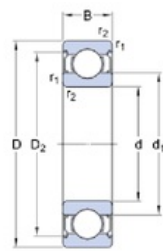
Fig. 37. The housing bore was machined with an improper taper, causing the uneven load distribution and GSC spalling in this cylindrical roller bearing outer ring.

Figure 182: Uneven load distribution and ball path due to bearing misalignment [13]

6306-2Z

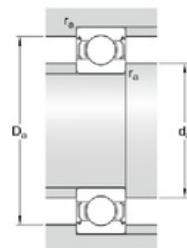
SKF Explorer

Dimensions



d	30	mm
D	72	mm
B	19	mm
d ₁	≈ 44.6	mm
D ₂	≈ 61.88	mm
r _{1,2}	min. 1.1	mm

Abutment dimensions



d _a	min. 37	mm
d _a	max. 44.5	mm
D _a	max. 65	mm
r _a	max. 1	mm

Calculation data

Basic dynamic load rating	C	29.6	kN
Basic static load rating	C ₀	16	kN
Fatigue load limit	P _u	0.67	kN
Reference speed		20000	r/min
Limiting speed		11000	r/min
Calculation factor	k _r	0.03	
Calculation factor	f ₀	13.1	

Mass

Mass bearing	0.363	kg
--------------	-------	----

Figure 183: SKF 6306-2Z single row deep groove ball bearing specifications [20]

Bearing type	Coefficient of friction μ
Deep groove ball bearings	0,0015
Angular contact ball bearings	
– single row	0,0020
– double row	0,0024
– four-point contact	0,0024
Self-aligning ball bearings	0,0010
Cylindrical roller bearings	
– with a cage, when $F_a \approx 0$	0,0011
– full complement, when $F_a \approx 0$	0,0020
Needle roller bearings with a cage	0,0020
Tapered roller bearings	0,0018
Spherical roller bearings	0,0018
CARB toroidal roller bearings with a cage	0,0016
Thrust ball bearings	0,0013
Cylindrical roller thrust bearings	0,0050
Needle roller thrust bearings	0,0050
Spherical roller thrust bearings	0,0018

Figure 184: Coefficient of Friction for various SKF bearings [21]

Consultation Meetings Attendance Form

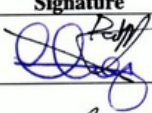
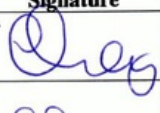
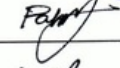

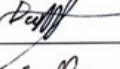
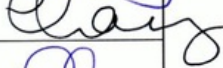
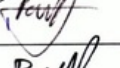


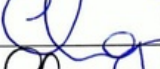










Week	Date	Comments (if applicable)	Student's Signature	Supervisor's Signature
2	11/8/16	discussed plan, work so far, potential experiments		
3	17/8/16	borrowed book on materials discussed plan/bearings		
4	22/8/16			
5	29/8/16	Belt has arrived! will be dismantled		
6	13/9/16	Bearing wear note!		
7	19/9/16	Still dismantling		
8	28/9/16	not sign with pyrex -melting, profilemeter -bearings cut		
9	5/10/16			
10	17/10/16			
11	25/10/16			

Figure 185: Consultation sheet